

5-2011

Stromal derived growth factor alpha (SDF-1 α) induces the differentiation of bone marrow progenitor cells (BMCs) into pericytes by regulating platelet derived growth factor B (PDGF-B) transcription

Randala Hamdan

Follow this and additional works at: https://digitalcommons.library.tmc.edu/utgsbs_dissertations

 Part of the [Laboratory and Basic Science Research Commons](#)

Recommended Citation

Hamdan, Randala, "Stromal derived growth factor alpha (SDF-1 α) induces the differentiation of bone marrow progenitor cells (BMCs) into pericytes by regulating platelet derived growth factor B (PDGF-B) transcription" (2011). *The University of Texas MD Anderson Cancer Center UTHealth Graduate School of Biomedical Sciences Dissertations and Theses (Open Access)*. 118.
https://digitalcommons.library.tmc.edu/utgsbs_dissertations/118

This Dissertation (PhD) is brought to you for free and open access by the The University of Texas MD Anderson Cancer Center UTHealth Graduate School of Biomedical Sciences at DigitalCommons@TMC. It has been accepted for inclusion in The University of Texas MD Anderson Cancer Center UTHealth Graduate School of Biomedical Sciences Dissertations and Theses (Open Access) by an authorized administrator of DigitalCommons@TMC. For more information, please contact digitalcommons@library.tmc.edu.

Stromal derived growth factor alpha (SDF-1 α) induces the differentiation of bone marrow progenitor cells (BMCs) into pericytes by regulating platelet derived growth factor B (PDGF-B) transcription

By Randala Hamdan, B.S.

APPROVED:

Eugenie S. Kleinerman, MD, Supervisory Professor

Alexander Lazar, MD, PhD

Gary Gallick, PhD

Qing Ma, PhD

Aarif Khakoo, MD

APPROVED:

George M. Stancel, PhD, Dean, The University of Texas
Graduate School of Biomedical Sciences at Houston

Stromal derived growth factor alpha (SDF-1 α) induces the differentiation of bone marrow progenitor cells (BMCs) into pericytes by regulating platelet derived growth factor B (PDGF-B) transcription

A

DISSERTATION

Presented to the Faculty of
The University of Texas
Health Science Center at Houston

And

The University of Texas
M.D. Anderson Cancer Center
Graduate School of Biomedical Sciences

in Partial Fulfillment
of the Requirements
for the Degree of

DOCTOR of PHILOSOPHY

By

Randala Hamdan

Houston, Texas
May, 2011

Dedications

To my parents whom I respect and adore; for all the emotional and financial support they have offered me, for the continuous encouragement and belief they have shown in me, for the sacrifices they have made to make my dream a reality and to their love, which has been the wind beneath my wings throughout my long journey.

To my dad, whose words of wisdom have taught me that success is not measured by what you own, but by the person you become; and that patience, dedication, honesty, selflessness and love, are a man's true wealth.

To my mom, who symbolizes all that is pure and beautiful in this world; you are the rock who has held strong the weight of our lives. Your love is unconditional and knows no boundaries; you are a true inspiration to us all. I just hope that I can be as great as a mother as you have been to us.

To my brother and sister, the two most wonderful people in my life and my partners in crime over the years. Thank you for making my experience as a middle child so amazing. You have truly shaped my personality and made me into the person I am today. I love you both very much.

Finally, to the love of my life, Nadeem, who is a blessing sent from God. You always know how to bring a smile to my face; thank you for being so supportive, so patient and so loving.

Acknowledgements

I am forever thankful to my mentor Dr. Eugenie S. Kleinerman for making me into the scientist I am today. Dr. Kleinerman is a true inspiration, she represents the definition of the ideal career yet family oriented woman of our generation. I feel blessed to have had the opportunity to be mentored by her. Dr. Kleinerman has guided me, encouraged me and, believed in me even when my project took a wrong turn. She allowed me to question when I had my doubts, she pushed me to challenge myself when I was feeling defeated and, she taught me to stay truthful to my scientific values. I could not have asked for better training as a Ph.D. student.

I would also like to thank all my previous and current committee members, Dr. Alan Schroit, Dr. Janet Price, Dr. Joseph McCarty, Dr. Suyun Huang, Dr. Alexander Lazar, Dr. Qing Ma, Dr. Gary Gallick and Dr. Aarif Khakoo. I am grateful for all their guidance, helpful suggestions and, for constantly challenging me to keep moving forward. I am especially thankful to Dr. Alan Schroit, for being a co-mentor at times and for serving as the chair of my candidacy committee. I have a lot of respect for Dr. Schroit and thank him for both the emotional and scientific support he has given me over the last few years.

I will always be grateful to my fellow student Chantale Charo for helping me become part of the graduate school and to Dr. Jean-Pierre Issa for his support towards my education and his generosity in sponsoring my tuition as a first year graduate student at the Graduate School of Biomedical Sciences (GSBS).

Two of my most rewarding experiences as a student at GSBS were receiving the City Federation of Women's Clubs Endowed Scholarship in the Biomedical Sciences and,

being nominated and awarded the Marilyn and Frederick R. Lummis, Jr., M.D., Fellowship in the Biomedical Sciences. I would like to thank the selection committees as well as the donors for their generosity. I would also like to thank Dr. Thomas Goka, Dr. Jon R. Wiener and, the Dean of GSBS, Dr. George Stancel for giving me this opportunity. I thank you for believing in me as a scientist, for constantly encouraging me, for allowing me to speak up when I needed to and, for showing me that at the end of the day, hard work will be recognized.

A special thank you goes to Dr. Nabil Ahmed, one of our collaborators at Texas Children's Hospital, for his teachings, guidance and his constant support. I would also like to thank Dr. Vidya Gopalakrishnan in the Department of Pediatrics at the University of Texas, MD Anderson Cancer center, for all her support, advice and guidance especially planning my future career goals.

I would not have survived all these years without all the emotional and scientific support of my co-workers, fellow students, lab members and friends. I would especially like to thank Christy Le, Dr. Nancy Gordon, Dr. Gangxiong Huang, Dr. Ling Yu, Dr. Zhichao Zhou, Dr. Mario Holloman, Dr. Nadya Koshkina and Krithi Rao in the Department of Pediatrics. Thank you for all your patience, teachings and advice. I would like to especially thank my dearest friend and fellow student at the time, Dr. Keri S. Stewart, who has constantly encouraged me and shared with me every step of this amazing life experience. I would also like to thank Talia Lapushin who has truly been like a sister to me. Thank you to all of you for creating such a wonderful work environment and the strong support network I need; I can honestly say I found my home away from home amongst you all.

Stromal derived growth factor alpha (SDF-1 α) induces the differentiation of bone marrow progenitor cells (BMCs) into pericytes by regulating platelet derived growth factor B (PDGF-B) transcription

Randala Hamdan, B.S.

Supervisory Professor, Eugenie S. Kleinerman, M.D.

We previously demonstrated that bone marrow cells (BMCs) migrate to TC71 and A4573 Ewing's sarcoma tumors where they can differentiate into endothelial cells (ECs) and pericytes and, participate in the tumor vascular development. This process of neo-vascularization, known as vasculogenesis, is essential for Ewing's sarcoma growth with the soluble vascular endothelial growth factor, VEGF₁₆₅, being the chemotactic factor for BMC migration to the tumor site. Inhibiting VEGF₁₆₅ in TC71 tumors (TC/siVEGF₇₋₁) inhibited BMC infiltration to the tumor site and tumor growth. Introducing the stromal-derived growth factor (SDF-1 α) into the TC/siVEGF₇₋₁ tumors partially restored vasculogenesis with infiltration of BMCs to a perivascular area where they differentiated into pericytes and rescued tumor growth. RNA collected from the SDF-1 α -treated TC/siVEGF₇₋₁ tumors also revealed an increase in platelet-derived growth factor B (PDGF-B) mRNA levels. PDGF-B expression is elevated in several cancer types and the role of PDGF-B and its receptor, PDGFR- β , has been extensively described in the process of pericyte maturation. However, the mechanisms by which PDGF-B expression is up-regulated during vascular remodeling and the process by which BMCs differentiate into pericytes during tumor vasculogenesis remain areas of investigation. In this study, we are the first to demonstrate that SDF-1 α regulates the expression of PDGF-B via a transcriptional mechanism which involves binding of the ELK-1 transcription factor to the *pdgf-b* promoter. We are also first to validate the critical role of the SDF-1 α /PDGF-B pathway in the differentiation of BMCs

into pericytes both *in vitro* and *in vivo*. SDF-1 α up-regulated PDGF-B expression in both TC/siVEGF₇₋₁ and HEK293 cells. In contrast, down-regulating SDF-1 α , down-regulated PDGF-B. We cloned the 2 kb *pdgf-b* promoter fragment into the pGL3 reporter vector and showed that SDF-1 α induced *pdgf-b* promoter activity. We used chromatin immunoprecipitation (ChIP) and demonstrated that the ELK-1 transcription factor bound to the *pdgf-b* promoter in response to SDF-1 α stimulation in both TC/siVEGF₇₋₁ and HEK293 cells. We collected BMCs from the hind femurs of mice and cultured the cells in medium containing SDF-1 α and PDGF-B and found that PDGFR- β^+ BMCs differentiated into NG2 and desmin positive pericytes *in vitro*. In contrast, inhibiting SDF-1 α and PDGF-B abolished this differentiation process. *In vivo*, we injected TC71 or A4573 tumor-bearing mice with the SDF-1 α antagonist, AMD3100 and found that inhibiting SDF-1 α signaling in the tumor microenvironment decreased the tumor microvessel density, decreased the tumor blood vessel perfusion and, increased tumor cell apoptosis. We then analyzed the effect of AMD3100 on vasculogenesis of Ewing's sarcoma and found that BMCs migrated to the tumor site where they differentiated into ECs but, they did not form thick perivascular layers of NG2 and desmin positive pericytes. Finally, we stained the AMD3100-treated tumors for PDGF-B and showed that inhibiting SDF-1 α signaling also inhibited PDGF-B expression. All together, these findings demonstrated that the SDF-1 α /PDGF-B pathway plays a critical role in the formation of BM-derived pericytes during vasculogenesis of Ewing's sarcoma tumors.

Table of Contents

Approval

Signatures.....	i
Title Page.....	ii
Dedications.....	iii
Acknowledgements.....	iv
Abstract.....	vi
Table of Contents.....	viii
List of Figures.....	xiii
List of Tables.....	xvi
CHAPTER 1. Introduction.....	1
Ewing's Sarcoma.....	2
Blood vessel development by vasculogenesis.....	3
Vasculogenesis in Ewing's sarcoma.....	4
Bone marrow transplant model.....	5
Vasculogenesis is essential for Ewing's sarcoma.....	6
The role of vascular endothelial growth factor (VEGF ₁₆₅) in vasculogenesis.....	6
Stromal-derived growth factor (SDF-1 α) and BMC chemotaxis.....	7
SDF-1 α partially rescues vasculogenesis in VEGF ₁₆₅ -inhibited TC/siVEGF ₇₋₁	
Ewing's sarcoma tumors.....	8
Pericytes/vascular smooth muscle cells (vSMCs).....	10
The role of pericytes in tumor vessel development.....	11

Platelet derived growth factor B (PDGF-B) is critical for pericyte maturation.....	13
The role of PDGF-B in pericyte maturation during tumor growth.....	13
A link between pericyte maturation and PDGF-B in Ewing's sarcoma.....	14
The ELK-1 transcription factor.....	14
SDF-1 α activates ELK-1.....	15
Hypothesis.....	16
CHAPTER 2. SDF-1α regulates PDGF-B expression <i>in vitro</i> and <i>in vivo</i>.....	18
Rationale.....	19
Results.....	21
SDF-1 α up-regulates PDGF-B mRNA levels <i>in vitro</i>	21
SDF-1 α up-regulates PDGF-B protein levels <i>in vitro</i> and <i>in vivo</i>	23
Down-regulating SDF-1 α down-regulates PDGF-B expression.....	26
Summary.....	29
CHAPTER 3. SDF-1α regulates PDGF-B via a transcriptional mechanism which involves binding of the ELK-1 transcription factor to the <i>pdgf-b</i> promoter.....	30
Rationale.....	31
Results.....	33
SDF-1 α regulates PDGF-B expression via transcription.....	33
SDF-1 α induces binding of the ELK-1 transcription factor to the <i>pdgf-b</i> promoter.....	35
The ELK-1 transcription factor is phosphorylated at serine 383 in response to SDF-1 α in HEK293 ChIP samples.....	40
Summary.....	42

CHAPTER 4. The SDF-1α/PDGF-B pathway induces the differentiation of bone marrow progenitor cells (BMCs) into pericytes <i>in vitro</i>.....	44
Rationale.....	45
Results.....	47
Fresh BMCs express PDGFR- β but do not express NG2 and desmin mature pericyte markers.....	47
BMCs differentiate into pericytes when cultured in conditioned medium from 10T1/2 cells.....	49
BMCs do not differentiate into pericytes when cultured in 10T1/2-sh-SDF-1 conditioned medium compared to 10T1/2-sh-control medium.....	51
Summary.....	53
CHAPTER 5. The SDF-1α antagonist AMD 3100 negatively impacts tumor vessel development in the Ewing's sarcoma tumor model.....	55
Rationale.....	56
The SDF-1 α antagonist AMD 3100.....	56
AMD 3100 and Ewing's sarcoma.....	57
Results.....	58
AMD3100 leads to smaller vessels with smaller lumens in both TC71 and A4573 Ewing's sarcoma tumors.....	58
AMD 3100 decreases the overall microvessel density in both TC71 and A4573 Ewing's sarcoma tumors.....	60
AMD3100 decreases the amount of perfused vessels in both TC71 and A4573 Ewing's sarcoma tumors.....	62

AMD3100 increases apoptosis in both TC71 and A4573 Ewing's sarcoma tumors.....	64
Summary.....	66
CHAPTER 6. The SDF-1α/PDGF-B pathway plays a critical role in the differentiation of BMCs into pericytes in Ewing's sarcoma tumors.....	68
Rationale.....	69
Results.....	72
BMCs migrate to AMD 3100-treated tumors where they predominantly differentiate into ECs but do not form thick perivascular layers.....	72
AMD 3100 decreases the differentiation of BMCs into NG2 and desmin (+) pericytes in TC71 and A4573 tumors.....	74
AMD 3100 decreases the total NG2 and desmin ⁺ pericyte content in TC71 and A4573 Ewing's tumors.....	76
AMD3100 decreases PDGF-B expression in Ewing's sarcoma tumors.....	78
Summary.....	79
CHAPTER 7. AMD 3100 does not display a therapeutic effect in the treatment of primary Ewing's sarcoma tumors.....	80
Rationale.....	81
Results.....	83
AMD 3100 treatment leads to a trend towards decreased overall tumor volume in both TC71 and A4573 Ewing's tumors.....	83
AMD 3100 did not increase the survival of TC71 or A4573-tumor bearing mice...	85
Summary.....	87

CHAPTER 8. Appendix	89
The <i>pdgf-b</i> /pGL3 vector is functional.....	90
SDF-1 α induces the phosphorylation of the ELK-1 transcription factor at serine 383 with a peak at 30 minutes in TC/siVEGF ₇₋₁ cells.....	91
CHAPTER 9. Discussion and future directions.....	93
Discussion.....	94
SDF-1 α regulates PDGF-B by a transcriptional mechanism which involves the ELK-1 transcription factor.....	94
The SDF-1 α /PDGF-B pathway plays a critical role in BM-derived pericyte differentiation during vasculogenesis of Ewing's sarcoma.....	97
AMD 3100 as anti-vascular therapeutic agent.....	103
Conclusion.....	108
Future directions.....	110
Investigate the therapeutic effect of AMD 3100 on Ewing's sarcoma metastasis..	110
Investigate the possibility of a BM pre-metastatic niche in the lungs which could function to support Ewing's sarcoma metastasis post treatment with AMD3100..	111
Investigate the therapeutic effect of AMD 3100 in combination with DC101 anti- VEGFR-2 in Ewing's sarcoma.....	113
CHAPTER 10. Materials and Methods.....	115
Bibliography.....	129
Vita.....	141

List of figures

Figure 1. Bone marrow transplant model.....	5
Figure 2. Hypothesis.....	17
Figure 3. SDF-1 α up-regulates PDGF-B mRNA levels <i>in vitro</i>	22
Figure 4. SDF-1 α up-regulates PDGF-B protein levels.....	25
Figure 5. Down-regulating SDF-1 α decreases PDGF-B mRNA levels.....	28
Figure 6. SDF-1 α regulates PDGF-B expression via transcription.....	34
Figure 7. The ELK-1 transcription factor binds to <i>pdgf-b</i> promoter in response to SDF-1 α	39
Figure 8. ELK-1 is phosphorylated at S383 in response to SDF-1 α in HEK293 ChIP samples.....	41
Figure 9. Freshly isolated BMCs express the early pericyte marker PDGFR- β but do not express desmin and NG2 mature pericyte markers.....	48
Figure 10. 10T1/2 conditioned medium induces BMCs to differentiate into pericytes as defined by morphology and the expression of NG2 and desmin.....	50
Figure 11. BMCs cultured in 10T1/2-sh-SDF-1 conditioned medium do not differentiate into pericytes as defined by morphology and expression of NG2 and desmin.....	52
Figure 12. Tumor vessels are smaller with smaller lumens in response to AMD 3100 in both TC71 and A4573 Ewing's sarcoma tumors.....	59
Figure 13. The total microvessel density is decreased in response to AMD 3100 in both TC71 and A4573 Ewing's sarcoma tumors.....	61

Figure 14. AMD 3100 decreased the total amount of perfused vessels in both TC71 and A4573 Ewing's tumors.....	63
Figure 15. AMD 3100 increases apoptosis in both TC71 and A4573 Ewing's tumors.....	65
Figure 16. BMCs migrate to both TC71 and A4573 AMD 3100-treated tumors where they differentiate into ECs but do not form thick perivascular layers.....	73
Figure 17. AMD 3100 decreases the differentiation of BMCs into desmin and NG2 positive pericytes in both TC71 and A4573 Ewing's tumors.....	75
Figure 18. AMD 3100 decreases the total amount of desmin and NG2 pericytes in both TC71 and A4573 Ewing's tumors.....	77
Figure 19. AMD 3100 decreases PDGF-B expression in both TC71 and A4573 Ewing's tumors.....	78
Figure 20. AMD 3100 does not statistically decrease the final TC71 and A4573 tumor volumes compared to PBS.....	84
Figure 21. AMD 3100 did not increase the survival of TC71 and A4573 tumor-bearing mice.....	86
Figure 22. Summary.....	107
Figure A1. The <i>pdgf-b</i>/pGL3 construct is functional.....	90
Figure A2. The ELK-1 transcription factor is phosphorylated at S383 in response to SDF-1α stimulation in TC/siVEGF₇₋₁ cells.....	92

List of tables

Table 1. Forward and reverse primers.....	121
Table 2. Immunohistochemistry primary and secondary antibodies.....	126

Chapter 1.

Introduction

Ewing's sarcoma

Ewing's sarcoma is a member of the Ewing's sarcoma family of tumors (ESFT), an aggressive form of childhood cancer. While bone tumors account for about 5% of all childhood and adolescent cancers, Ewing's sarcoma is the second most common pediatric bone tumor after osteosarcoma (1, 2). Ewing's sarcoma tumors are more prevalent in males than females with a peak incidence in young adults around the age of 15. Although the tumors most commonly occur in bone, especially the pelvis, the long bones and the bones of the chest wall; the cancer can arise in any bone or soft tissue (2). ESFT display an aggressive behavior with a tendency towards recurrence following resection and are highly metastatic to the lungs (50%), bone (25%) and bone marrow (20%) (1-3).

Most patients with Ewing's sarcoma present with tumor-related symptoms such as pain and tumor mass and are diagnosed using biopsy, imaging and molecular DNA testing (1). In more than 85% of cases, patients with Ewing's sarcoma are characterized with the translocation and fusion of the *EWSR1* gene to the ETS family *FLI1* gene t(11;22)(q24;q12) resulting in the formation of the EWS/FLI1 protein (4). Additional translocations between the EWS gene and members of the ETS family of transcription factors have also been reported (*EWS/ERG* fusion) (2). While the role of the EWS/FLI1 gene has been established as a prognostic factor, the many implications of this fusion in the treatment plan and patient clinical outcome remains an area of investigation (4).

The current therapy regimen for patients with Ewing's sarcoma includes surgery, radiation therapy, and chemotherapy with surgery being the preferred method of local control (2). In cases where surgery is not possible due to the site or size of the tumor mass, then radiation therapy becomes the preferred treatment regimen (4). Most patients with

Ewing's sarcoma present with micrometastasis at the time of diagnosis or after the first round of therapy; therefore, despite a survival of about 65 – 75% in non-metastatic Ewing's sarcoma patients, patients with recurrent disease or metastasis at time of diagnosis still have only about 20 – 25% overall survival (5). The need for improvement in therapy is evident. Therefore, it becomes important for us to better understand the tumor biology and the role of the tumor microenvironment in supporting tumor growth in order to devise new therapeutic approaches.

Blood vessel development by vasculogenesis

Solid tumors are highly angiogenic; they depend on a vascular network for their growth, invasion and metastasis (6). While angiogenesis is the process by which new blood vessels form from pre-existing capillaries by vessel sprouting or endothelial budding (7), vasculogenesis is the process involving the migration and homing of bone marrow-progenitor cells (BMCs) from the bone marrow (BM) to the sites of neo-vascularization where they can participate in the blood vessel development (8, 9). Vasculogenesis was thought to be limited to early embryogenesis and not occur in adults. However, recent studies have shown that both angiogenesis and vasculogenesis contribute to embryonic development, adult wound healing and, tumor growth (8-11).

During embryonic development, vasculogenesis involves growth and fusion of multiple blood islands that ultimately give rise to the yolk sac capillary network. After the onset of blood circulation, this capillary network differentiates into an arteriovenous vascular system. While hematopoietic stem cells (HSCs) are situated in the center of the blood island and are destined to generate hematopoietic cells, endothelial progenitor cells (EPCs) or angioblasts are located at the periphery of the blood islands (9, 12).

In 1997, Asahara and his colleagues first reported the isolation of EPCs from human peripheral blood on the basis of cell surface expression of CD34 and other endothelial markers (12). In response to certain cytokines or tissue ischemia, BM-derived EPCs are increased in the systemic circulation. These cells home to, and incorporate into sites of neo-vascularisation (9, 12, 13).

The first evidence of BMC migration and incorporation into sites of tumor neo-angiogenesis was provided by Rafii and his colleagues in 2001. They showed that tumor did not form in the Id- (inhibitor of differentiation)-mutant mice. These mice cannot support neo-angiogenesis due to impaired vascular endothelial growth factor (VEGF) - driven mobilization of VEGFR2⁺ and impaired proliferation and incorporation of VEGFR1⁺ EPCs. However, transplantation of the Id-mutant mice with wildtype BMCs or VEGF-mobilized stem cells restored neo-angiogenesis and tumor growth (14). These findings demonstrated that vasculogenesis can be essential to tumor neo-vascularization.

Vasculogenesis in Ewing's sarcoma

Ewing's sarcoma tumors rely on an extensive vascular network for survival and growth (6, 15). We investigated the role of vasculogenesis in Ewing's sarcoma tumors and found that about 10% of the tumor vessels possess at least one BM-derived endothelial cell. CD34⁺ BM progenitor cells were shown to migrate from the BM to the tumor site and participate in the process of tumor neo-vascularization (10, 16). In order to further investigate the role of vasculogenesis in the Ewing's sarcoma tumor models, we needed a more efficient way of tracking BMC migration and infiltration into the tumor site. We therefore designed a bone marrow transplant model (BMT) in which GFP⁺ transgenic mice were used as donor mice, and nude mice were used as recipients.

Bone marrow transplant model

Nude mice (recipients) were submitted to whole body lethal irradiation to eradicate the existing BM constituents and then rescued by an intravenous injection of GFP⁺ BMCs collected from the donor transgenic mice. Engraftment was confirmed one month later by flow cytometry then, the mice received subcutaneous injections of the Ewing's sarcoma tumor cells. The Tumors were resected 2-3 weeks after tumor cell injection and analyzed by immunohistochemistry staining (IHC). If the mice or tumors were to receive any form of treatment, we administered the treatment once the tumors were palpable.

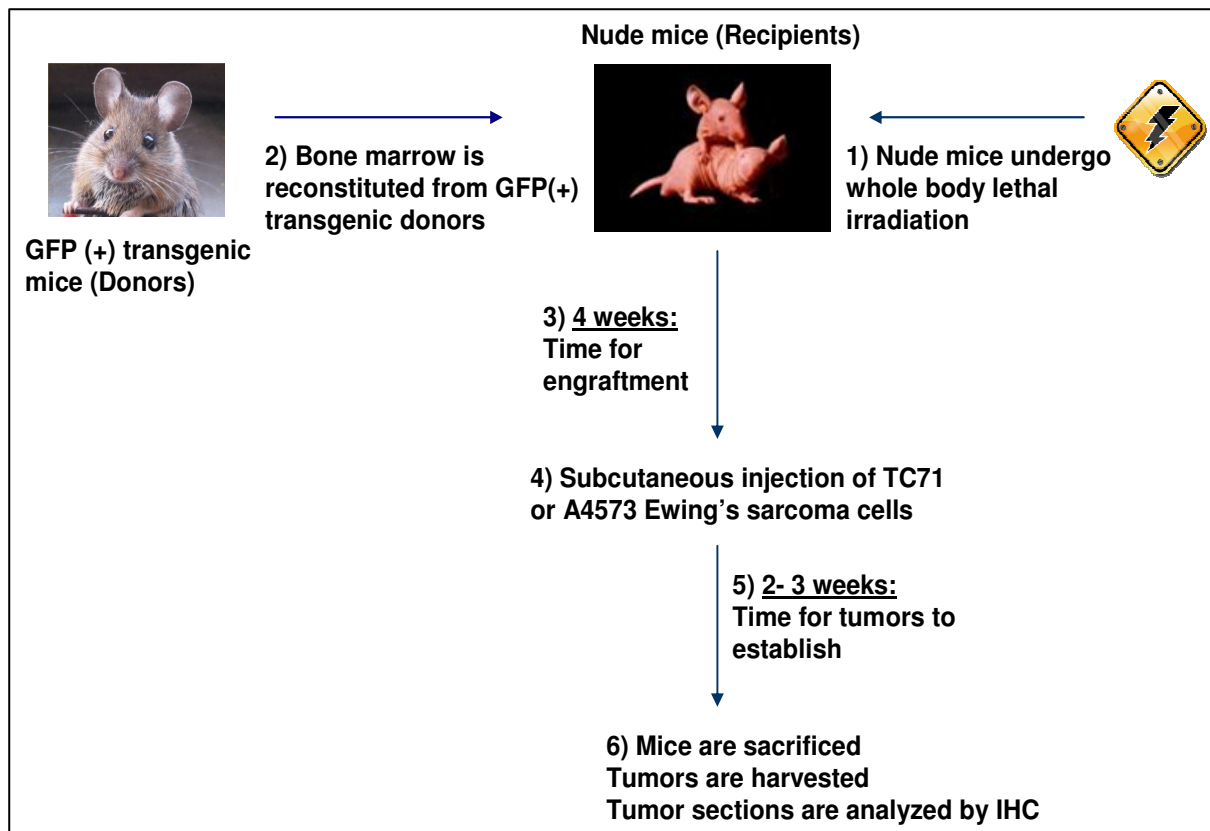


Figure 1. Bone marrow transplant model.

Vasculogenesis is essential for Ewing's sarcoma

To investigate whether BMCs and vasculogenesis was an essential process for Ewing's sarcoma tumor growth, we used the Mekk3-deficient conditional knockout mice. Mekk3⁻ BM cells cannot form vessels and therefore will not contribute to the tumor vessel development. Transplanting Mekk3-deficient BMCs into mice resulted in decreased tumor vessel density and tumor growth (17).

We also analyzed the different BMC sub-populations that support vasculogenesis of Ewing's sarcoma. We found that the human CD34⁺/CD45⁺ and CD34⁺/CD38⁻ cells, synonymous to the murine VEGFR2⁺ and Sca1⁺/Gr1⁺ cells, co-localized with the tumor vascular network, and differentiated into CD31⁺ or human vascular endothelial cadherin⁺ endothelial cells. These cell populations were also found to be in close proximity to the vessel wall, differentiating into desmin and alpha-smooth muscle actin (α -SMA) positive pericytes. The human CD34⁻/CD45⁺ population synonymous to the mouse Sca1⁻/Gr1⁺ cells, migrated predominantly to sites in the tumor paranchema outside of the tumor vasculature and differentiated into monocytes/macrophages expressing F4/80 or CD14 (18). All together, these findings demonstrated that vasculogenesis plays a critical role in the formation of Ewing's sarcoma tumor vessels.

The role of the vascular endothelial growth factor (VEGF₁₆₅) in vasculogenesis

We next investigated the mechanism by which BMCs migrated to the tumor site. Vascular endothelial growth factor (VEGF) is a very well characterized cytokine and its role in angiogenesis and tumor vessel remodeling has been extensively described (19-21). We analyzed several Ewing's sarcoma cell lines and patient samples for the expression of VEGF. We found that Ewing's sarcoma over-express VEGF and that there was a shift in

isoforms from the extracellular matrix-bound VEGF₁₈₉ isoform, to the smaller and more soluble VEGF₁₆₅ isoform (16, 22). Further studies confirmed that VEGF₁₆₅ stimulated BMC migration to the tumor and the tumor vessels (10, 16, 23).

To characterize the role of VEGF₁₆₅ in vasculogenesis of Ewing's sarcoma, we used an si-RNA specific for VEGF₁₆₅ and generated the TC/siVEGF₇₋₁ cell line with decreased VEG₁₆₅. Using our BMT model (Figure 1), we found that TC/siVEGF₇₋₁ tumors were smaller with decreased infiltration of BMCs into the tumor site and decreased vasculogenesis (24). Introducing VEGF₁₈₉ into TC/siVEGF₇₋₁ tumors did not rescue tumor growth or increase the tumor vessel density (25). These findings demonstrated that VEGF₁₆₅ was the chemotactic stimulus for BMC migration to the tumor site.

Stromal derived growth factor (SDF-1 α) and BMC chemotaxis

Chemokines are small highly charged molecules, secreted or membrane-bound, ranging from 6-14 kDa in size (26) . They are involved in a variety of immune reactions such as infection, inflammation and tissue repair (27). To date, there are more than fifty different chemokines that have been identified along with over twenty chemokine receptors that have been cloned (28). Chemokines are classified into four major classes based on the arrangement of the conserved cysteine (C) residues near the NH₂-terminus of the mature protein; the CXC or α -chemokine, the CC or β -chemokines, the C or γ -chemokines and, the CXXXXC or δ -chemokines (29). Chemokines bind to G-protein-coupled seven transmembrane receptors present on the surface of target cells; they can bind to multiple receptors and, the same receptor can bind to more than one chemokine (28).

The α -chemokine, stromal derived growth factor (SDF-1) has two main isoforms SDF-1 α and β , with SDF-1 α being the predominant isoform (26). SDF-1 α or CXCL12

binds specifically to the G-protein coupled receptor CXCR4 which can only bind to SDF-1 α (28). Recent studies suggested that SDF-1 α can also bind to the orphan receptor RDC1 also known as CXCR7; however, the signaling properties of this receptor remain unclear (30). The SDF-1 α chemokine is constitutively expressed. It is produced by multiple BM-stromal cell types and by the epithelial cells in several organs such as the liver, heart, lung, brain and bone marrow. Its receptor, CXCR4, is also expressed on the surface of many cell types including hematopoietic, endothelial, stromal and neuronal cells (31). SDF-1 α /CXCR4 knockout studies in mice are embryonic lethal and no SDF-1 α /CXCR4 deficiencies have been described in humans (28). In contrast, patients with a mutation leading to the activation of CXCR4 suffer from warts, hypogammaglobulinemia, immunodeficiency and myelokathesis (WHIM) syndrome (32).

The SDF-1 α /CXCR4 axis has been implicated in several biological processes. It is involved in homeostasis and functions to regulate hematopoietic cell trafficking and secondary lymphoid tissue architecture (31, 33). In adult life, SDF-1 α plays an important role in the retention and homing of BM progenitor cells to the BM (28, 34). SDF-1 α provides a chemotactic gradient for CXCR4 (+) BM progenitor cells and its implication in embryonic and adult postischemia and tumor angiogenesis has been extensively described (35-37).

SDF-1 α partially rescues vasculogenesis in VEGF₁₆₅-inhibited TC/siVEGF₇₋₁ Ewing's sarcoma tumors

The expression of various angiogenic growth factors such as VEGF and b-FGF is enhanced during tumor development and play a critical role in tumor blood vessel development (35). The SDF-1 α serum levels have been shown to become elevated in

response to ischemia and tumor growth and induce the mobilization of mature and immature hematopoietic progenitor and stem cells into the peripheral blood (38). Furthermore, a study by Gabriele Bergers and colleagues in 2008 demonstrated that HIF-1 α , a direct effector of hypoxia, induced the recruitment of BM-progenitor myeloid cells, as well as endothelial and pericyte progenitor cells to sites of neo-vascularization in glioblastoma tumors through increases in SDF-1 α (39).

As previously described, findings from our lab demonstrated that vasculogenesis plays a critical role in Ewing's sarcoma growth and that VEGF₁₆₅ is the chemotactic factor for BMC migration to the site of neo-vascularization (10, 16). Inhibiting VEGF₁₆₅ in TC71 tumors (TC/siVEGF₇₋₁), decreased infiltration of BMCs into the tumor site, decreased vasculogenesis and inhibited tumor growth. We analyzed SDF-1 α expression in TC/siVEGF₇₋₁ tumors and found that inhibiting VEGF₁₆₅ also decreased SDF-1 α (24, 40).

Given the role of SDF-1 α as a chemotactic factor for BM-progenitor cells, we introduced SDF-1 α into the TC/siVEGF₇₋₁ tumors using an adenoviral vector containing the SDF-1 α gene (Ad-SDF-1 α) to determine if BMCs could rescue tumor growth in the absence of VEGF₁₆₅. We found that SDF-1 α restored the infiltration of BMCs into the tumor site, increased tumor vessel density and, enhanced the growth of TC/siVEGF₇₋₁ tumors (31, 40, 41). SDF-1 α , while having no effect on VEGF₁₆₅ expression, induced the infiltration of BMCs predominantly to the perivascular area. Immunohistochemistry analysis (IHC) demonstrated that the majority of these BMCs differentiated into pericytes or vascular smooth muscle cells (vSMCs) (40). These findings once again emphasized the critical role of BMCs and the process of vasculogenesis in Ewing's sarcoma tumor growth. Furthermore, our data suggested a correlation between SDF-1 α and BM-derived pericyte

maturation and indicated a critical role for these BM-derived pericytes in supporting tumor neo-vascular development and tumor growth.

Pericytes/vascular smooth muscle cells (vSMCs)

Small blood vessels such as capillaries have two types of cell layers, the inner lining of the vessel wall composed of endothelial cells (EC) and the surrounding perivascular layer of cells, referred to as pericytes, vascular smooth muscle cells or mural cells which envelop the surface of the vascular tube. Both layers together form the basement membrane of microvessels (42). Pericytes were identified over a 100 years ago by Charles Rouget and are referred to as vascular smooth muscle cells (vSMCs) because of their contractile filaments (43). Pericytes possess a cell body with a prominent nucleus, a small amount of cytoplasm, and long processes that embrace several endothelial cells at once or extend to more than one capillary. Pericytes communicate with endothelial cells by direct physical contact and/or through paracrine signaling pathways (42).

Pericytes/vSMCs vary in location and have diverse characteristics and functions (42). They regulate vascular diameter and capillary blood flow by vasoconstriction and vasodilatation of the capillary beds. Pericytes are described as multipotent mesenchymal cells. They have been shown to be precursors to SMCs capable of becoming adipocytes, osteoblasts and phagocytes. Majno and colleagues first demonstrated the role of pericytes as phagocytes using electron microscopy. Several other studies since have described the importance of pericytes as phagocytes or precursors to macrophages in the brain (43-45). Pericytes have also been shown to regulate capillary growth. During wound healing, pericytes can either form from pre-existing microvessels or come into contact with ECs that

are forming new vessels to exert an inhibitory effect on EC proliferation and regulate vessel growth (46).

Pericytes are derived from mesenchymal stem cells. It remains unclear whether pericytes are smooth-muscle cells or cells with smooth-muscle-cell characteristics and whether these cells even have a distinct progenitor. Therefore, it is very common for pericytes to be referred to as vascular smooth muscle cells. Defining a pericyte remains a challenge; no general pan-pericyte molecular marker has yet been found. Currently, a few molecular markers, although not exclusive to pericytes, have been used for the identification of these cells. Depending on the tissue and developmental or angiogenic state of a blood vessel, the expression pattern of pericyte markers can vary. The most commonly used markers are desmin and alpha smooth muscle actin α -SMA, (contractile filaments), regulator of G protein signaling 5 RGS-5, (a GTPase- activating protein), neuron-gial 2 NG2, (a chondroitin sulfate proteoglycan) and platelet-derived growth factor receptor beta PDGFR- β , (a tyrosine kinase receptor) (42).

The role of pericytes in tumor vessel development

Pericytes are found as a single-cell layer or as a solitary cell in close association with ECs in the normal vasculature. Both ECs and pericytes are embedded within the basement membrane of capillaries where pericytes communicate with ECs or other components of the vessel wall to prevent vessel leakage (47). Although the vasculature remains quiescent and angiogenesis is an infrequent event in the normal adult, the latter still occurs during wound healing or pathological conditions such as diabetic retinopathy and tumor growth. However, the difference between normal physiological angiogenesis and

pathological angiogenesis lies in the imbalance between the positive and negative regulators being expressed in the microenvironment (42).

During tumor growth, the hypoxic nature of the microenvironment leads to vasodilatation, increased vascular permeability and degradation of the vascular basement membrane. As a result, the strong and quiescent association between ECs and pericytes is destabilized, leakage is increased and tumor vessels appear to be in a constant state of remodeling. All together, these dynamic changes lead to vessels that are chaotic, poorly organized, tortuous and irregularly shaped (42, 47).

Tumor vessels as well as pericyte coverage are different depending on the tumor type. In general, pericytes within tumors are less abundant and more loosely attached to the vessel wall with cytoplasmic structures that can extend deep within the surrounding tumor tissue. Until recently, pericytes have been considered abnormal and dysfunctional in tumors and therefore, they have been neglected as potential targets for anti-vascular therapy (42). However, recent studies have demonstrated that although pericytes are present in a smaller number within tumors, targeting pericytes in addition to endothelial cells, resulted in more efficient reduction in tumor vasculature than targeting one or the other alone (48).

The above findings, combined with our observations that SDF-1 α gene therapy increased the infiltration and differentiation of BMCs into pericytes/vSMCs within TC/siVEGF₇₋₁ tumors and subsequently rescued tumor growth, emphasize the importance of pericytes as functional cell-components of the tumor vasculature which promote tumor growth. These cells therefore may be a potential target for anti-angiogenic therapy.

Platelet derived growth factor B (PDGF-B) is critical for pericyte maturation

Platelet derived growth factor B (PDGF-B) is a member of the PDGF family of growth factors which are mitogens for many cells of mesenchymal origin including fibroblasts and smooth muscle cells and for some cell populations of neuroectodermal origin. The PDGF family is composed of four different polypeptide chains PDGF-A, B, C and D. These four polypeptides are encoded by four different genes and can form homo or heterodimers. The ligands can bind the two tyrosine kinase receptors, PDGFR- α and PDGFR- β . When synthesized and secreted in its homodimer form, PDGF-BB binds to its tyrosine kinase receptor, PDGFR- β (49).

PDGF-B and PDGFR- β are mainly expressed in the developing vasculature, where PDGF-B is produced by the endothelial cells and PDGFR- β is expressed by mural cells such as pericytes and vSMCs (50). The role of PDGF-B and PDGFR- β in the maturation process of pericytes has been extensively described. Blocking the signaling through the PDGF-B/PDGFR- β pathway leads to pericyte loss and to endothelial changes followed by capillary dilation and rupture (51, 52).

The role of PDGF-B in pericyte maturation during tumor growth

The expression of PDGF-B is normally restricted to a limited number of cell types. However, many cancers including colorectal cancer, pancreatic cancer, glioma, and sarcoma, have been shown to over-express PDGF-B (53, 54). PDGF-B is produced by the tumor endothelium and is required for the recruitment of an adequate number of PDGFR- β^+ pericytes to the tumor vessels and their integration in the vascular wall (55). Studies by Rajantie and colleagues reported the detection of BM-derived periendothelial vascular mural cells at sites of tumor growth (56). Shortly after, another study by Gabriele Bergers

and her group reported the discovery of PDGFR- β -expressing pericyte progenitor cells (PPPs) which possess the capacity to differentiate into NG2 (+), desmin (+) and, alpha-smooth muscle actin (+) pericytes within tumors (57).

On the other hand, inhibiting PDGFR- β in a mouse model of pancreatic cancer was found to deplete tumor pericytes and to induce their detachment from the vascular endothelium which resulted in blood vessel hyperdilation and disruption (48). Another study using the novel DNA oligonucleotide aptamer (AX102) that selectively binds PDGF-B showed that inhibiting PDGF-B in Lewis lung carcinomas reduced pericyte coverage and tumor vascularity (58).

A link between pericyte maturation and PDGF-B in Ewing's sarcoma

Previous findings from our lab demonstrated that treating VEGF₁₆₅ inhibited Ewing's sarcoma tumors, TC/siVEGF₇₋₁, with an adenoviral vector containing the SDF-1 α gene (Ad-SDF-1 α) partially restored vasculogenesis with infiltration of BMCs predominantly to a perivascular area where they differentiated into pericytes/vSMCs and, rescued tumor growth. Given the critical role of PDGF-B in pericyte maturation, RNA was extracted from the Ad-SDF-1 α treated tumors and analyzed for PDGF-B mRNA expression. We found that SDF-1 α gene therapy increased PDGF-B mRNA levels in TC/siVEGF₇₋₁ tumors (40). These findings suggested a correlation between SDF-1 α , PDGF-B and BM-derived pericyte differentiation during vasculogenesis of Ewing's sarcoma.

The ELK-1 transcription factor

The ELK-1 nuclear transcription factor, a member of the three ternary complex factors (TCFs), is one of the 30 or more members of the ETS (E twenty-six) family of

transcription factors. All family members share a conserved ~ 85 amino acid DNA-binding domain, termed the ETS domain that directs binding to recognition sites containing GGA cores. ETS proteins are important mediators of growth-regulating and differentiation signaling pathways. Particularly, ETS proteins are effectors of growth factor signaling pathways involving RAS/MAPK-dependent signaling (59, 60). Recent evidence suggests that ELK-1 is a target of all three classes of MAP kinases ERK, JNK, and p38 MAPK and functions as a nuclear transcriptional activator (61). TCFs are involved in several biological processes and have been shown to be important in regulating angiogenesis and vasculogenesis (62, 63).

SDF-1 α activates ELK-1

Signaling through the SDF-1 α /CXCR4 pathway initiates a cascade of several signal transduction pathways linked to transcription and expression through MEK1/2 and ERK1/2. ERK can then phosphorylate and activate other cellular proteins as well as translocate to the nucleus, phosphorylate and/or, activate transcription factors (33). Binding of SDF-1 α to CXCR4 induces phosphorylation of the mitogen-activated protein kinases (MAPKs) p44 ERK-1 and p42 ERK-2, which subsequently initiates the phosphorylation of several downstream transcription factors including the nuclear transcription factor ELK-1 (64).

Altogether, these findings and observations suggested a link between SDF-1 α signaling and PDGF-B expression involving the ELK-1 transcription factor and a role for the SDF-1 α /PDGF-B pathway in BM-derived pericyte differentiation during vasculogenesis of Ewing's sarcoma.

Hypothesis

To summarize, we know that

- 1) BMCs migrate to VEGF₁₆₅-inhibited TC/siVEGF₇₋₁ Ewing's sarcoma tumors in response to SDF-1 α and differentiate into pericytes/vSMCs
- 2) PDGF-B mRNA levels are up-regulated in TC/siVEGF₇₋₁ tumors by SDF-1 α with no effect on VEGF₁₆₅
- 3) PDGF-B is critical for pericyte maturation
- 4) SDF-1 α signaling can activate the ELK-1 transcription factor, a member of the ETS family of transcription factors

We therefore formulated the following hypothesis that **SDF-1 α up-regulates the expression of PDGF-B via a transcriptional mechanism involving the ELK-1 transcription factor and in turn, PDGF-B induces the differentiation of bone marrow progenitor cells into pericytes during vasculogenesis of Ewing's sarcoma.**

\

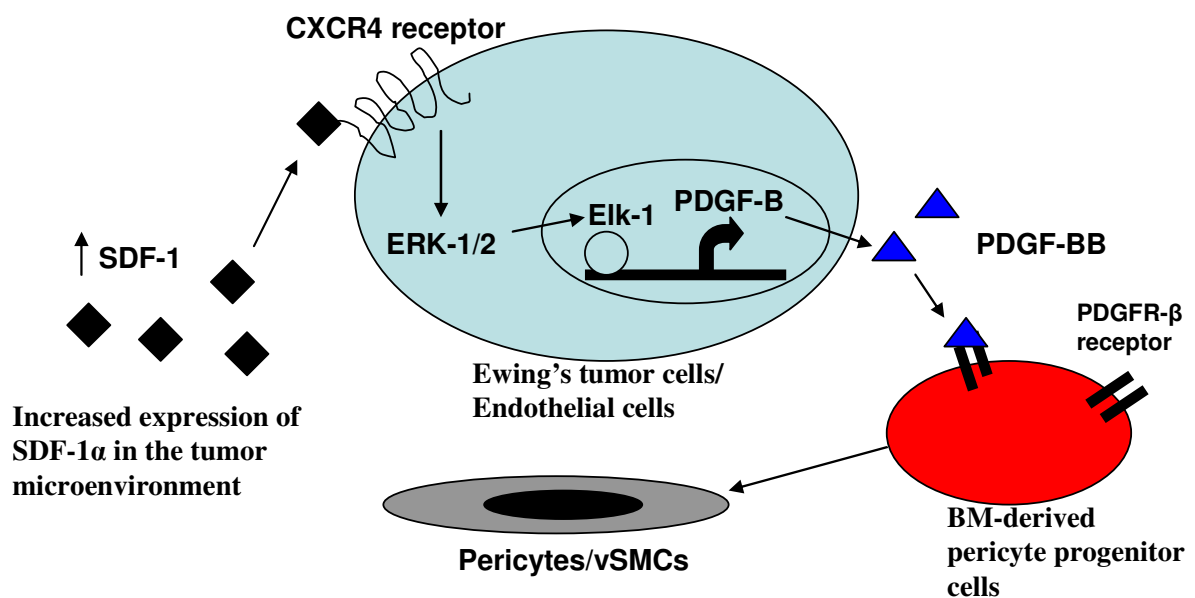


Figure 2. Hypothesis. SDF-1 α expression is increased in the tumor microenvironment, binds to its receptor CXCR4 expressed on either tumor cells or endothelial cells and, induces the ERK-1/2 (MAPKs) signaling cascade which activates the ELK-1 transcription factor. ELK-1 binds to the PDGF-B promoter and activates the expression and secretion of the PDGF-BB protein. PDGF-BB then binds to its PDGFR- β receptor expressed on pericyte progenitor cells and induces their differentiation into mature pericytes.

Chapter 2.

SDF-1 α regulates PDGF-B expression *in vitro* and *in vivo*

Rationale

We previously demonstrated that vasculogenesis is essential for Ewing's sarcoma growth and that VEGF₁₆₅ is the chemotactic stimulus for bone marrow cell (BMC) migration to the tumor site. In fact, inhibiting VEGF₁₆₅ in TC71 Ewing's sarcoma tumors (TC/siVEGF₇₋₁) inhibited both BMC infiltration into the tumor and tumor growth (16, 24, 25, 65). However, introducing stromal derived growth factor (SDF-1 α) into TC/siVEGF₇₋₁ tumors using an adenoviral vector containing the SDF-1 α gene (Ad-SDF-1 α), increased infiltration of BMCs to a perivascular area where they differentiated into pericytes/vSMCs and, partially rescued tumor growth. RNA collected from the Ad-SDF-1 α treated TC/siVEGF₇₋₁ tumors also showed an increase in platelet derived growth factor B (PDGF-B) mRNA levels (40). These observations suggested a correlation between SDF-1 α and PDGF-B expression.

PDGF-B is a member of the PDGF family of growth factors which have been described as mitogens for cells of mesenchymal origin such as fibroblasts and smooth muscle cells (49, 53). PDGF-B binds to its tyrosine kinase receptor PDGFR- β and both proteins are mainly expressed in the developing vasculature (51, 66). PDGF-B expression has been shown to be up-regulated in tumors, especially the ones established from sarcoma and glioma (54, 66). However, the mechanism by which PDGF-B expression is up-regulated during vascular remodeling remains unclear.

In this section, we investigated SDF-1 α as a regulator of PDGF-B expression. We first confirmed up-regulation of PDGF-B protein levels *in vivo* in the Ad-SDF-1 α treated TC/siVEGF₇₋₁ tumors by IHC. We then treated both the TC/siVEGF₇₋₁ and HEK293 cells

with the recombinant human SDF-1 α protein and demonstrated that SDF-1 α up-regulated PDGF-B mRNA and protein levels *in vitro* using real time PCR (qPCR) and enzyme linked immunosorbent assay (ELISA). By contrast, an shRNA specific for SDF-1 α which down-regulated SDF-1 α mRNA and protein levels also down-regulated PDGF-B. We are the first to demonstrate that SDF-1 α regulates PDGF-B expression.

Results

SDF-1 α up-regulates PDGF-B mRNA levels *in vitro*

We previously demonstrated that treating VEGF₁₆₅-inhibited TC/siVEGF₇₋₁ tumors with an adenoviral vector containing the SDF-1 α gene (Ad-SDF-1 α) in order to up-regulate SDF-1 α expression also up-regulated PDGF-B mRNA levels (40). To confirm that SDF-1 α up-regulates PDGF-B mRNA *in vitro*, we used both the TC/siVEGF₇₋₁ and the HEK293 cell lines which express low levels of endogenous PDGF-B. The cells were plated in the absence of growth factors and supplements for 8 hours and then treated with 100ng/ml of either the recombinant human SDF-1 α protein or the 9SDF-1 α inactive protein for 24 hours. Total RNA was collected and the PDGF-B mRNA levels were quantified using q-PCR. SDF-1 α up-regulated PDGF-B mRNA levels compared to 9SDF-1 α in both TC/siVEGF₇₋₁ and HEK293 cells (Figure 3).

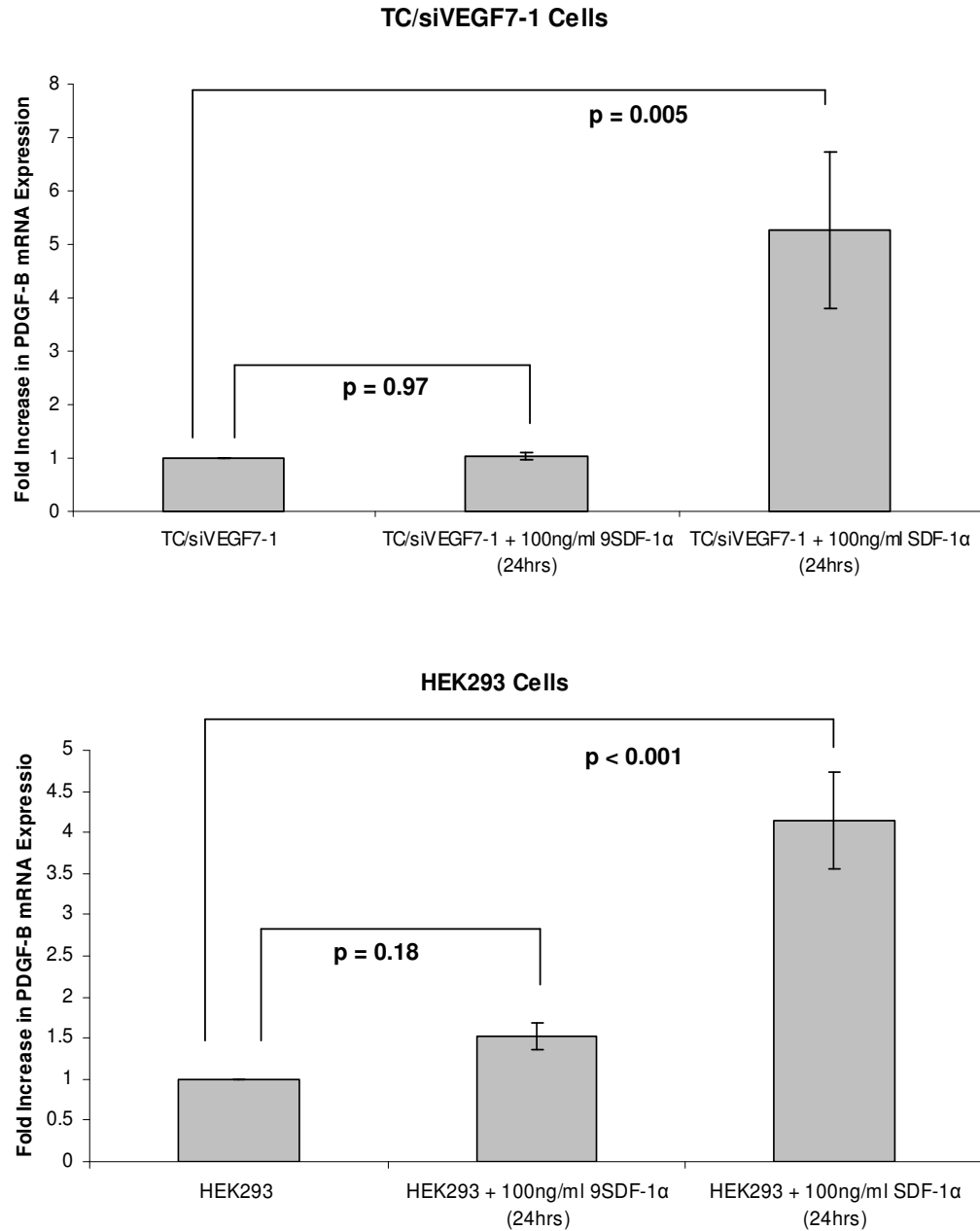


Figure 3. SDF-1 α up-regulates PDGF-B mRNA levels *in vitro*. TC/siVEGF₇₋₁ and HEK293 cells were plated in the absence of growth factors and supplements for 8 hours and then treated with 100ng/ml of either SDF-1 α or the 9SDF-1 α inactive protein for 24 hours. RNA was collected and analyzed by q-PCR for the expression of PDGF-B. Bar graph shows pooled data from 3 independent experiments each performed in triplicate. $P < 0.05$ was considered significant. SDF-1 α up-regulates PDGF-B mRNA levels compared to 9SDF-1 α .

SDF-1 α up-regulates PDGF-B protein levels *in vitro* and *in vivo*

To demonstrate that SDF-1 α up-regulates PDGF-B protein levels *in vitro*, TC/siVEGF₇₋₁ and HEK293 cells were plated in the absence of growth factors and supplements for 8 hours and then treated with 100ng/ml of either the recombinant human SDF-1 α protein or 9SDF-1 α inactive protein for 36 hours. Since the ~27kD PDGF-B protein is a secreted protein, the PDGF-B protein levels were quantified using ELISA. SDF-1 α up-regulated PDGF-B protein levels compared to 9SDF-1 α in both TC/siVEGF₇₋₁ and HEK293 cells (Figure 4A).

In order to analyze the effect of SDF-1 α on PDGF-B protein levels *in vivo*, PDGF-B protein levels were analyzed in the Ad-SDF-1 α versus the Ad-control-treated TC/siVEGF₇₋₁ tumors. Briefly, TC/siVEGF₇₋₁ tumors received 5 intratumoral injections of either Ad-SDF-1 α or Ad-control over a period of 3 weeks. The tumors were then resected, snap frozen in OCT and, stored at - 80°C for further analysis by IHC. Tumor sections were obtained and analyzed by IHC for PDGF-B protein expression (brown staining). Ad-SDF-1 α up-regulated PDGF-B protein levels compared to Ad-control in TC/siVEGF₇₋₁ tumors (Figure 4B).

Figure 4A. ELISA assay to quantify PDGF-B protein levels

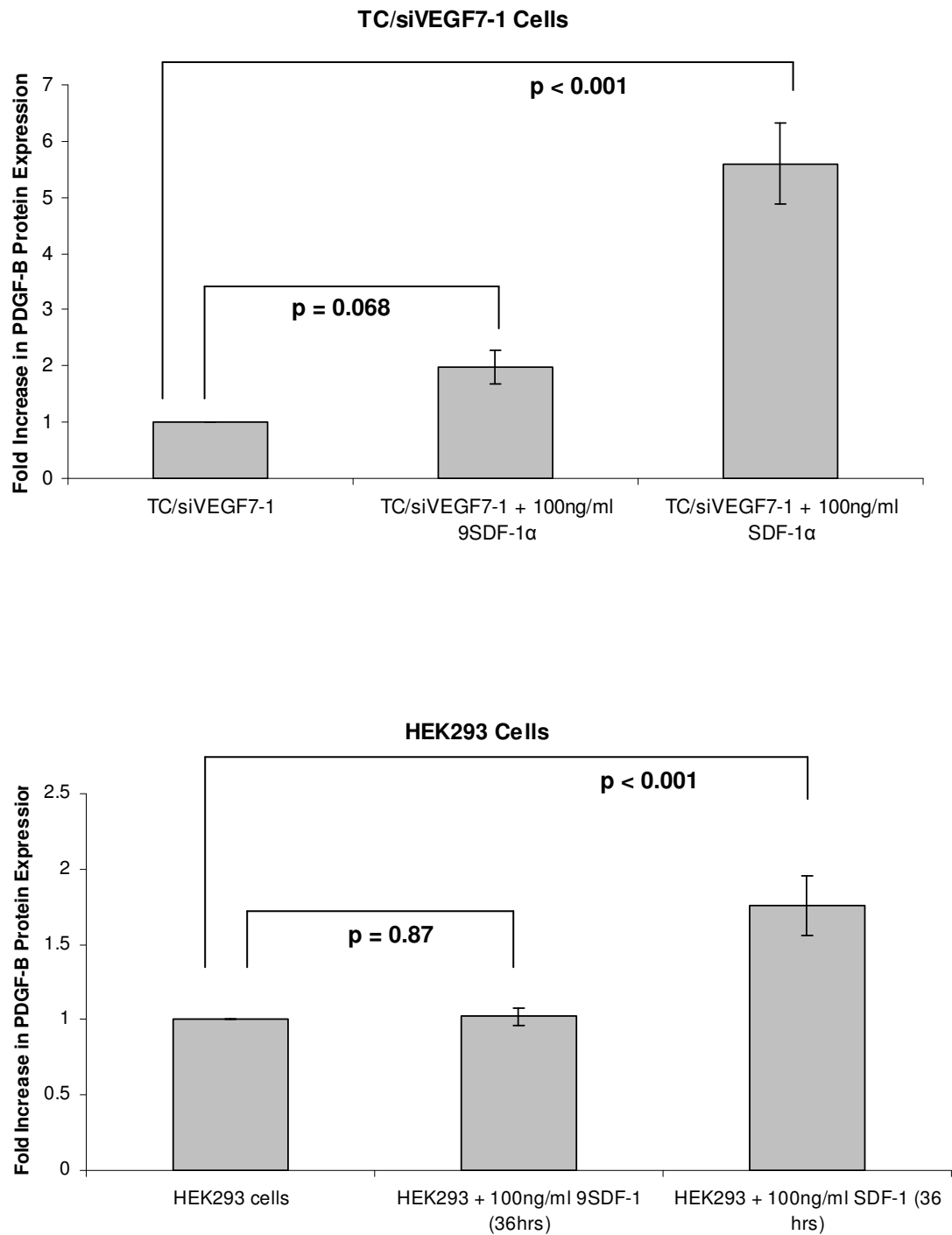


Figure 4B. Immunohistochemistry staining to detect PDGF-B protein expression in Ad-SDF-1 α -treated TC/siVEGF₇₋₁

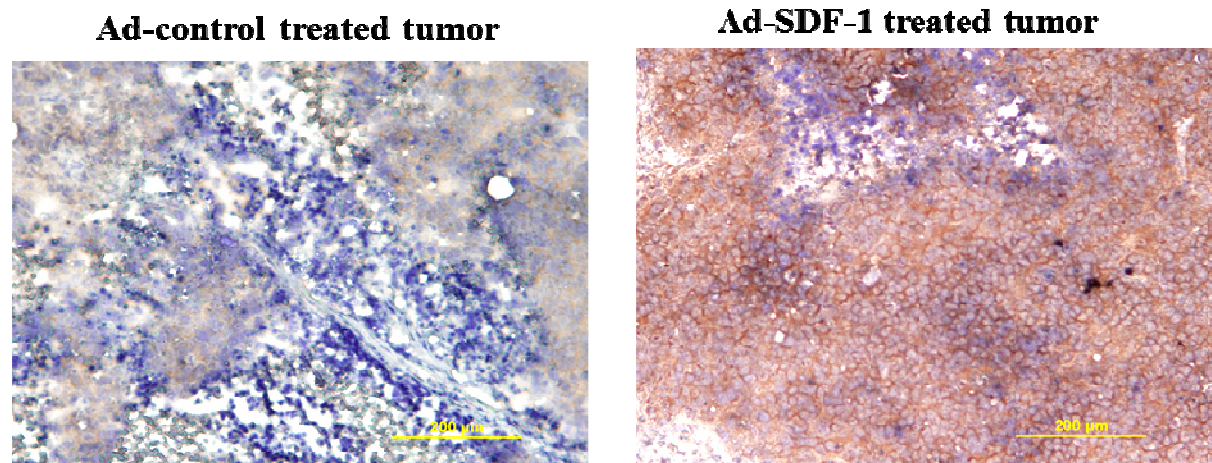


Figure 4. SDF-1 α up-regulates PDGF-B protein levels. A) ELISA assay for the PDGF-B protein. TC/siVEGF₇₋₁ and HEK293 cells were plated in the absence of growth factors and supplements for 8 hours and then treated with 100ng/ml of either SDF-1 α or the 9SDF-1 α inactive protein for 36 hours. The supernatant was collected, concentrated and, the ~ 27kD soluble PDGF-B protein levels quantified by ELISA. Bar graph shows pooled data from three independent experiments each performed in triplicate. $P < 0.05$ was considered significant. **B) IHC for PDGF-B protein.** TC/siVEGF₇₋₁ tumors were injected 5 days following tumor cell inoculation with either Ad-SDF-1 α or Ad-control twice weekly for 3 weeks. On day 23, the tumors were resected and tumor sections were cut, fixed and analyzed for expression of PDGF-B (brown staining). Ad-SDF-1 α up-regulates PDGF-B protein levels compared to Ad-control both in vitro and in vivo.

Down-regulating SDF-1 α down-regulates PDGF-B expression

To further confirm that SDF- α regulates the expression of PDGF-B, an shRNA plasmid specific for SDF-1 α (shSDF-1 α) was used to down-regulate SDF-1 α mRNA and protein levels in C3H/10T1/2 (10T1/2) mouse mesenchymal-like cells and to look for its effect on PDGF-B. 10T1/2 cells, which endogenously express SDF-1 α and PDGF-B, were transfected with 1 μ g of either the shSDF-1 α or shcontrol plasmid and maintained under puromycin selection (2 μ g/mL) for the duration of the experiments. Using PCR, qPCR (Figure 5A and B) and ELISA (Figure 5C), down-regulation of SDF-1 α mRNA and protein levels in 10T1/2 cells transfected with either shSDF-1 α (10T1/2-sh-SDF-1 α) or shcontrol (10T1/2-sh-control) was quantified. We found that down-regulating SDF-1 α expression in 10T1/2 cells also down-regulated PDGF-B mRNA levels (Figure 5A and B).

Figure 5A. PCR to detect SDF-1 α and PDGF-B mRNA

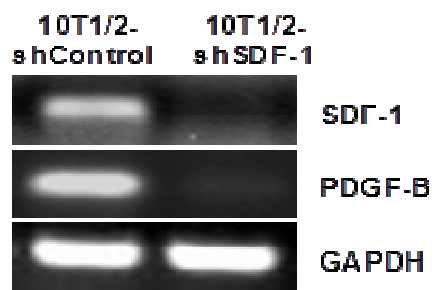


Figure 5B. qPCR to confirm SDF-1 α and PDGF-B mRNA down-regulation

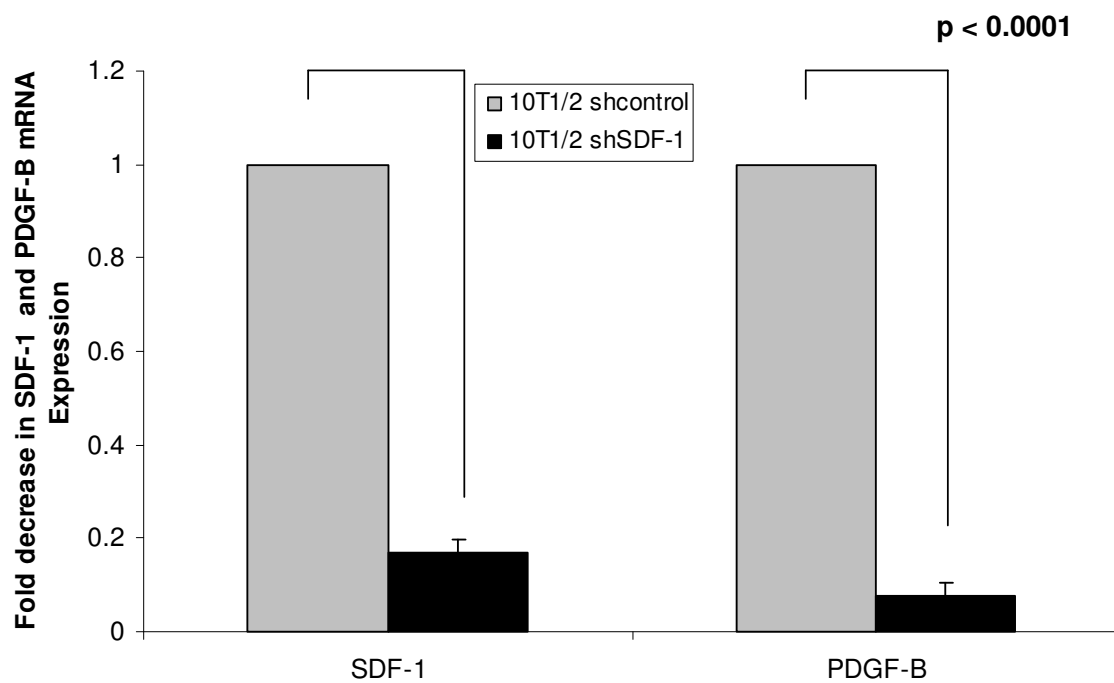


Figure 5C. ELISA assay to confirm down-regulation of SDF-1 α protein levels

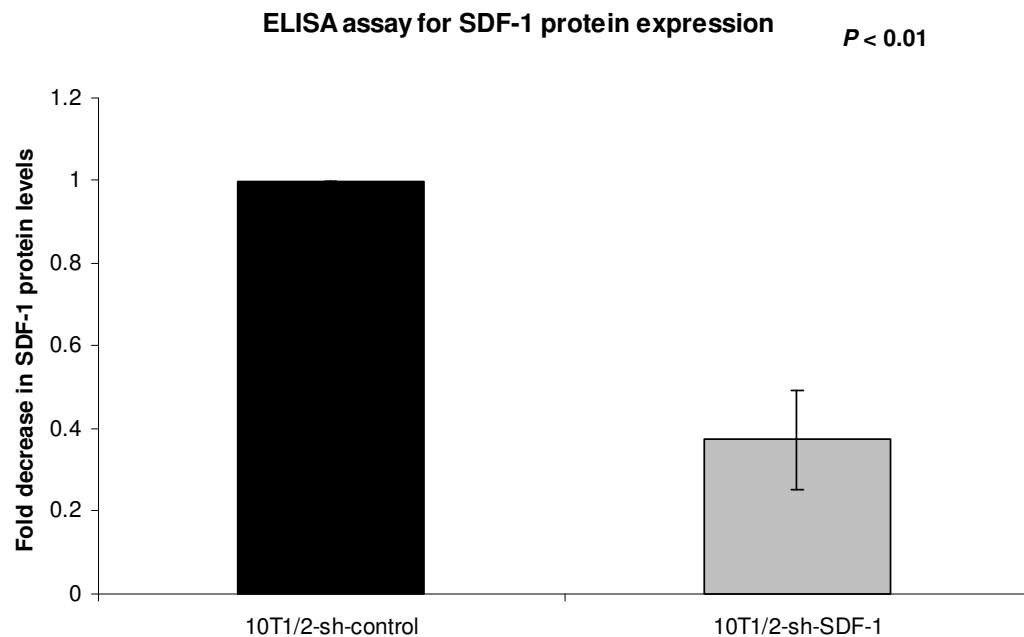


Figure 5. Down-regulating SDF-1 α decreases PDGF-B mRNA levels. 10T1/2 cells were transfected with 1 μ g shSDF-1 α (10T1/2-sh-SDF-1) or shcontrol (10T1/2-sh-control) using FuGENE 6 and maintained under puromycin selection for the duration of the experiments. SDF-1 α and PDGF-B mRNA levels were analyzed and quantified by (A) PCR and (B) qPCR. SDF-1 α and PDGF-B mRNA levels were down-regulated in 10T1/2-shSDF-1 compared to 10T1/2-shcontrol. (C) Supernatant from either 10T1/2-sh-SDF-1 or 10T1/2-sh-control was collected, concentrated and, analyzed by ELISA. Bar graph shows pooled data from three independent experiments each performed in triplicate. $P < 0.05$ was considered significant. SDF-1 α protein levels are down-regulated in 10T1/2-shSDF-1 compared to 10T1/2-shcontrol.

Summary

We previously demonstrated that treating TC/siVEGF₇₋₁ tumors with Ad-SDF-1 α up-regulated PDGF-B mRNA levels (40). In this section, we investigated the role of SDF-1 α as a regulator of PDGF-B expression both *in vitro* and *in vivo*.

We treated both the TC/siVEGF₇₋₁ and HEK293 cells with either the recombinant human SDF-1 α or the inactive 9SDF-1 α protein and found that SDF-1 α up-regulated PDGF-B mRNA and protein levels *in vitro*. To confirm that SDF-1 α also up-regulated PDGF-B protein levels *in vivo*, tumor sections from the Ad-SDF-1 α treated tumors were stained for PDGF-B. We found that SDF-1 α up-regulated PDGF-B protein levels *in vivo*. In contrast, we used an shRNA plasmid specific for SDF-1 α and down-regulated SDF-1 α mRNA and protein levels in 10T1/2 cells. We found that down-regulating SDF-1 α also down-regulated PDGF-B.

Many cancers, including colorectal cancer, pancreatic cancer, glioma, and sarcoma, overexpress PDGF-B (53). However, the mechanism by which PDGF-B is up-regulated remains unclear. Studies by Onimaru and colleagues demonstrated that VEGFC can regulate vascular stabilization by controlling PDGF-B expression (67). In the current study, we are the first to demonstrate the SDF-1 α regulates PDGF-B. These findings illustrate the importance of SDF-1 α in the tumor microenvironment not only as a chemotactic factor for BMC migration, but also, as a regulator of other angiogenic factors such as PDGF-B which are critical for tumor blood vessel development.

Chapter 3.

SDF-1 α regulates PDGF-B via a transcriptional mechanism which involves binding of the ELK-1 transcription factor to the *pdgf-b* promoter

Rationale

Stromal derived growth factor (SDF-1 α) binds to its 7-transmembrane G-protein coupled receptor CXCR4 expressed on the surface of cells. Once SDF-1 α binds to CXCR4, several down-stream signaling pathways linked to transcription and expression through the MEK1/2 and ERK1/2 are induced. ERK can then phosphorylate and activate other cellular proteins as well as translocate to the nucleus and phosphorylate and /or activate transcription factors such as the ELK-1 transcription factor (64, 68). The ELK-1 nuclear transcription factor is a member of the three ternary complex factors (TCFs), a subfamily of the E twenty-six (Ets) domain transcription factors. TCFs are involved in several biological processes and have been shown to be important in regulating angiogenesis and vasculogenesis (59, 62, 63).

PDGF-B expression has been shown to be over-expressed in several cancers such as sarcomas and gliomas (53, 54). However, the mechanism by which PDGF-B is up-regulated during vascular remodeling remains unclear. In the previous section, we demonstrated that SDF-1 α regulates PDGF-B expression both *in vitro* and *in vivo*. Since PDGF-B is regulated via several mechanisms, including transcriptional regulation (60), we investigated whether SDF-1 α regulates PDGF-B via a transcriptional mechanism and whether this regulation involves binding of the ELK-1 transcription factor to the *pdgf-b* promoter.

We cloned the 2kb *pdgf-b* promoter into the pGL3 luciferase reporter vector (*pdgf-b*/pGL3) and showed that SDF-1 α activates the *pdgf-b* promoter in both the TC/siVEGF₇₋₁ and HEK293 cell lines. We then used the GeneRegulation.com software and identified

potential ELK-1 binding sites. 3 sites which scored above 85% were investigated at -600 bp, and the transcription start site (TS) within the *pdgf-b* promoter and, at +1 Kb within the transcribed region. We used chromatin immunoprecipitation and showed that ELK-1 binds to the *pdgf-b* promoter at the -600 bp site with a peak at 30 minutes after SDF-1 α stimulation in both the TC/siVEGF₇₋₁ and HEK293 cell lines. In contrast, ELK-1 did not bind to the TS site in either cell lines while it bound to the + 1Kb site only in the TC/siVEGF₇₋₁ cells. We are the first to demonstrate that SDF-1 α regulates PDGF-B via a transcriptional mechanism which involves binding of the ELK-1 transcription factor to the *pdgf-b* promoter.

Results

SDF-1 α regulates PDGF-B expression via transcription

To demonstrate that SDF-1 α regulates the expression of PDGF-B via a transcriptional mechanism, both the TC/siVEGF₇₋₁ and HEK293 cell lines were transfected with 50ng/mL of either the *pdgf-b*/pGL3 construct we generated or the pGL3 control vector for 48 hours. The cells were then plated in the absence of growth factors and supplements for 24 hours and treated with 100ng/ml of either the human recombinant SDF-1 α or the 9SDF-1 α inactive protein for 8 hours. The cells were lysed and the luciferase signal was measured and quantified to analyze *pdgf-b* promoter activity. SDF-1 α activated the *pdgf-b* promoter compared to 9SDF-1 α in both TC/siVEGF₇₋₁ and HEK293 cells (Figure 6).

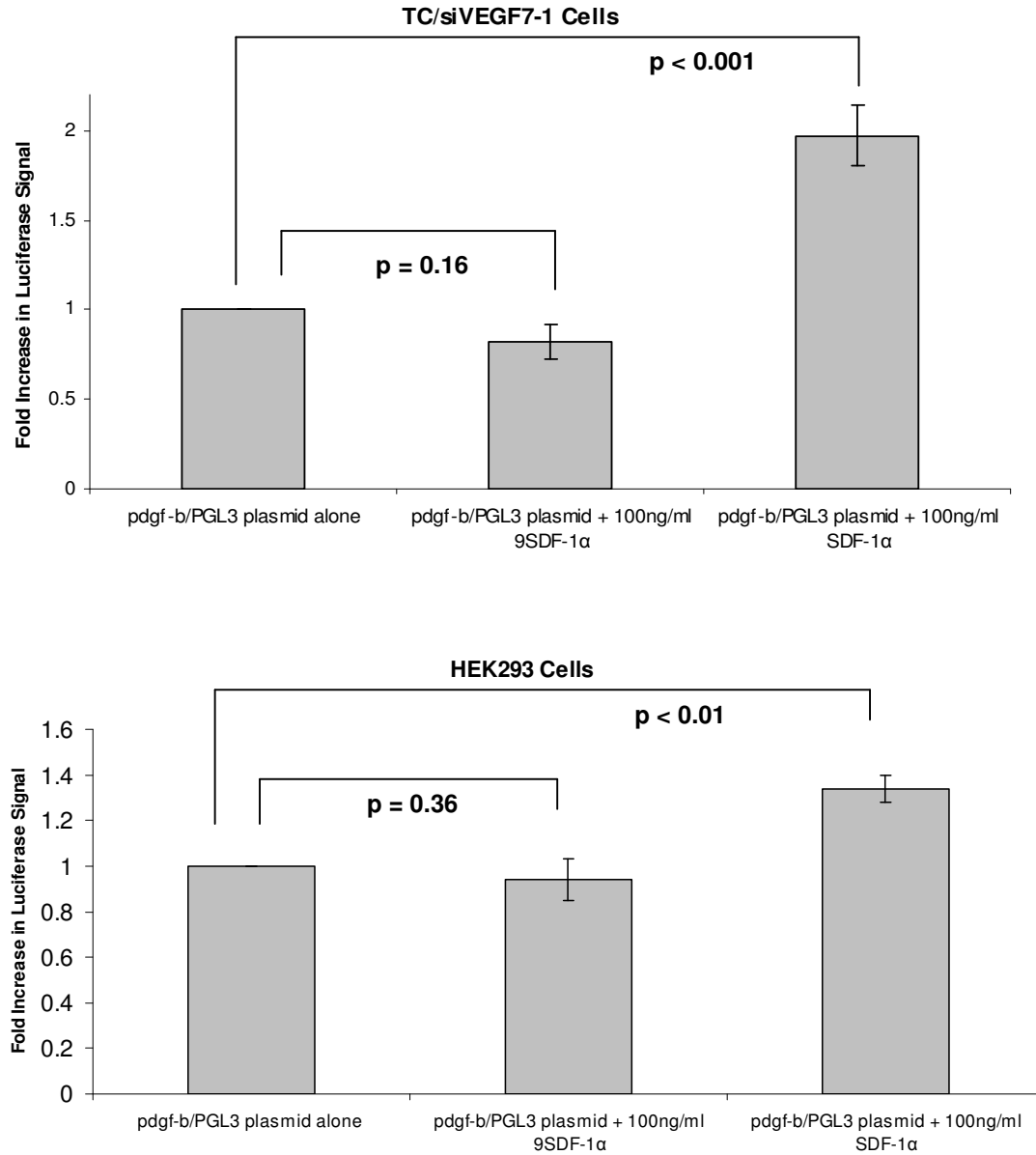


Figure 6. SDF-1 α regulates PDGF-B expression via transcription. TC/siVEGF₇₋₁ and HEK293 cells were transfected with either the pdgf-b/pGL3 luciferase construct or the pGL3 control vector for 48 hours. The cells were plated in the absence of growth factors and supplements for 24 hours and then treated with 100ng/ml of either SDF-1 α or 9SDF-1 α inactive protein for 8 hours. The cells were lysed and the luciferase signal quantified. Bar graph shows pooled data from three independent experiments each performed in triplicate. $P < 0.05$ was considered significant. SDF-1 α activates the *pdgf-b* promoter in both TC/siVEGF₇₋₁ and HEK293 cells.

SDF-1 α induces binding of the ELK-1 transcription factor to the *pdgf-b* promoter

To determine whether the ELK-1 transcription factor binds to the *pdgf-b* promoter in response to SDF-1 α stimulation, ELK-1 binding sites were identified both within the *pdgf-b* promoter and the transcribed region using the GeneRegulation.com MATCH software. Three binding sites which scored above 85% were investigated at -600 bp, the transcription start site (TS) and, at the +1 kb site (Figure 7A). TC/siVEGF₇₋₁ and HEK293 cells were plated in the absence of growth factors and supplements for 24 hours and then treated with 100ng/ml of the SDF-1 α recombinant human protein for 15, 30 and, 60 minutes. Chromatin immunoprecipitation (ChIP) was performed and ELK-1 binding was quantified using q-PCR.

ELK-1 binds to the *pdgf-b* promoter with high affinity at the -600 bp site in both TC/siVEGF₇₋₁ and HEK293 cells ($P < 0.05$; Figure 7B and C), does not bind with high affinity at the TS site ($P > 0.05$; Figure 7D) and, binds to the + 1 Kb site in the TC/siVEGF₇₋₁ but not in the HEK293 cells (Figure 7E). We speculate that the large error bars observed at the TS site (Figure 7D) are due to the cycling of the ELK-1 transcription factor between a bound and unbound state. ELK-1 recognizes and binds the TS binding site but is quickly released suggesting that this site is not critical for the activation of the *pdgf-b* promoter in response to SDF-1 α . As for binding of ELK-1 to the +1 kb site in the TC/siVEGF₇₋₁ cells, further studies are required to analyze its potential role in promoting PDGF-B transcription in response to SDF-1 α .

Figure 7A. Schematic representing the 3 investigated ELK-1 binding sites

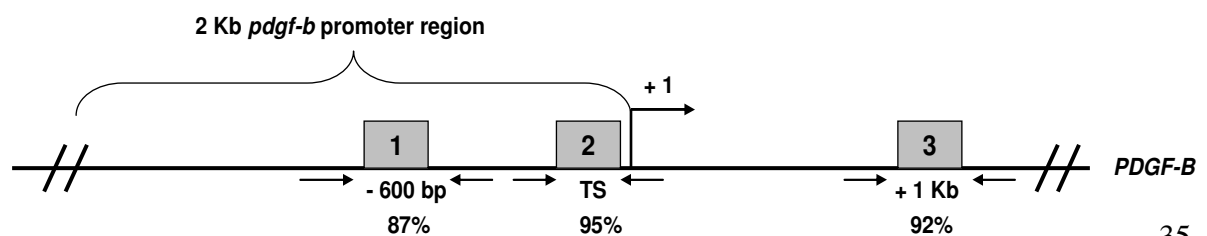


Figure 7B. qPCR quantification of ELK-1 binding at the – 600bp site

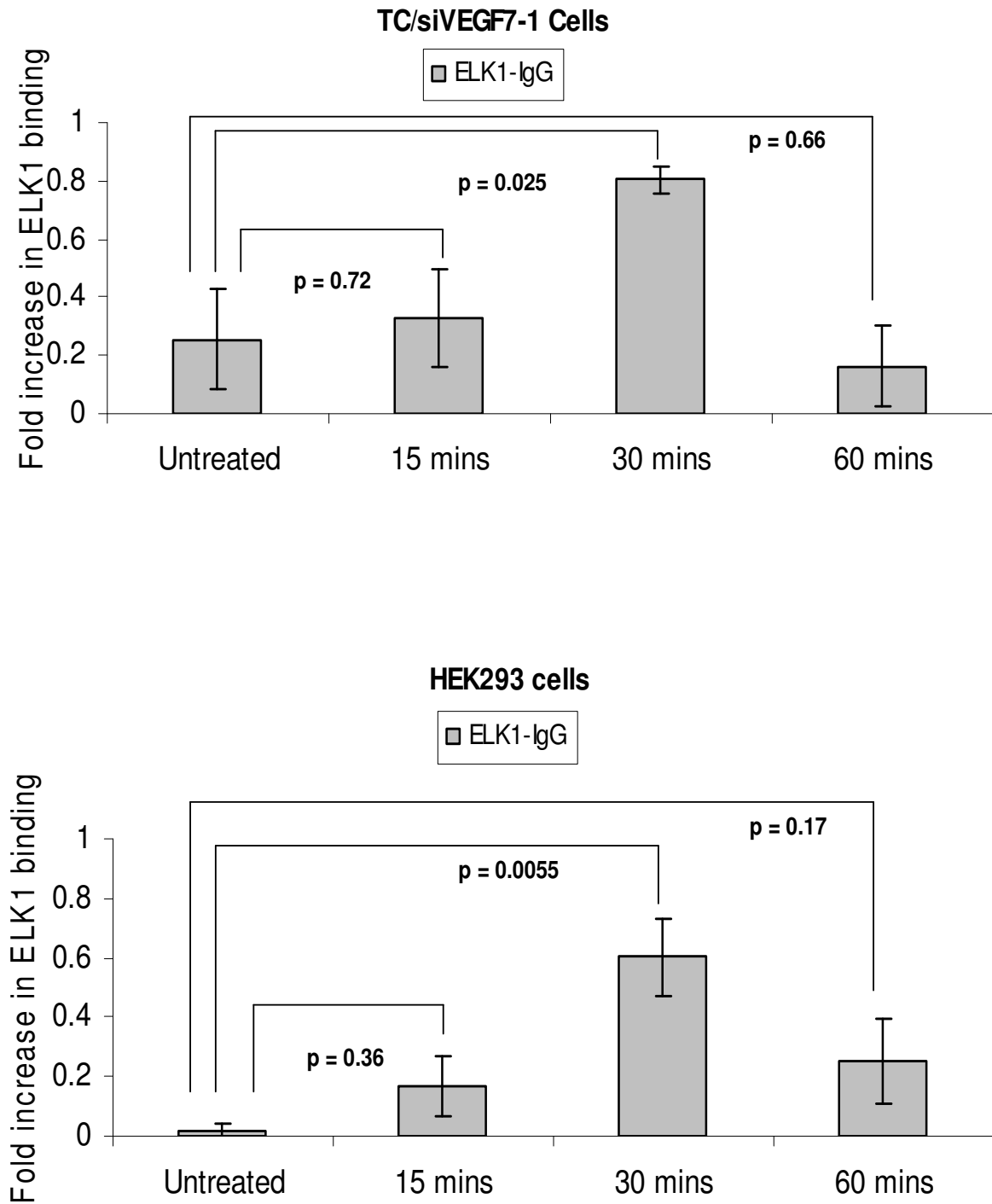


Figure 7C. Representative gel depicting ELK-1 binding at the – 600bp site in TC/siVEGF₇₋₁ cells with a peak at 30 minutes post stimulation with SDF-1 α

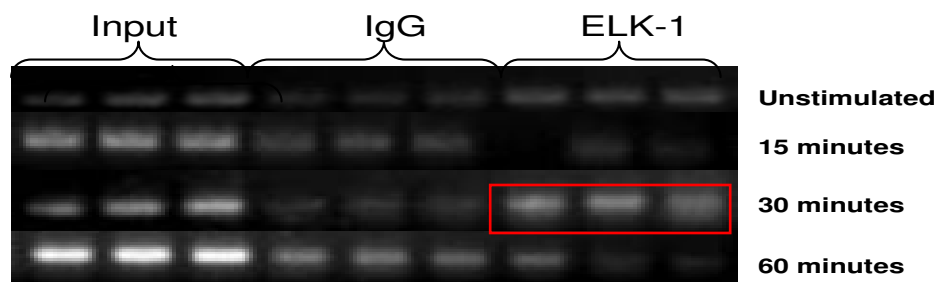


Figure 7D. qPCR quantification of ELK-1 binding at the transcription start (TS) site

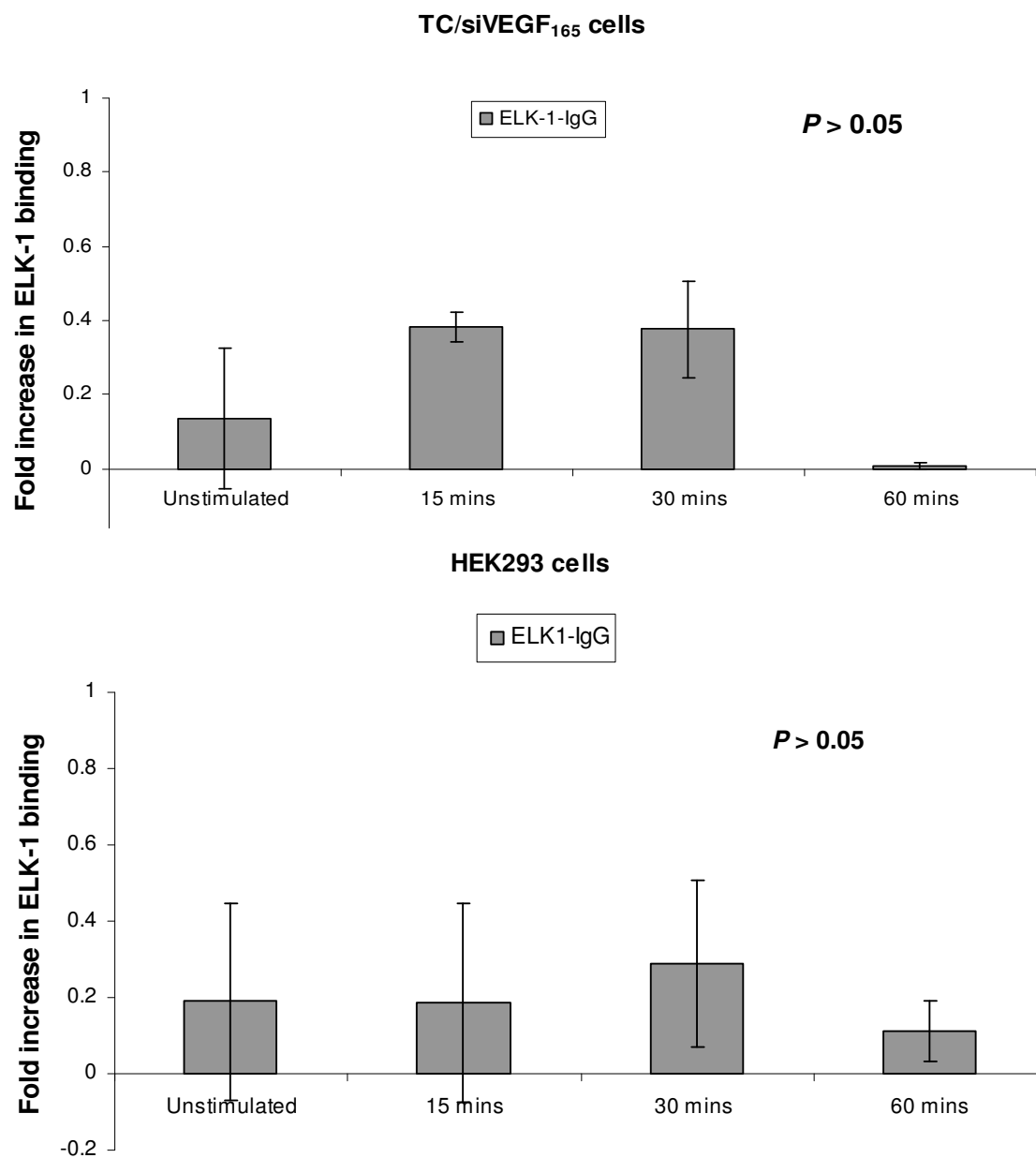


Figure 7E. qPCR quantification of ELK-1 binding at the + 1 kb site

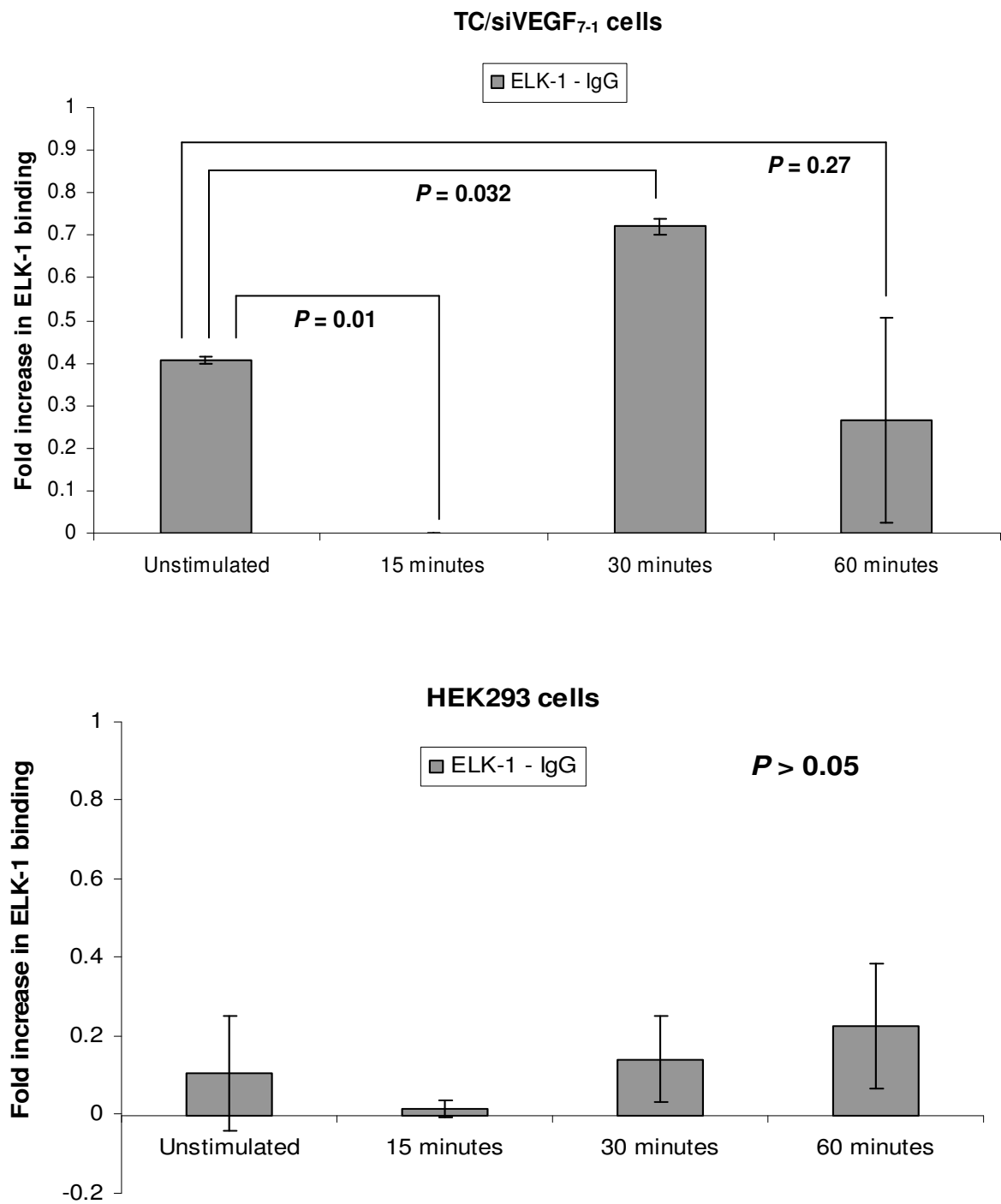


Figure 7. The ELK-1 transcription factor binds to *pdgf-b* promoter in response to SDF-1 α . (A)

Schematic representation of the potential ELK-1 binding sites within the promoter and the transcribed region. Using GeneRegulation.com MATCH software, 3 potential ELK-1 binding sites which scored >85% were investigated at -600 bp (blue box 1), at the transcription start site (TS; blue box 2) and, at the + 1 Kb site (blue box 3). Primer binding sites for the corresponding regions are also illustrated. **(B,C,D,E)** TC/siVEGF₇₋₁ and HEK293 cells were plated and cultured in the absence of growth factors and supplements for 24 hours, then treated with 100ng/ml of SDF-1 α for 15, 30 or 60 minutes. Chromatin immunoprecipitation (ChIP) was performed and ELK-1 binding at each of the 3 different sites was quantified using qPCR. The data is represented as fold increase in ELK-1 binding scaled from 0 (non-binding) to 1 (complete binding). Bar graph shows pooled data from three independent experiments each performed in triplicate. The sample values minus the control values were used in one-way analysis of variance. Negative numbers were replaced with 0 indicating non-binding. $P < 0.05$ was considered significant. **(B, C)** ELK-1 binds to the *pdgf-b* promoter at the -600bp site with a peak at 30 minutes post stimulation with SDF-1 α . The qPCR samples were run on a 1% agarose gel confirming ELK-1 binding at the – 600 bp site with a peak at 30 minutes. **(D)** ELK-1 does not bind with high affinity at the TS site; however, **(E)** it binds at the +1 Kb site in TC/siVEGF₇₋₁ cells but not in the HEK293 cells.

The ELK-1 transcription factor is phosphorylated at serine 383 in response to SDF-1 α in HEK293 ChIP samples

To further demonstrate that the ELK-1 transcription factor is activated in response to SDF-1 α stimulation, a fraction of the lysates from the HEK293 cells collected for ChIP (as previously described) were also used in a western blot analysis to detect both phosphorylated ELK-1(S383) and total ELK-1. The ELK-1 transcription factor is a member of the ETS family of transcription factors which has been reported to be activated in response to the MAPK (ERK1/2) pathway by phosphorylation, specifically at serine 383 (61, 64). We found that SDF-1 α induced phosphorylation of the ELK-1 transcription factor at S383 with a peak at 30 minutes post stimulation coinciding with the previous ChIP findings (Figure 8A and B). These observations suggest that the ELK-1 transcription factor plays a critical role in the transcription of PDGF-B in response to SDF-1 α .

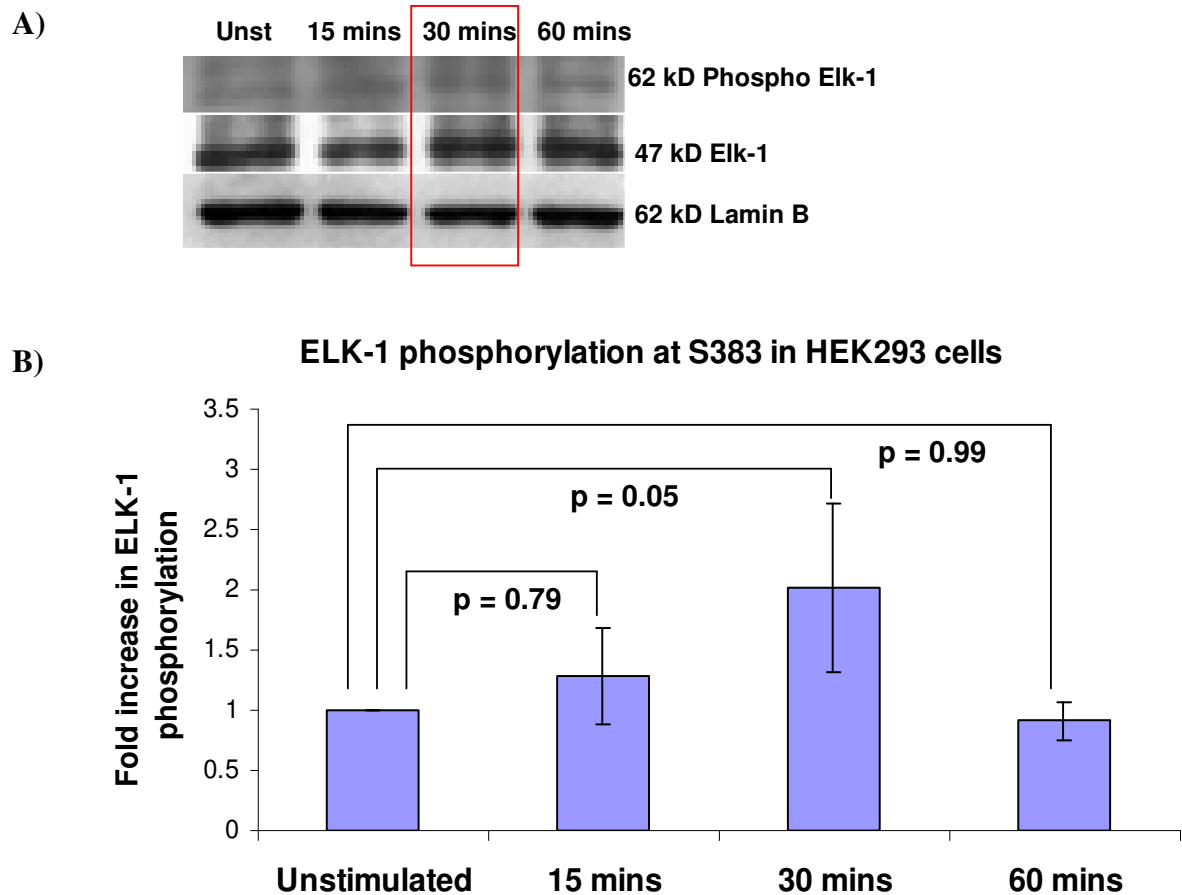


Figure 8. ELK-1 is phosphorylated at S383 in response to SDF-1 α in HEK293 ChIP samples. HEK293 cells were plated and cultured in the absence of growth factors and supplements for 24 hours then treated with 100ng/ml of SDF-1 α for 15, 30 or 60 minutes. The nuclear protein fractions were isolated as described for the ChIP assay, combined with 2x SDS loading buffer and boiled at 100 °C for 5 minutes. Western blot analysis was performed and the membrane was probed for phospho-ELK-1(S383). **(A)** Representative blot illustrating phospho-ELK-1(S383), total ELK-1 and, Lamin B nuclear loading control bands. **(B)** Bar graph from 3 independent western blots depicting the fold increase in phospho-ELK-1(S383) as measured from the corresponding densitometry. Both phospho-ELK-1(S383) and total ELK-1 were normalized to Lamin B and the densitometry was calculated as the ratio of normalized phospho-ELK-1(S383) to normalized total ELK-1. $P < 0.05$ was considered significant. SDF-1 α induced phosphorylation of ELK-1 at S383 with a peak at 30 minutes.

Summary

Many cancers, including colorectal cancer, pancreatic cancer, glioma, and sarcoma, over-express PDGF-B (53). However, the mechanisms by which PDGF-B expression is up-regulated during vascular remodeling remains unclear. In the previous sections, we demonstrated that SDF-1 α regulated PDGF-B expression *in vitro* in both TC/siVEGF₇₋₁ and HEK293 cells and *in vivo* in TC/siVEGF₇₋₁ tumors. PDGF-B expression can be regulated by several mechanisms, including transcriptional regulation (60).

Signaling through the SDF-1 α /CXCR4 pathway initiates a cascade of several signal transduction pathways linked to transcription and expression through MEK1/2 and ERK1/2. ERK can then phosphorylate and activate other cellular proteins as well as translocate to the nucleus, phosphorylate and/or, activate transcription factors (33). Binding of SDF-1 α to CXCR4 induces phosphorylation of the mitogen-activated protein kinases (MAPKs) p44 ERK-1 and p42 ERK-2, which subsequently initiates the phosphorylation of several downstream transcription factors including the nuclear transcription factor ELK-1 (64). Here, we investigated whether SDF-1 α regulated PDGF-B expression via a transcriptional mechanism which involves binding of the ELK-1 transcription factor.

We cloned the 2 Kb *pdgf-b* promoter into the pGL3 reporter vector and showed that SDF-1 α regulates PDGF-B expression via a transcriptional mechanism in both TC/siVEGF₇₋₁ and HEK293 cells. We then used the GeneRegulation Match software and identified potential ELK-1 binding sites within the *pdgf-b* promoter and transcribed region. Using ChIP, we then demonstrated that the ELK-1 transcription factor binds to the *pdgf-b* promoter in response to SDF-1 α at the -600 bp site in both TC/siVEGF₇₋₁ and HEK293

cells with a peak at 30 minutes post stimulation. Furthermore, we performed western blot analysis on a portion of the nuclear proteins obtained from the ChIP assay to confirm phosphorylation and activation of the ELK-1 transcription factor in response to SDF-1 α . SDF-1 α induced activation and phosphorylation of ELK-1 at serine 383 with a peak at 30 minutes which coincided with its binding to the *pdgf-b* promoter with a peak at 30 minutes post stimulation.

We are first to demonstrate that SDF-1 α regulates PDGF-B via a transcriptional mechanism which involves binding of the ELK-1 transcription factor to the *pdgf-b* promoter.

Chapter 4.

The SDF-1 α /PDGF-B pathway induces the differentiation of bone marrow progenitor cells (BMCs) into pericytes *in vitro*

Rationale

We previously demonstrated that treating VEGF₁₆₅-inhibited TC/siVEGF₇₋₁ tumors with Ad-SDF-1 α partially restored vasculogenesis and induced infiltration of BMCs to a perivascular area. These BMCs differentiated into pericytes/vSMCs. We also showed that Ad-SDF-1 α up-regulated PDGF-B mRNA levels in TC/siVEGF₇₋₁ tumors (40). In the previous sections we confirmed that SDF-1 α regulates PDGF-B RNA and protein levels both *in vitro* and *in vivo* via a transcriptional mechanism which involved binding of the ELK-1 transcription factor to the *pdgf-b* promoter.

When secreted in its homodimer form, PDGF-BB binds to its tyrosine kinase receptor PDGFR- β . PDGF-B and PDGFR- β are expressed in the developing vasculature, where PDGF-B is produced by endothelial cells, and PDGFR- β is expressed by mural cells such as pericytes and vascular smooth muscle cells (49). The role of PDGF-B and PDGFR- β in pericyte differentiation has been extensively described (53, 66). Pericytes are recruited by PDGF-B-expressing endothelial cells to remodel, stabilize and mature the new vascular tube. In fact, PDGFR- β + pericyte progenitor cells (PPPs) have been reported to migrate to sites of tumor growth where they differentiate into NG2+, desmin+ and α -SMA+ pericytes (57).

All together, these observations suggested a correlation between the up-regulation of PDGF-B by SDF-1 α and the differentiation of BMCs into pericytes observed in the Ad-SDF-1 α treated TC/siVEGF₇₋₁ tumors. In this section, we investigated whether the SDF-1 α /PDGF-B pathway plays a role in the differentiation of BMCs into pericytes *in vitro*.

We established an *in vitro* pericyte differentiation model where BMCs were flushed from the hind femurs of mice and cultured in either DMEM complete medium alone or, in conditioned medium from 10T1/2, 10T1/2-sh-SDF-1 or, 10T1/2-sh-control cells which we previously generated (chapter 2; Figure 3). Although no general marker exists for the detection of pericytes, several markers are currently used for the identification of these cells. Depending on the tissue and developmental or angiogenic state of a blood vessel, the expression pattern of pericyte markers can vary. The most commonly used markers are, the early pericyte marker PDGFR- β also expressed on BM-derived progenitor cells; RGS-5, which detects differentiating pericytes and, desmin, α -SMA and, NG2 which are expressed on mature pericytes (42). α -SMA is also highly expressed by vascular smooth muscle cells so for the purpose of our studies, we used NG2 and desmin as markers for mature differentiated pericytes.

As expected, we found that fresh BMCs expressed the PDGFR- β early pericyte marker but did not express both NG2 and desmin mature pericyte markers. However, PDGFR- β^+ BMCs differentiated into mature pericytes, as defined by their morphology and the expression of desmin and NG2, when cultured in conditioned medium from 10T1/2 cells or 10T1/2-conditioned medium compared to DMEM medium alone or 10T1/2-sh-SDF-1 conditioned medium. These findings, combined with our previous observations that 10T1/2-sh-SDF-1 cells express low or no SDF-1 α and PDGF-B, confirmed the critical role of the SDF-1 α /PDGF-B pathway in BM-derived pericyte differentiation *in vitro*.

Results

Fresh BMCs express PDGFR- β but do not express NG2 and desmin mature pericyte markers

We investigated the expression of the 3 pericyte markers PDGFR- β , desmin and, NG2 on freshly collected BMCs prior to culture *in vitro*. BMCs were flushed from the hind femurs of mice, immediately cytopun onto glass slides, fixed and stained for the expression of PDGFR- β , NG2 and desmin (red staining). As anticipated, we found that fresh BMCs express the early pericyte marker PDGFR- β but do not express the mature pericyte markers desmin and NG2 (Figure 9). Therefore and for the rest of this study, we identified mature pericytes as cells with pericyte-like morphology (Figure 10A) and which express both the desmin and NG2 mature pericyte markers.

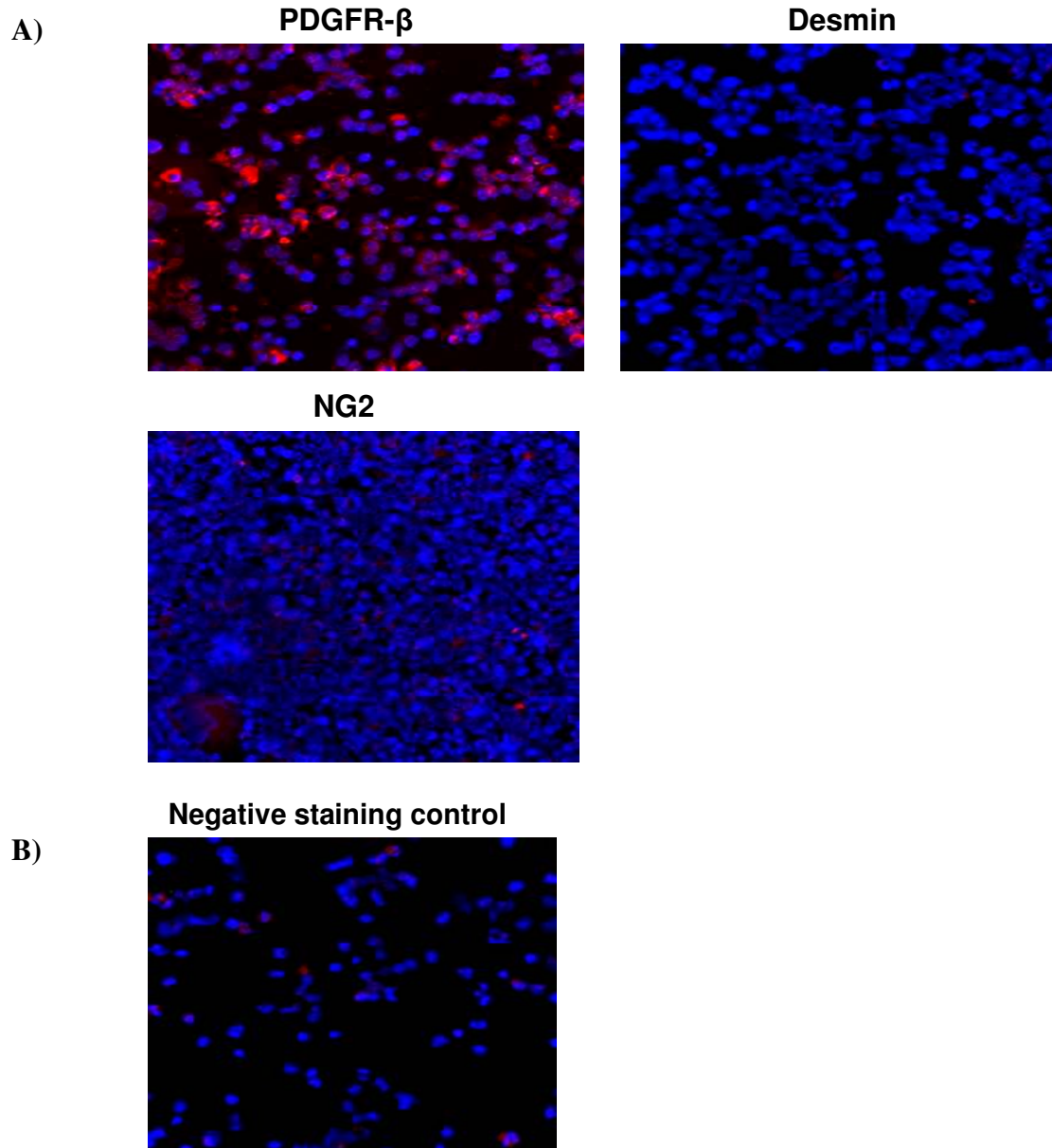


Figure 9. Freshly isolated BMCs express the early pericyte marker PDGFR- β but do not express desmin and NG2 mature pericyte markers. Immunocytochemistry staining. BMCs were flushed from the hind femurs of mice, cytospun onto glass slides, fixed, and stained for (A) PDGFR- β , desmin, and NG2 (red). (B) Negative staining control. No primary IgG was added, only the goat anti-rabbit Alexa fluor 594 secondary alone (red). Blue represents Hoechst nuclear staining. Fresh BMCs express the early PDGFR- β pericyte marker but do not express desmin and NG2 mature pericyte markers.

BMCs differentiate into pericytes when cultured in conditioned medium from 10T1/2 cells

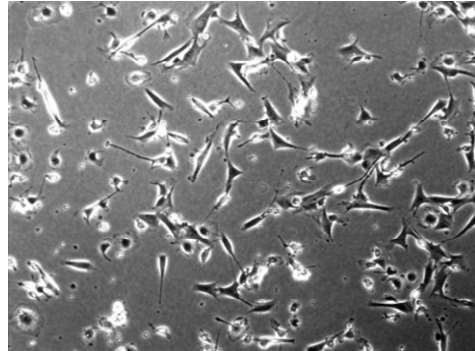
To confirm that BMCs differentiate into mature pericytes in response to soluble growth factors present in the 10T1/2 conditioned medium, whole BMCs were flushed from the hind femurs of mice and cultured in a 2-well chamber slide in either DMEM complete medium alone or, in conditioned medium obtained from 10T1/2 cells for a period of 2 weeks. 10T1/2 cells endogenously express SDF-1 α and PDGF-B. We found that BMCs differentiate into pericytes, as judged by morphology (Figure 10A) and for the expression of NG2 and desmin mature pericyte markers (red staining; Figure 10B) when cultured in conditioned medium from 10T1/2 cells compared to DMEM complete medium alone.

A)

BM cells + DMEM complete medium

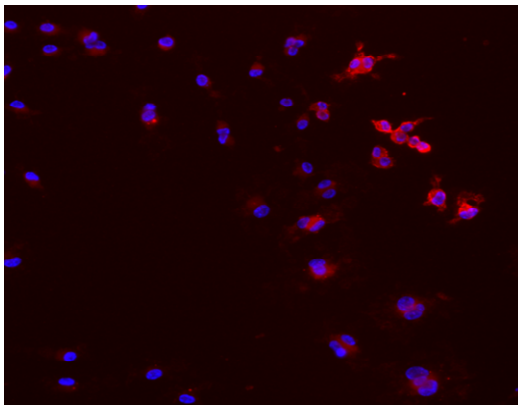


BM cells + 10T1/2 conditioned medium



B)

Desmin



NG2

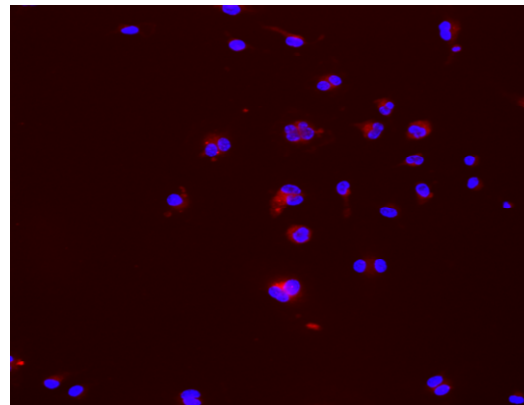


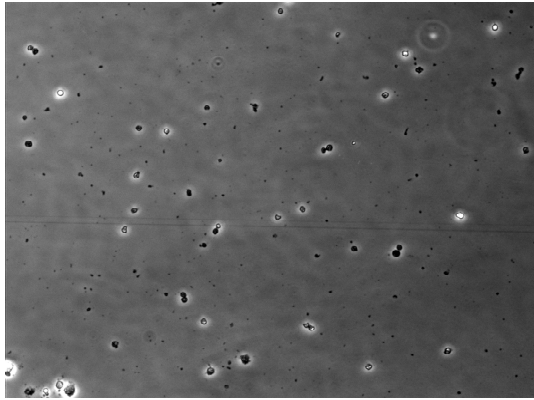
Figure 10. 10T1/2 conditioned medium induces BMCs to differentiate into pericytes as defined by morphology and the expression of NG2 and desmin. In vitro pericyte differentiation model. BMCs were flushed from the hind femurs of mice and cultured in either conditioned medium from 10T1/2 cells or DMEM complete medium alone for 2 weeks. When cultured in 10T1/2 conditioned medium, (A) PDGFR- β^+ BMCs attach to the plate and acquire pericyte-like morphology and (B) express the mature pericyte markers desmin and NG2 (red). Blue represents Hoechst nuclear staining. The negative staining control was the same as in Figure 9B. BMCs differentiate into mature pericytes that express NG2 and desmin when cultured in 10T1/2 conditioned medium.

BMCs do not differentiate into pericytes when cultured in 10T1/2-sh-SDF-1 conditioned medium compared to 10T1/2-sh-control medium

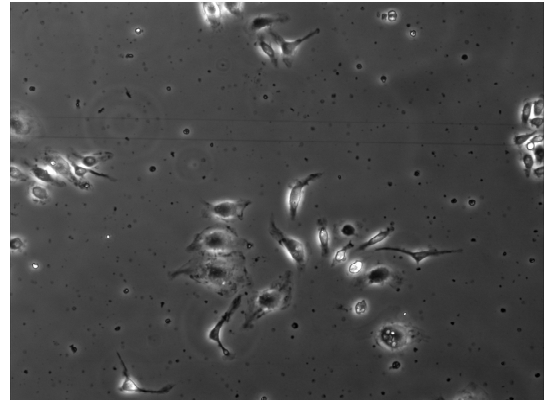
We showed that PDGFR- β^+ BMCs can differentiate into mature pericytes as judged by morphology and expression of NG2 and desmin mature pericyte markers (Figure 10) when cultured in conditioned medium from 10T1/2 cells. To confirm that the SDF-1 α /PDGF-B pathway plays a role in this differentiation process, we investigated whether PDGFR- β^+ BMCs can differentiate into mature pericytes when cultured in conditioned medium collected from 10T1/2-sh-SDF-1. 10T1/2-shSDF-1 cells do not express SDF-1 α and PDGF-B (Figure 5). BMCs were collected from the hind femurs of mice and cultured in a 2-well chamber slide in conditioned medium from either 10T1/2-shSDF-1 or 10T1/2-shcontrol for 2 weeks. We found that PDGFR- β^+ BMCs behave in a manner similar to cells cultured in DMEM medium alone; they do not differentiate into mature pericytes (Figure 11A). On the other hand, PDGFR- β^+ BMCs differentiate into mature pericytes when cultured in 10T1/2-sh-control medium (Figure 11B).

A)

BM cells + shSDF-1 10T1/2 conditioned media

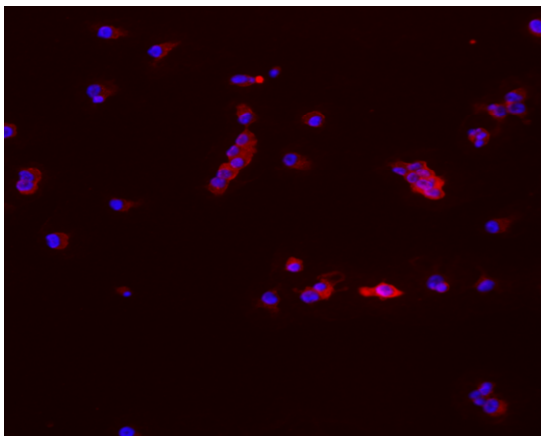


BM cells + shcontrol 10T1/2 conditioned media



B)

Desmin



NG2

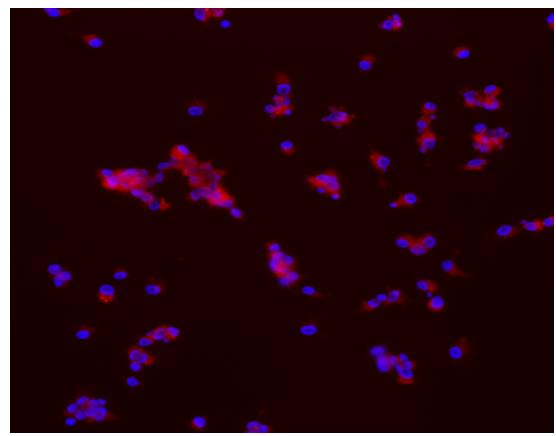


Figure 11. BMCs cultured in 10T1/2-sh-SDF-1 conditioned medium do not differentiate into pericytes as defined by morphology and expression of NG2 and desmin. In vitro pericyte differentiation model. BMCs were flushed from the hind femurs of mice and cultured in conditioned medium from either 10T1/2-sh-SDF-1 cells or 10T1/2-sh-control cells for 2 weeks. PDGFR- β^+ BMCs (**A**) attach to the plate, acquire pericyte-like morphology and, (**B**) stain positive for desmin and NG2 (red) when cultured in 10T1/2-sh-control compared to 10T1/2-sh-SDF-1 conditioned medium. Blue represents Hoechst nuclear staining. The negative staining control was the same as in Figure 9B. BMCs do not attach to the plate and differentiate into desmin and NG2 expressing pericytes when cultured in 10T1/2-sh-SDF-1 conditioned medium.

Summary

Previous findings from our group showed that treating TC/siVEGF₇₋₁ tumors with Ad-SDF-1 α increased BMC migration to the tumor site where they predominantly differentiated into pericytes while synonymously increasing PDGF-B mRNA levels (40). In the previous sections, we investigated the correlation between SDF-1 α and PDGF-B and found that SDF-1 α regulated PDGF-B both *in vitro* and *in vivo* via a transcriptional mechanism involving the ELK-1 transcription factor. PDGF-B and its receptor, PDGFR- β , have been extensively described in the process of pericyte maturation and in fact, a lack of signaling through the PDGF-B/PDGFR- β pathway leads to pericyte loss and to endothelial changes followed by capillary dilation and rupture (51, 52). Therefore, we hypothesized that the SDF-1 α /PDGF-B pathway plays a critical role in BM-derived pericyte differentiation.

To test our hypothesis, we established an *in vitro* pericyte differentiation model. BMCs were collected from the hind femurs of mice and cultured in DMEM medium alone or in medium from 10T1/2 cells. We found that BMCs differentiate into PDGFR- β , desmin and, NG2 positive pericytes when cultured in 10T1/2 medium. A study by Gabriele Bergers and colleagues reported the discovery of PDGFR- β -expressing pericyte progenitor cells (PPPs) which possess the capacity to differentiate into NG2⁺, desmin⁺ and, alpha-smooth muscle actin⁺ pericytes within tumors (57).

In order to confirm that BMCs differentiated into pericytes when cultured in 10T1/2 conditioned medium due to soluble growth factors present within the 10T1/2 conditioned medium, we collected fresh BMCs and immediately tested them for the expression of

PDGFR- β , desmin and, NG2. As expected, we found that fresh BMCs expressed the early pericyte marker PDGFR- β but did not express the desmin and NG2 mature pericyte markers.

Furthermore and to characterize the role of the SDF-1 α /PDGF-B pathway in the process of BM-derived pericyte differentiation *in vitro*, we collected PDGFR- β^+ BMCs from hind femurs of mice and cultured them in either 10T1/2-sh-SDF-1 or 10T1/2-sh-control medium. As described in chapter 2, 10T1/2-sh-SDF-1 cells do not express SDF-1 α and PDGF-B compared to 10T1/2-sh-control cells (Figure 5). We found that PDGFR- β^+ BMCs did not differentiate into mature pericytes when cultured in 10T1/2-sh-SDF-1 medium.

Our data confirmed that the SDF-1 α /PDGF-B pathway plays a critical role in BM-derived pericyte differentiation *in vitro*. In the next sections, we investigated the role of this pathway in BM-derived pericyte differentiation *in vivo* in Ewing's sarcoma tumors.

Chapter 5.

The SDF-1 α antagonist AMD 3100 negatively impacts tumor vessel development in the Ewing's sarcoma tumor model

Rationale

Our group previously demonstrated that the soluble vascular endothelial growth factor VEGF₁₆₅ is the chemotactic stimulus for BMC migration during vasculogenesis of Ewing's sarcoma (10, 16, 23). We used an siRNA specific for VEGF₁₆₅ and generated the TC/siVEGF₇₋₁ cell line and showed that inhibiting VEGF₁₆₅ decreased vasculogenesis, inhibited TC/siVEGF₇₋₁ tumor growth and, decreased SDF-1 α expression (40). SDF-1 α is a chemotactic factor for BMCs and plays a critical role in the mobilization of BMCs from the BM to the peripheral blood (28, 31); therefore, we re-introduced SDF-1 α into the TC/siVEGF₇₋₁ tumors and showed that SDF-1 α rescued tumor growth by restoring the infiltration of BMCs to a perivascular area and inducing their differentiation into pericytes (40).

These observations suggested a critical role for the SDF-1 α chemokine in Ewing's sarcoma tumor growth. Specifically, we hypothesized that SDF-1 α plays a critical role in Ewing's sarcoma neo-vascularization. In order to investigate this hypothesis, we needed to specifically inhibit SDF-1 α signaling *in vivo* and document its effect on the tumor blood vessels.

The SDF-1 α antagonist AMD 3100

AMD3100 is a bicyclam derivative (1,1'-[1,4-phenylenebis(methylene)]-bis-1,4,8,11-tetraazacyclotetradecane) which selectively and reversibly blocks SDF-1 α from binding to its CXCR4 receptor. AMD3100 is currently used in the clinic in patients undergoing allogeneic transplantation due its low toxicity and its specificity in disrupting the SDF-1 α /CXCR4 axis (69, 70).

AMD 3100 and Ewing's sarcoma

In this section, we investigated the role of SDF-1 α on Ewing's sarcoma tumor blood vessel development by specifically inhibiting SDF-1 α signaling using the SDF-1 α antagonist, AMD 3100. Nude mice were subcutaneously injected with either TC71 or A4573 Ewing's sarcoma cells and once the tumors became palpable, the mice received daily subcutaneous injections of either PBS or 5mg/kg of the AMD3100 drug for the duration of the experiment. The experiment was terminated, the mice were all sacrificed and, the tumors resected for further analysis once the longest tumor measurement in the PBS control group reached the size of 2 centimeters. This constitutes the maximum size allowed by the Institutional Animal Care and Use Committee at The University of Texas M.D. Anderson Cancer Center. The tumors were resected and the vessel morphology and density analyzed by staining for the CD31 endothelial cell marker. In order to analyze whether AMD 3100 decreased blood flow to the tumors compared to PBS, we repeated the experiment; however, prior to resecting the tumors, we injected the mice with the Hoechst nuclear dye to label perfused blood vessels. We also stained the tumor sections for apoptosis using terminal deoxynucleotidyl transferase dUTP nick end labeling (TUNEL) to confirm vascular deficiency in response to AMD 3100.

We found that inhibiting SDF-1 α signaling in both TC71 and A4573 Ewing's sarcoma tumors resulted in smaller vessels with smaller lumens, decreased the microvessel density, decreased blood vessel perfusion and, increased tumor cell apoptosis.

Results

AMD 3100 leads to smaller vessels with smaller lumens in both TC71 and A4573 Ewing's sarcoma tumors

To investigate the role of SDF-1 α on blood vessel morphology in Ewing's sarcoma tumors, nude mice were subcutaneously injected with either TC71 or A4573 Ewing's sarcoma cells. Once the tumors became palpable, the mice received a daily subcutaneous injection of either PBS alone or 5mg/kg AMD 3100 for the duration of the experiment. All animals were sacrificed once the longest tumor measurement in the PBS control group reached 2 centimeters. The tumors were resected, snap frozen in OCT and, stored for further analysis by IHC. Tumor sections were stained for the CD31 endothelial cell marker (red staining) in order to label all the tumor vessels. We found that inhibiting SDF-1 α signaling, led to smaller more punctuated vessels with smaller lumens compared to the PBS group (Figure 12).

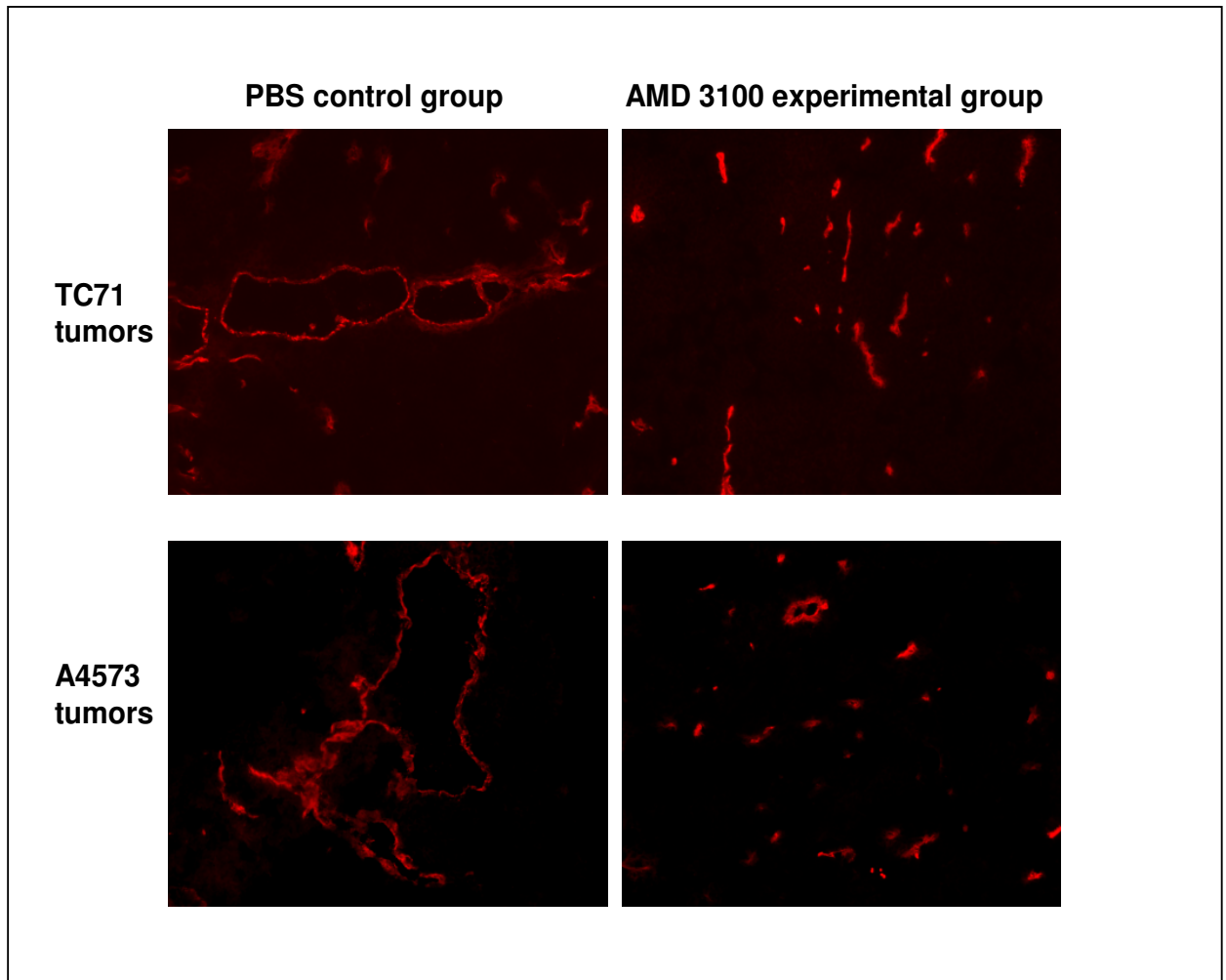


Figure 12. Tumor vessels are smaller with smaller lumens in response to AMD 3100 in both TC71 and A4573 Ewing's sarcoma tumors. Immunohistochemistry (IHC). Nude mice were implanted subcutaneously with either TC71 (top row) or A4573 (bottom row) Ewing's sarcoma cells. Once the tumors became palpable, the mice received daily subcutaneous injections of either PBS or 5 mg/kg AMD 3100. The tumors were resected once the longest tumor side measurement in the PBS control group reached a size of 2 centimeters (3 weeks post cell injection) and stained for the CD31 endothelial cell marker to label the tumor vasculature (red). Pictures were captured with a Zeiss Axioplan fluorescence microscope. 10x magnification. AMD 3100 treatment leads to tumors with smaller vessels and smaller lumens compared to PBS.

AMD 3100 decreases the overall microvessel density in both TC71 and A4573 Ewing's sarcoma tumors

We demonstrated that inhibiting SDF-1 α in both TC71 and A4573 tumors changed the vessel morphology and led to smaller vessels with smaller lumens (Figure 12). To investigate whether AMD 3100 decreased the tumor microvessel density in both TC71 and A4573 tumors as well, tumor sections were stained for the CD31 endothelial cell marker (red staining) as previously described to label the tumor vasculature and, the total amount of positive pixels for CD31 from both the PBS and AMD 3100 treated mice was quantified using the SimplePCI software. Note that any CD31⁺ cell, whether a single cell or a vessel-like structure, was included in the quantification. Treating the mice with AMD 3100 decreased the tumor microvessel density compared to PBS in both TC71 and A4573 Ewing's tumors (Figure 13).

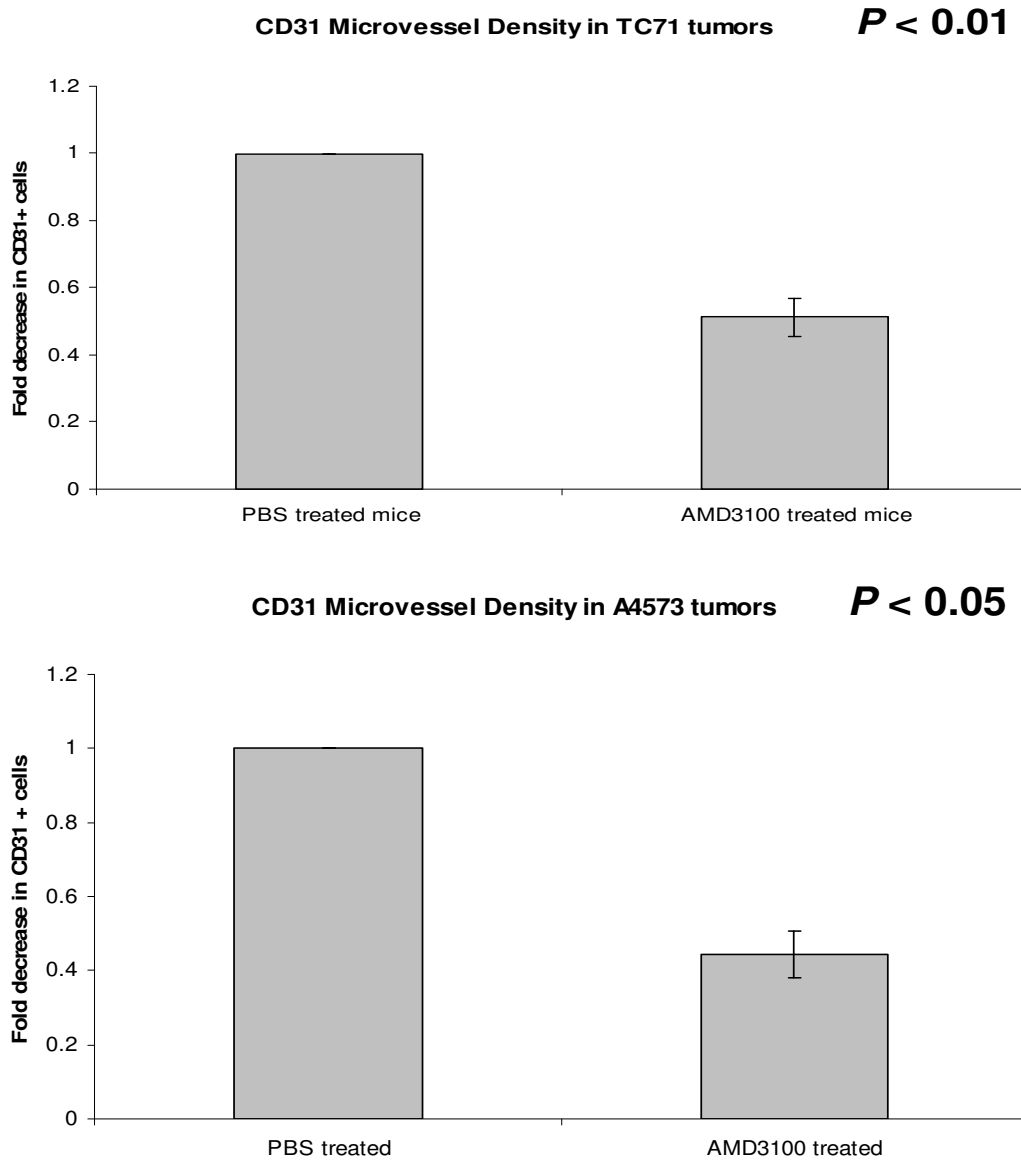


Figure 13. The total microvessel density is decreased in response to AMD 3100 in both TC71 and A4573 Ewing's sarcoma tumors. Microvessel density. Nude mice were implanted subcutaneously with either TC71 or A4573 Ewing's sarcoma cells. Once the tumors became palpable, the mice received daily subcutaneous injections of either PBS or 5 mg/kg AMD 3100. All tumors were resected 3 weeks post cell injection and stained for the CD31 endothelial cell marker. 10 x magnification. The total positive pixels for CD31 were quantified using the SimplePCI software. $P < 0.05$ was considered significant. The total microvessel density was reduced by 49 % in TC71 tumors and by 55.5 % in A4573 tumors.

AMD 3100 decreases the amount of perfused blood vessels in both TC71 and A4573 Ewing's sarcoma tumors

So far, our results demonstrated that using AMD 3100 to inhibit SDF-1 α from binding CXCR4 negatively impacted the tumor vasculature; it led to smaller vessels with smaller lumens and decreased the microvessel density. To investigate whether the blood vessels in the AMD 3100-treated mice were less efficient in delivering blood to the tumor site, the experiment was repeated as previously described; however and, prior to sacrificing the mice, we performed an intravenous (i.v.) injection using the Hoechst33342 dye in order to label any perfused blood vessels in both the PBS and AMD 3100 treated mice. Hoechst33342 is a nuclear dye which will label any cell it comes in contact with blue. Tumor sections were fixed and the total amount of positive pixels for Hoechst33342 (blue staining) was quantified using the SimplePCI software. Inhibiting SDF-1 α signaling not only changed the vessel morphology and decreased the total microvessel density but, it also decreased the total amount of perfused blood vessels compared to the mice treated with PBS (Figure 14).

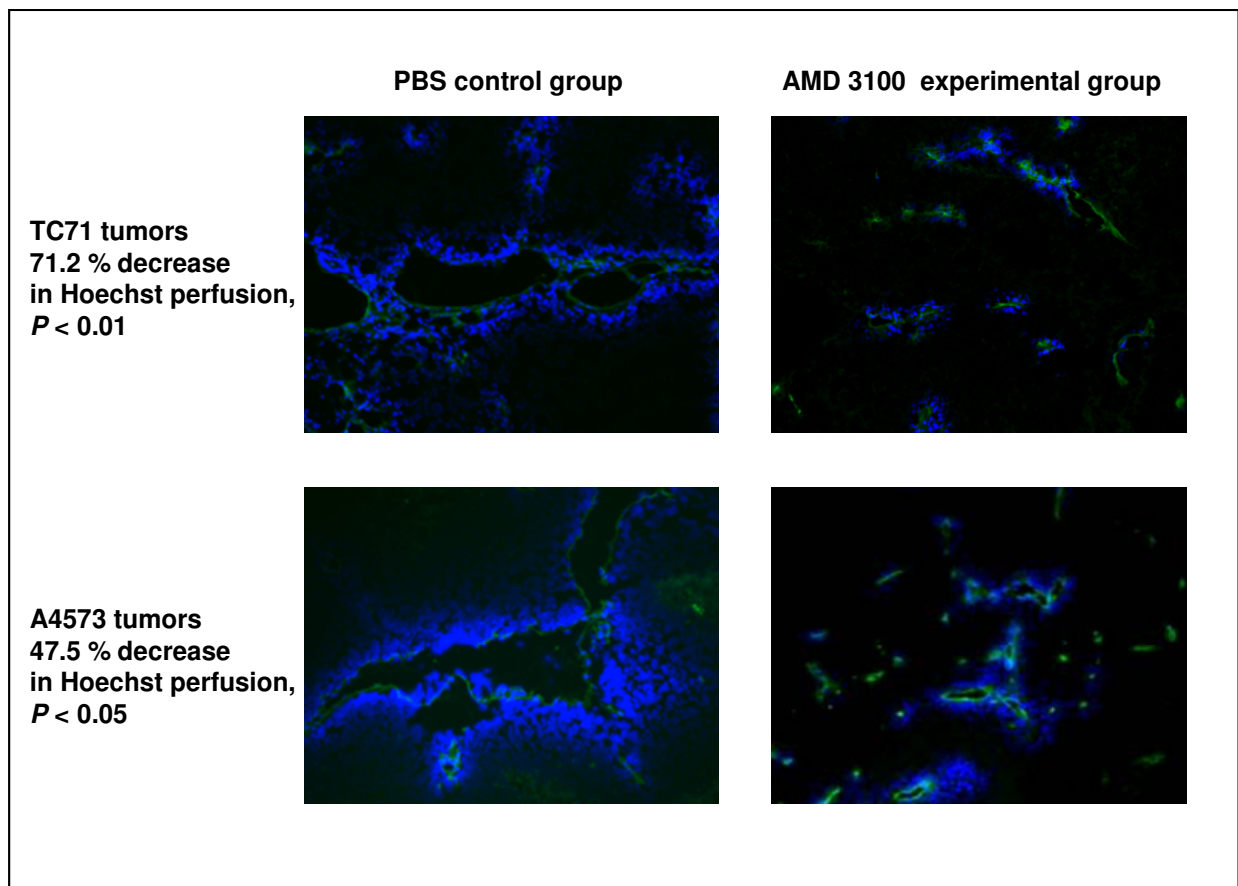


Figure 14. AMD 3100 decreased the total amount of perfused blood vessels in both TC71 and A4573 Ewing's tumors. Immunohistochemistry (IHC). Nude mice were implanted subcutaneously with either TC71 (top row) or A4573 (bottom row) Ewing's sarcoma cells. Once the tumors became palpable, the mice received daily subcutaneous injections of either PBS or 5 mg/kg AMD 3100. Immediately prior to resecting the tumors, the mice received an i.v. injection of the Hoechst33342 dye to label perfused vessels (blue). 10x magnification. The total positive pixels for Hoechst33342 were quantified using the SimplePCI software. $P < 0.05$ was considered significant. Vessel perfusion was reduced by 71.2 % in TC71 tumors and by 47.5 % in A4573 tumors.

AMD 3100 increases tumor cell apoptosis in both TC71 and A4573 Ewing's sarcoma tumors

To investigate the effect of the observed changes in vessel morphology, density and, perfusion on tumor cell viability in both TC71 and A4573 Ewing's sarcoma tumors in response to AMD 3100 and inhibiting SDF-1 α signaling, we performed TUNEL staining (brown) on the tumor sections to look for tumor cell apoptosis. The total amount of positive brown pixels was quantified using the SimplePCI software. AMD 3100 increased tumor cell apoptosis in both TC71 and A4573 Ewing's sarcoma tumors compared to PBS (Figure 15).

Figure 15A. TUNEL staining to detect tumor cell apoptosis

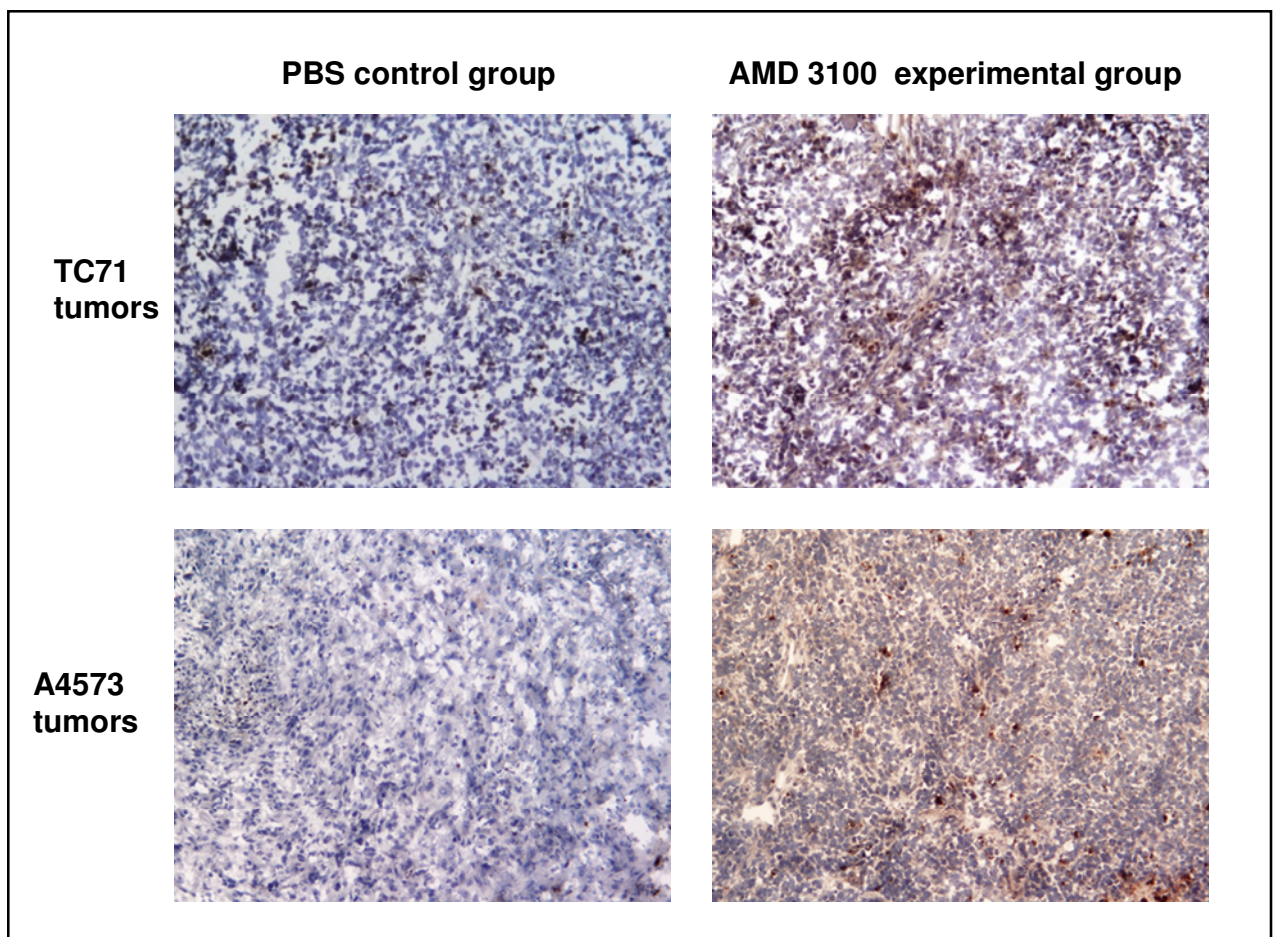


Figure 15B. Quantification for TUNEL staining

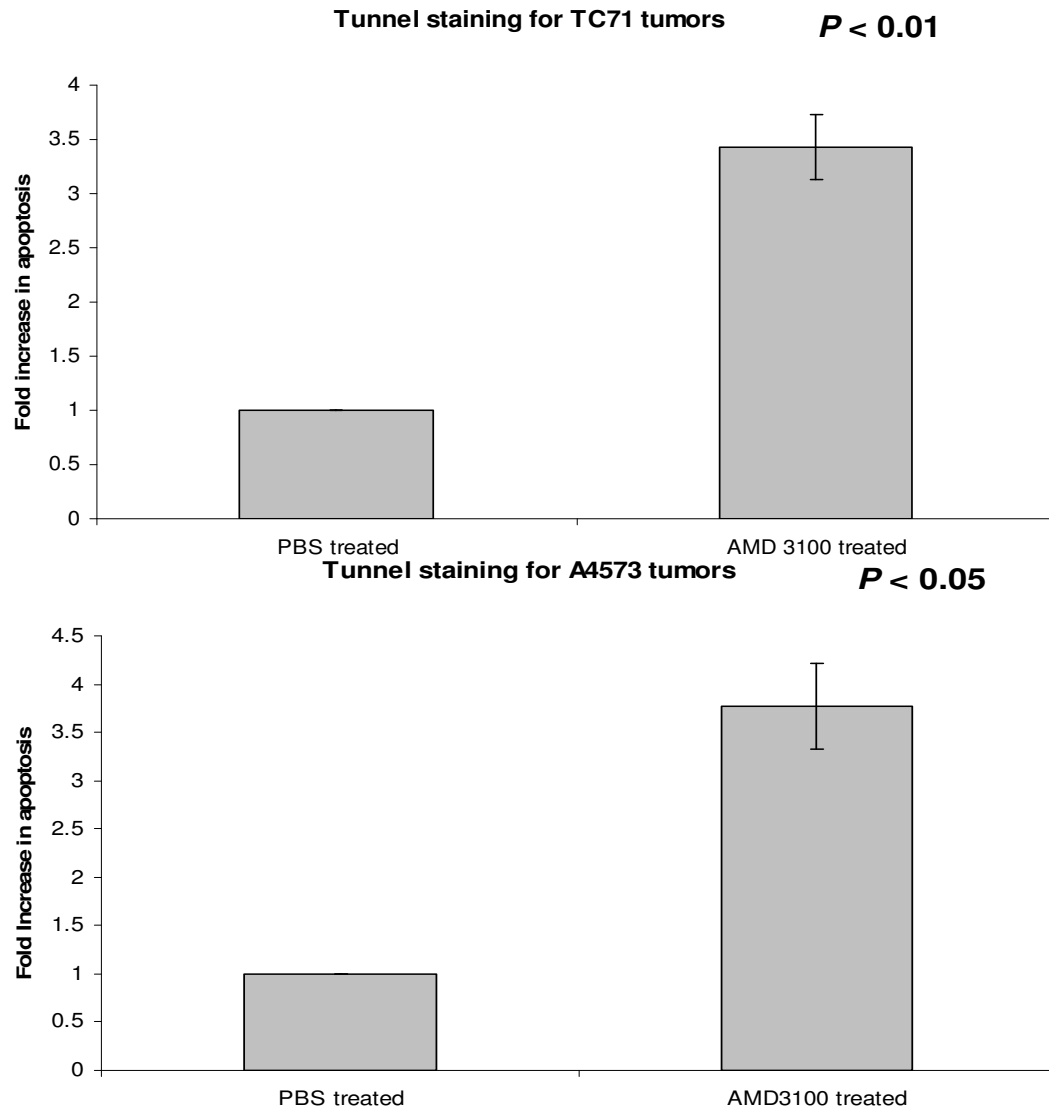


Figure 15. AMD 3100 increases tumor cell apoptosis in both TC71 and A4573 Ewing's sarcoma tumors. (A) TUNEL staining (brown). Nude mice were implanted subcutaneously with either TC71 (top row) or A4573 (bottom row) Ewing's sarcoma cells. Once the tumors became palpable, the mice received daily subcutaneous injections of either PBS or 5 mg/kg AMD 3100 for 3 weeks. Tumors were resected and tumor sections stained for tumor cell apoptosis using TUNEL. 10x magnification. (B) The total positive pixels for TUNEL were quantified using the SimplePCI software. $P < 0.05$ was considered significant. Apoptosis was increased by 2.4 folds in TC71 tumors and by 2.77 folds in A4573 tumors in response to AMD3100.

Summary

The SDF-1 α /CXCR4 axis has been implicated in several biological processes; it is involved in homeostasis and functions to regulate hematopoietic cell trafficking and secondary lymphoid tissue architecture (31, 33). In adult life, SDF-1 α plays an important role in the retention and homing of BM progenitor cells to the BM (28, 34). Overall, the role of SDF-1 α as a chemotactic gradient for CXCR4 (+) BM progenitor cells and its implication in embryonic and adult postischemia and in tumor angiogenesis has been extensively described (35-37). Our group demonstrated that introducing SDF-1 α into VEGF₁₆₅-inhibited TC/siVEGF₇₋₁ tumors partially restored vasculogenesis with infiltration of BMCs to a perivascular area and rescued tumor growth (40). These observations suggested a critical role for the SDF-1 α chemokine in blood vessel development during Ewing's sarcoma tumor growth.

In this section, in order to investigate the role of SDF-1 α in Ewing's sarcoma, we used the AMD 3100 drug which specifically disrupts the SDF-1 α /CXCR4 axis (69, 70) and analyzed its effect on tumor blood vessels in both TC71 and A4573 Ewing's sarcoma tumors. Nude mice were subcutaneously injected with either TC71 or A4573 Ewing's cells and once the tumors became palpable, the mice received daily subcutaneous injections of either PBS or 5 mg/kg AMD 3100 for the duration of the experiment.

The tumors were resected and tumor sections were stained for the CD31 endothelial cell marker to label the blood vessels. We found that inhibiting SDF-1 α signaling negatively impacted the tumor vessels; the vessel morphology indicated smaller and more punctuated vessels with smaller lumens. Furthermore, we quantified the total amount of

CD31⁺ cells and found that the overall microvessel density was decreased. We i.v. injected the mice with the Hoechst33342 dye and found that the vessels were also less perfused in response to AMD 3100. All these changes led to an increase in tumor apoptosis. Although our findings cannot determine vessel functionality, it is safe to conclude that the vessels in the AMD 3100 group are less efficient in delivering blood to the tumor mass compared to the vessels in the PBS control group. These findings confirm our hypothesis that SDF-1 α plays a critical role in the process of blood vessel development during Ewing's sarcoma tumor growth.

Chapter 6.

The SDF-1 α /PDGF-B pathway plays a critical role in BM- derived pericyte differentiation during Ewing's sarcoma tumor growth

Rationale

We demonstrated that SDF-1 α signaling plays a critical role during blood vessel development of Ewing's sarcoma tumors; inhibiting SDF-1 α signaling in both TC71 and A4573 tumors negatively impacted the tumor blood vessel morphology, decreased the microvessel density and perfusion and, increased tumor cell apoptosis (chapter 5). Given that SDF-1 α functions as a chemotactic stimulus for BMC migration (28, 31) and combined with the previous findings from our group showing that introducing SDF-1 α into VEGF₁₆₅ - inhibited tumors (TC/siVEGF₇₋₁) partially restored vasculogenesis with infiltration of BMCs to a perivascular area where they differentiated into pericytes (40), these observations suggested a role for SDF-1 α signaling in vasculogenesis of Ewing's sarcoma and specifically, in BM-derived pericyte differentiation which supports tumor neo-vascularization.

Furthermore, our studies also demonstrated that introducing SDF-1 α into TC/siVEGF₇₋₁ tumors increased PDGF-B mRNA levels (40). We investigated the correlation between SDF-1 α and PDGF-B and showed that SDF-1 α regulates PDGF-B expression both *in vitro* and *in vivo* (chapters 2 and 3). Given the role of PDGF-B and its receptor, PDGFR- β , in the process of pericyte maturation (51, 55) and studies showing that inhibiting PDGFR- β in a mouse model of pancreatic cancer depleted tumor pericytes and induced their detachment from the vascular endothelium which resulted in blood vessel hyperdilation and disruption (48), we investigated the role of the SDF-1 α /PDGF-B pathway in BM-derived pericyte differentiation. In chapter 4, we confirmed the critical role of the SDF-1 α /PDGF-B pathway *in vitro*. In this chapter, we investigated the role of this pathway

in vivo. We hypothesized that the differentiation of BMCs into pericytes observed in the Ad-SDF-1 α treated TC/siVEGF₇₋₁ tumors (40) and the negative impact observed from inhibiting SDF-1 α signaling using AMD3100 on both the TC71 and A4573 Ewing's sarcoma tumor vasculature, is in fact due to the role of SDF-1 α both as a chemotactic factor for CXCR4+ BMC progenitors and as a regulator of PDGF-B expression.

The effect of AMD3100 on BMC migration to both TC71 and A4573 Ewing's sarcoma tumors was analyzed by performing a BMT from GFP⁺ transgenic mice into nude mice (Figure 1) and staining for BMCs at the distant tumor site. Tumor sections were stained for both GFP and for the CD31 endothelial cell marker to label the tumor vasculature and characterize the distribution of BMCs relative to it. GFP⁺ BMCs migrated to both TC71 and A4573 tumors in both PBS and AMD3100 – treated tumors; however, the distribution and differentiation pattern of these cells was different in both groups. GFP⁺ BMCs predominantly differentiated into endothelial cells and did not form thick perivascular layers surrounding the CD31+ vessels in the AMD3100 – treated mice.

In order to confirm that BMCs do not differentiate into pericytes in the AMD3100 – treated group and to elucidate the role of the SDF-1 α /PDGF-B pathway on BM-derived pericyte differentiation during vasculogenesis of Ewing's sarcoma, we further stained the tumor sections for GFP in combination with both desmin and NG2, mature pericyte markers. We found that AMD3100 decreased BMC differentiation into pericytes in both TC71 and A4573 Ewing's sarcoma tumors. We further validated our hypothesis that SDF-1 α induces BMC differentiation into pericytes via its regulation of PDGF-B by staining the tumor sections for the expression of PDGF-B. We found that Inhibiting SDF-1 α signaling *in vivo* down regulated PDGF-B expression.

All together, our data validates the critical role of the SDF-1 α /PDGF-B pathway in BM-derived pericyte differentiation during vasculogenesis of Ewing's sarcoma.

Results

BMCs migrate to AMD 3100-treated tumors where they predominantly differentiate into ECs but do not form thick perivascular layers

To investigate the effect of AMD 3100 on the migration of GFP⁺ BMCs to both TC71 and A4573 Ewing's sarcoma tumors, we performed a BMT from GFP⁺ transgenic mice into nude mice as previously described (Figure 1). Following engraftment, the mice were subcutaneously implanted with either TC71 or A4573 Ewing's sarcoma cells. Once the tumors became palpable, the mice received a daily subcutaneous injection of either PBS or 5 mg/kg AMD 3100 for the duration of the experiment. Once the longest tumor measurement in the PBS control group reached 2 centimeters (3 weeks following tumor cell injection), all the mice were sacrificed and the tumors resected. Tumor sections were stained for GFP⁺ BM-derived cells (red staining) and for CD31 endothelial cell marker (green staining) in order to analyze the distribution of BMCs relative to the tumor vessels. We found that BMCs migrated to both the AMD 3100 and PBS treated tumors; however, the distribution of these cells within the tumor site was changed. BMCs preferentially co-localized with the CD31 marker within the AMD 3100 treated tumors, indicating that these BMCs differentiated into endothelial cells (yellow staining) but rarely formed perivascular layers surrounding the vessels like the ones observed in the PBS control group (Figure 16).

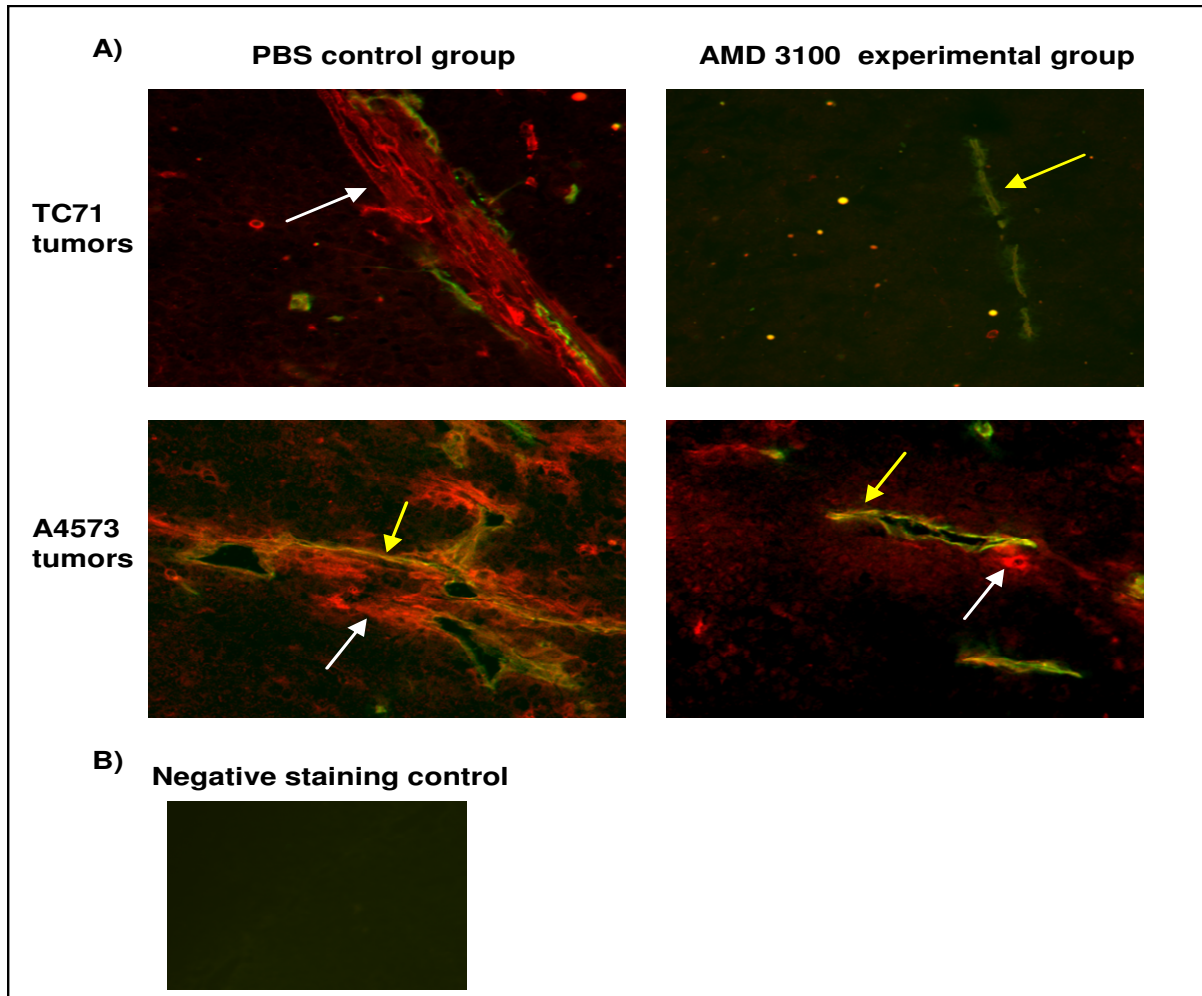


Figure 16. BMCs migrate to both TC71 and A4573 AMD 3100-treated tumors where they differentiate into ECs but do not form thick perivascular layers. Immunohistochemistry (IHC). TC71 (top row) or A4573 (bottom row) Ewing's sarcoma tumors were subcutaneously implanted in GFP⁺ BM-transplanted nude mice. Tumor-bearing mice received daily subcutaneous injections of either PBS or 5mg/kg AMD 3100 for the duration of the experiment. **(A)** Tumor sections were stained for GFP (red) in combination with CD31, an endothelial cell marker (green). GFP⁺ BMCs that migrated to the tumor and co-localized with CD31 (yellow) are depicted by the yellow arrows. GFP⁺ BMCs that formed perivascular layers are depicted by the white arrows. **(B)** Negative staining control. No primary IgG was added only the secondary. 20 x magnification. BMCs migrate to both PBS and AMD 3100-treated mice. BMCs predominantly differentiate into ECs and do not form thick perivascular layers in the AMD 3100 group compared to the PBS control group.

AMD 3100 decreases the differentiation of BMCs into NG2 and desmin positive pericytes in both TC71 and A4573 tumors

Our previous findings demonstrated that BMCs migrate to both AMD 3100 and PBS-treated tumors; however, they do not form thick perivascular layers surrounding the vasculature in the AMD 3100-treated mice. To demonstrate that the decrease in the perivascular layer corresponded to a decrease in BM-derived pericytes, we performed a BMT from GFP⁺ mice into nude mice, subcutaneously implanted the transplanted mice with either TC71 or A4573 Ewing's cells and, administered the AMD 3100 treatment as previously described. The tumors were harvested and tumor sections stained for GFP⁺ BMCs (red staining) in combination with desmin or NG2, pericyte markers (green staining). We found that inhibiting SDF-1 α signaling decreased desmin⁺ (Figure 17A) and NG2⁺ (Figure 17B) BM-derived pericytes in both TC71 and A4573 Ewing's tumors.

Figure 17A. Desmin⁺ BM-derived pericytes

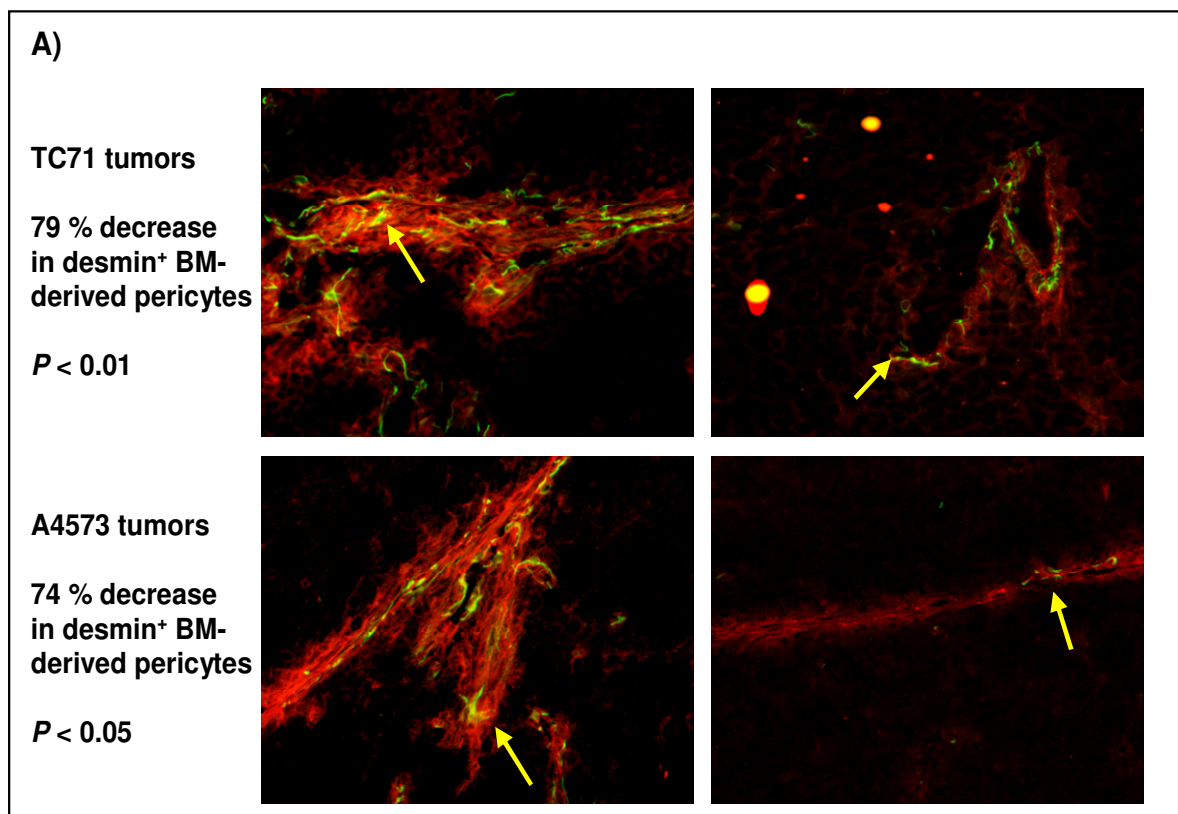


Figure 17B. NG2⁺ BM-derived pericytes

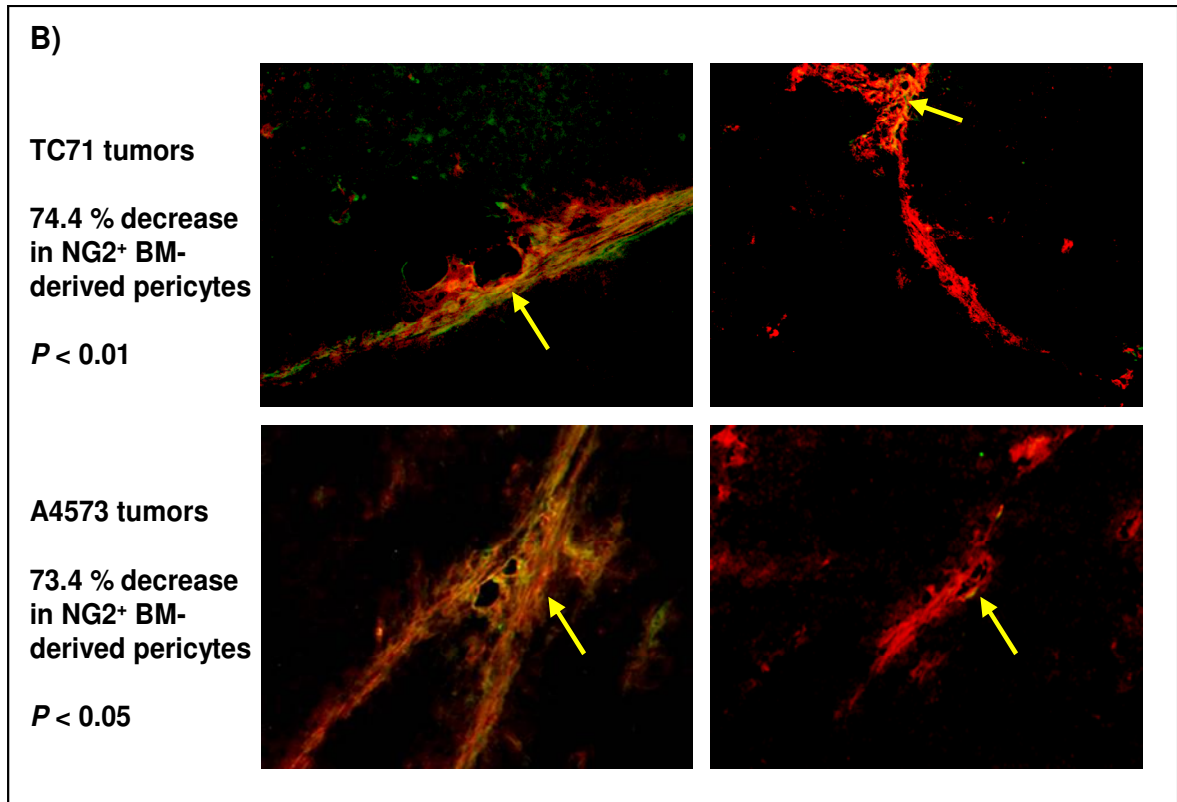


Figure 17. AMD 3100 decreases the differentiation of BMCs into desmin and NG2 positive pericytes in both TC71 and A4573 Ewing's tumors. Immunohistochemistry (IHC). TC71 (top row) or A4573 (bottom row) Ewing's sarcoma tumors were implanted subcutaneously in GFP⁺ BM-transplanted nude mice. The tumor-bearing mice received daily subcutaneous injections of either PBS or 5mg/kg AMD 3100 for the duration of the experiment. Tumors were harvested and tumor sections were stained for **(A)** GFP+ BMCs (red) in combination with desmin (green) and **(B)** GFP+ BMCs (red) in combination with NG2 (green) to identify pericytes. 20 x magnification. GFP+ BMCs that differentiated into pericytes (yellow) are depicted with the yellow arrows. The total amount of green and red pixels were quantified using the SimplePCI software and the ratio calculated to measure the percent decrease in BM-derived desmin and NG2 positive pericytes in response to AMD 3100 compared to PBS as indicated in both panels **(A)** and **(B)**. $P < 0.05$ was considered significant. AMD 3100 decreases the differentiation of BMCs into NG2⁺ pericytes in TC71 and A4573 tumors.

AMD 3100 decreases the total NG2 and desmin⁺ pericyte content in TC71 and A4573 Ewing's tumors

To investigate the effect of AMD 3100 on the overall tumor pericyte content, tumor sections from either the AMD 3100 or PBS treated mice were stained for the CD31 endothelial cell marker (red staining) in combination with either desmin or NG2 mature pericyte markers (green staining) to analyze the amount and distribution of pericytes relative to the vasculature. We then quantified the total amount of green pixels in five random 10x fields using the SimplePCI software. We found that the desmin (Figure 18A) and NG2 (Figure 18B) positive pericyte content was decreased in the AMD 3100 treated mice and that these cells did not form thick loose layers around the vessels as observed in the PBS group in both TC71 and A4573 Ewing's tumors.

Figure 18A. Overall desmin⁺ tumor-associated pericytes

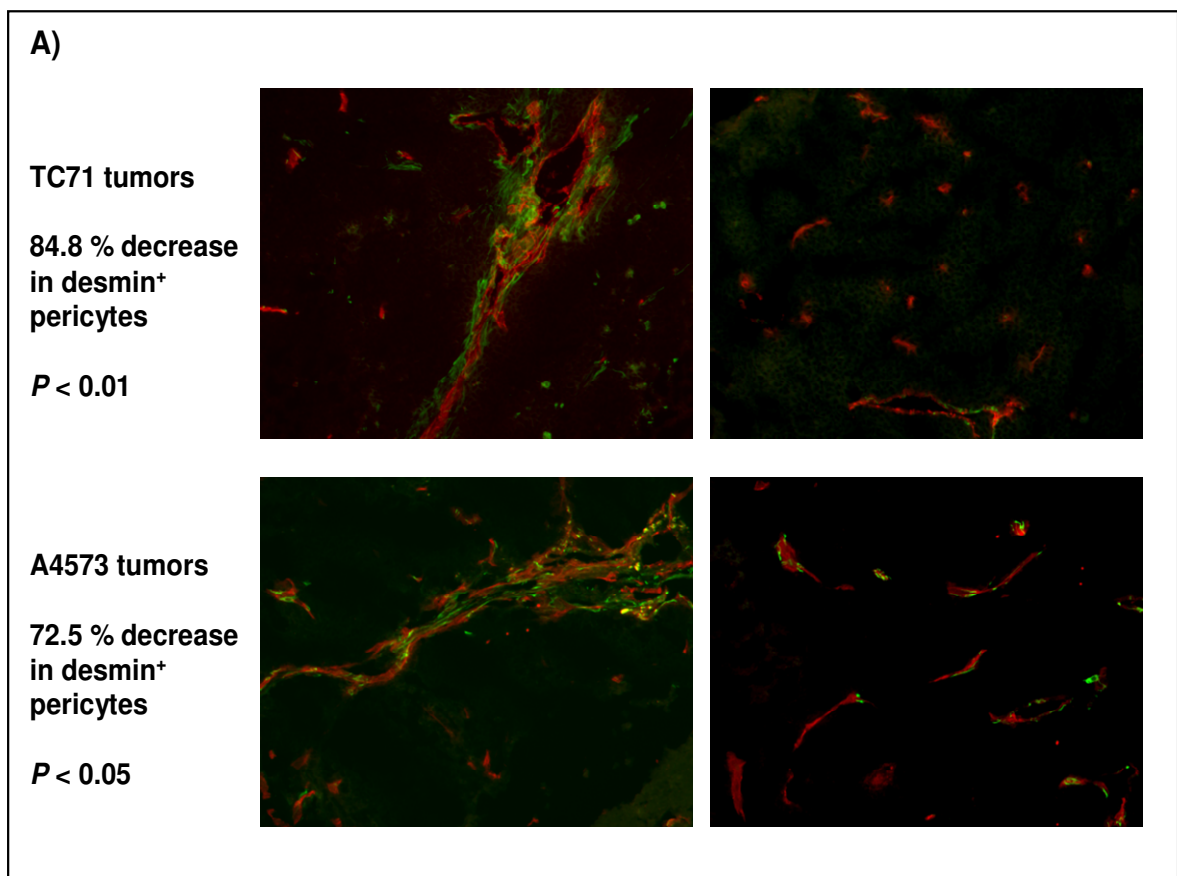


Figure 18B. Overall NG2⁺ tumor-associated pericytes

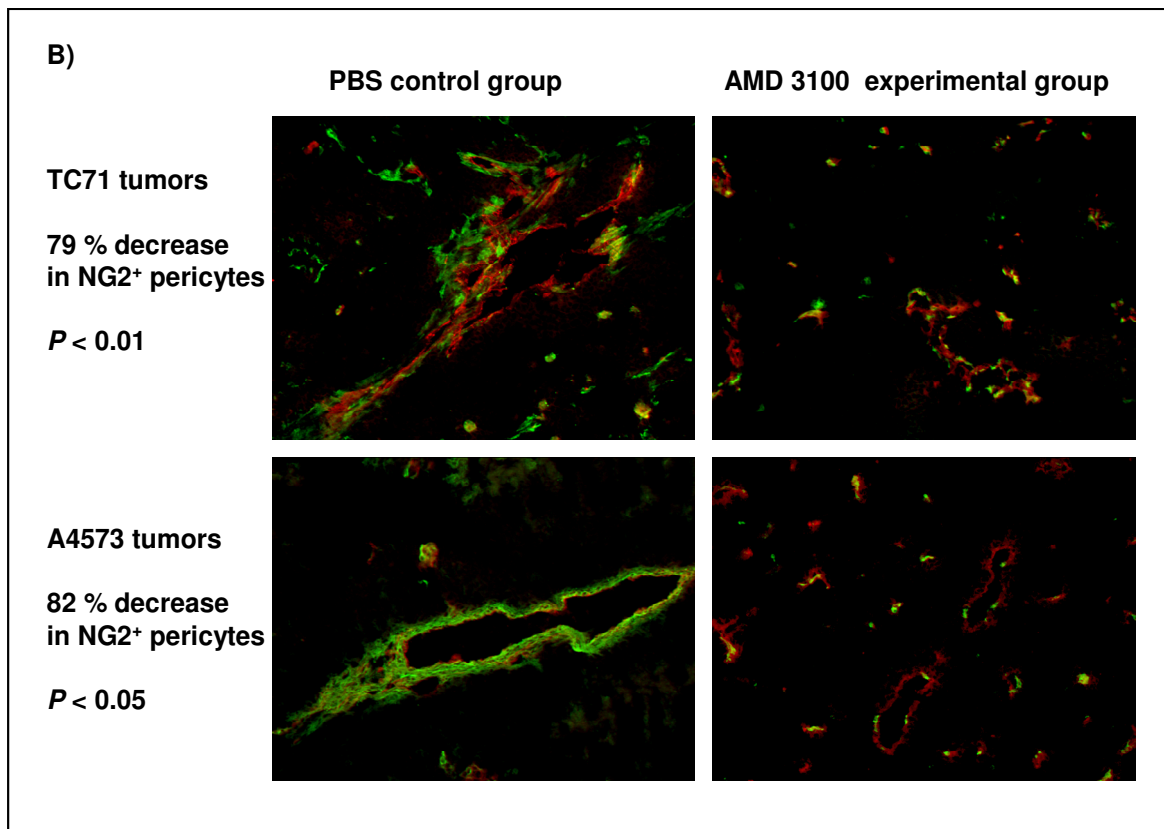


Figure 18. AMD 3100 decreases the total amount of desmin and NG2 pericytes in both TC71 and A4573 Ewing's tumors. Immunohistochemistry (IHC). Nude mice were subcutaneously implanted with either TC71 (top rows) or A4573 (bottom rows) Ewing's sarcoma cells. Once the tumors became palpable, the mice received daily subcutaneous injections of either PBS or 5 mg/kg AMD 3100. All tumors were resected once the longest tumor side measurement in the PBS control group reached a size of 2 centimeters (3 weeks post cell injection). Tumor sections were stained for (A) CD31 endothelial cell marker (red) in combination with desmin or (B) CD31 endothelial cell marker (red) in combination with NG2 (green) to identify pericytes. 10 x magnification. The total positive amount of green pixels for each pericyte marker was quantified and the reduction in overall pericyte content in AMD 3100 compared to PBS-treated tumors was determined using the SimplePCI software. Percent reductions are indicated within both panels (A) and (B). *P* < 0.05 was considered significant. AMD 3100 decreases the overall NG2⁺ pericyte content in the TC71 and A4573 tumors.

AMD3100 decreases PDGF-B expression in Ewing's sarcoma tumors

To demonstrate that inhibiting SDF-1 α signaling in both TC71 and A4573 tumors also down-regulated PDGF-B expression and that the SDF-1 α /PDGF-B pathway is playing a critical role in the differentiation of BMCs into pericytes *in vivo*, tumor sections from either PBS or AMD 3100 treated mice were fixed and analyzed for PDGF-B expression (brown staining). We found that AMD3100 decreased PDGF-B in both TC71 and A4573 tumors compared to PBS (Figure 19).

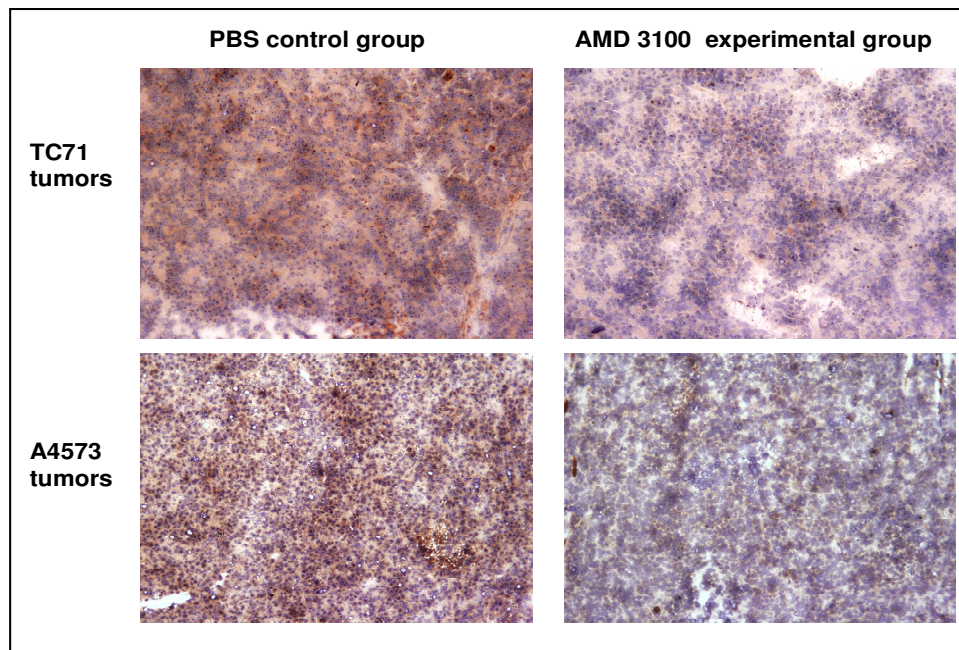


Figure 19. AMD 3100 decreases PDGF-B expression in both TC71 and A4573 Ewing's tumors.

Immunohistochemistry (IHC). Nude mice were subcutaneously implanted with either TC71 (top row) or A4573 (bottom row) Ewing's sarcoma cells. Once the tumors became palpable, the mice received daily subcutaneous injections of either PBS or 5 mg/kg AMD 3100. All tumors were resected once the longest side tumor measurement in the PBS control group reached a size of 2 centimeters (3 weeks post cell injection). Tumor sections were fixed and stained for PDGF-B (brown). 10 x magnification. AMD 3100 decreases PDGF-B expression in TC71 and A4573 tumors.

Summary

In this section, we investigated the role of the SDF-1 α /PDGF-B pathway in BM-derived pericyte differentiation during vasculogenesis of Ewing's sarcoma. SDF-1 α functions as a chemotactic stimulus for CXCR4⁺ BMCs and has been shown to play a role in tumor neo-angiogenesis (31, 35, 39). Previous findings from our lab demonstrated that introducing SDF-1 α into VEGF₁₆₅-inhibited TC71 tumors (TC/siVEGF₇₋₁) induced infiltration of BMCs to a perivascular area and their differentiation into pericytes. SDF-1 α treated TC/siVEGF₇₋₁ tumors also displayed an increase in PDGF-B mRNA levels (40).

In the previous sections, we investigated the correlation between SDF-1 α and PDGF-B and demonstrated that SDF-1 α regulates the expression of PDGF-B both *in vitro* and *in vivo* (chapters 2 and 3). Given the role of PDGF-B and its receptor PDGFR- β in the process of pericyte maturation (51), we then investigated the role of the SDF-1 α /PDGF-B pathway in BM-derived pericyte differentiation and demonstrated that this pathway plays a critical role in the differentiation of BMCs into pericytes *in vitro* (chapter 4).

Here, we treated both TC71 and A4573 tumor-bearing mice with AMD 3100 and showed that inhibiting SDF-1 α signaling decreased the infiltration of BMCs to a perivascular area and their differentiation into pericytes. Furthermore, we tested the AMD 3100-treated tumors for PDGF-B and found that PDGF-B protein expression was also decreased. All together, these findings validated the critical role of the SDF-1 α /PDGF-B pathway in BM-derived pericyte differentiation *in vivo* in the Ewing's sarcoma tumors.

Chapter 7.

**AMD 3100 does not display a therapeutic effect in the treatment of primary Ewing's
sarcoma tumors**

Rationale

Ewing's sarcoma tumors rely on an extensive vascular network for survival and growth (2, 6). We previously demonstrated that BMCs migrate to both TC71 and A4573 Ewing's sarcoma tumors, differentiate into endothelial cells and pericytes and, participate in tumor neo-vascularization. Further studies then confirmed that vasculogenesis is in fact essential for Ewing's sarcoma growth and that VEGF₁₆₅ is the chemotactic stimulus for BMC migration to the tumor site; inhibiting VEGF₁₆₅ inhibited vasculogenesis and tumor growth (10, 16, 25, 65). We introduced SDF-1 α into the VEGF₁₆₅-inhibited tumors (TC/siVEGF₇₋₁) and demonstrated that, while having no effect on VEGF₁₆₅ expression, SDF-1 α partially restored vasculogenesis and rescued tumor growth (40). All together, these findings emphasized the importance of vasculogenesis for Ewing's sarcoma growth and suggested a role for SDF-1 α in this process of tumor neo-vascularization.

In the current study, we investigated the role of SDF-1 α in vasculogenesis of Ewing's sarcoma; specifically, the role of the SDF-1 α /PDGF-B pathway in BM-derived pericyte differentiation. We found that inhibiting SDF-1 α signaling in TC71 and A4573 Ewing's sarcoma tumors down-regulated the expression of PDGF-B while simultaneously inhibiting the differentiation of BMCs into pericytes (chapters 5 and 6). These findings confirmed the critical role of the SDF-1 α /PDGF-B in the process of pericyte differentiation during vasculogenesis of Ewing's sarcoma.

Although pericytes are present in a smaller number within tumors, studies have shown that targeting pericytes in addition to endothelial cells, resulted in a more efficient reduction in tumor vasculature than targeting one or the other alone (48). We analyzed the

tumor vessels in the AMD 3100 treated TC71 and A4573 Ewing's sarcoma tumor-bearing mice and found that inhibiting SDF-1 α signaling resulted in smaller vessels with smaller lumens, decreased vessel perfusion and, increased tumor apoptosis. These observations prompted us to investigate the effect of AMD 3100 on the overall growth of the primary Ewing's sarcoma tumors and its potential as a therapeutic approach in the treatment of the disease.

We subcutaneously injected TC71 or A4573 Ewing's sarcoma cells into nude mice and once the tumors became palpable, the mice received subcutaneous daily injections of either PBS or AMD 3100. Tumor volume was measured starting on day 1 of treatment and twice a week thereafter for the duration of the experiment. Once the longest tumor measurement in the PBS control group reached 2 centimeters (3 weeks), the mice were sacrificed and the final tumor volumes recorded. We found that AMD 3100 did not statistically reduce the TC71 or A4573 tumor volume compared to PBS. We then performed a survival study to investigate whether AMD 3100 stabilized the disease and therefore prolonged the mice survival compared to PBS. For this purpose, the mice were each sacrificed individually once their longest tumor measurement reached 2 centimeters. AMD 3100 did not increase the survival of TC71 or A4573 tumor-bearing mice compared to PBS.

Results

AMD 3100 treatment leads to a trend towards decreased overall tumor volume in both TC71 and A4573 Ewing's tumors

To investigate the effect of inhibiting SDF-1 α signaling and BM-derived pericyte differentiation on the growth of the primary Ewing's sarcoma tumors, we subcutaneously injected mice with either TC71 or A4573 Ewing's sarcoma cells and once the tumors became palpable, the mice received daily subcutaneous injections of either PBS alone or 5mg/kg AMD 3100. The individual tumor volumes were recorded on day 1 of treatment and twice weekly thereafter for the duration of the experiment. All the mice were sacrificed and the tumors resected once the longest tumor measurement in the PBS control group reached 2 centimeters (3 weeks post injection). The volume of each individual tumor in either the PBS or the AMD 3100 group was recorded according to the following formula $\frac{1}{2} \cdot a^2 \cdot b$; a and b represent 2 dimensions of the tumor with a being the longest one. We found that although the tumors in the AMD 3100-treated mice displayed a delay in tumor growth and a trend towards a decreased tumor volume compared to the PBS-treated group, inhibiting SDF-1 α signaling and specifically, the differentiation of BMCs into pericytes, did not statistically inhibit the growth of the primary Ewing's tumors (Figure 20).

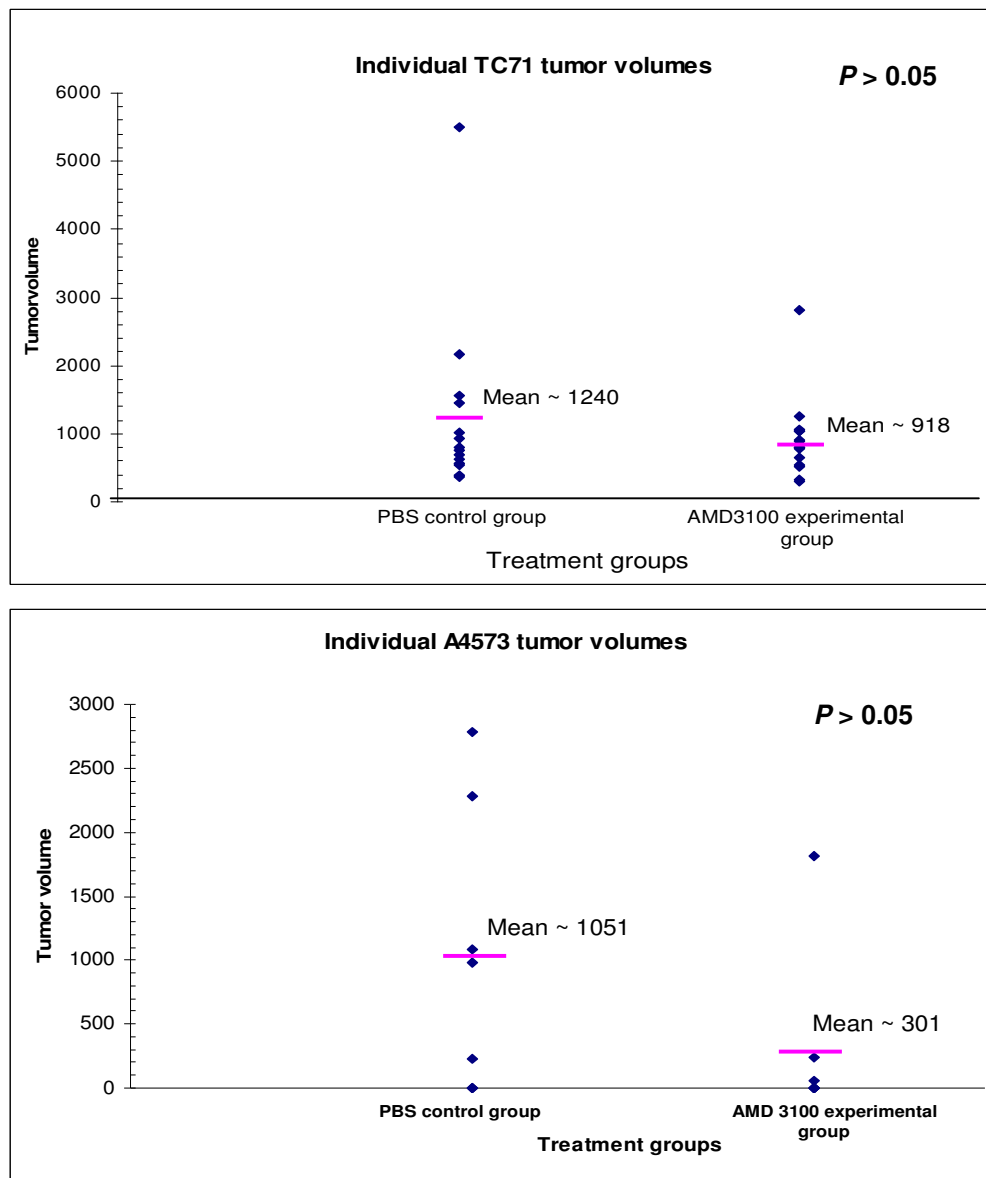


Figure 20. AMD 3100 does not statistically decrease the final TC71 and A4573 tumor volumes compared to PBS. Individual tumor volumes. Nude mice were subcutaneously implanted with either TC71 (top panel) or A4573 (bottom panel) Ewing's sarcoma cells. Tumor-bearing mice received daily subcutaneous injections of either PBS or 5 mg/kg AMD 3100 for the duration of the experiment. All mice were sacrificed 3 weeks post tumor cell inoculation. Individual tumor volumes were recorded on day 1 of treatment and twice weekly thereafter. The graphs indicate the final individual tumor volumes from both groups recorded on day of tumor resection. The data was analyzed using the Mann-Whitney 2-tailed U-test software. $P < 0.05$ was considered significant. AMD 3100 results in a trend towards decreased overall tumor volumes compared to PBS.

AMD 3100 did not increase the survival of TC71 or A4573-tumor bearing mice

Although inhibiting SDF-1 α signaling did not statistically decrease the overall final tumor volume in either the TC71 or A4573 tumors compared to the PBS control group, it led to a trend towards a decreased tumor growth rate. We speculated that maybe AMD 3100 prolonged the survival of the tumor-bearing mice compared to PBS by establishing a stable disease. In order to test this hypothesis, we repeated experiment as previously described; however, this time, we sacrificed the mice individually once each of the tumors' longest side measurement reached 2 centimeters. AMD 3100 did not increase the survival of the primary tumor –bearing mice compared to PBS (Figure 21).

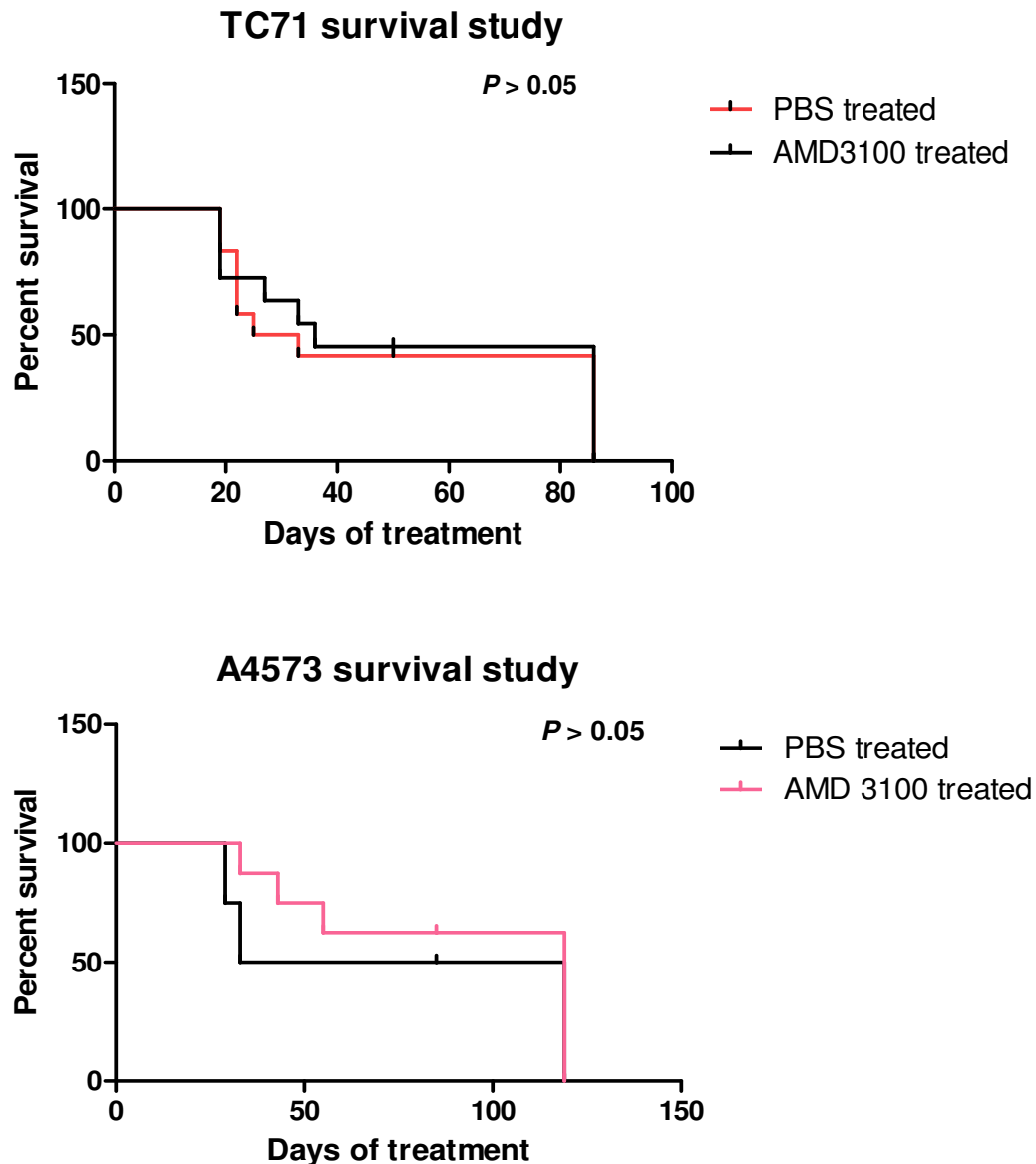


Figure 21. AMD 3100 did not increase the survival of TC71 and A4573 tumor-bearing mice. Survival curves. Nude mice were subcutaneously implanted with either TC71 (top panel) or A4573 (bottom panel) Ewing's sarcoma cells. Once the tumors became palpable, the mice received daily subcutaneous injections of either PBS or 5 mg/kg AMD 3100. Individual mice were sacrificed each at a time once their corresponding longest tumor side measurement reached a size of 2 centimeters. The data was analyzed using the GraphPad Prism software. $P < 0.05$ was considered significant. AMD 3100 did not increase the survival of the TC71 and A4573 primary tumor-bearing mice.

Summary

We previously demonstrated that inhibiting SDF-1 α signaling down-regulated PDGF-B, decreased BM-derived pericyte differentiation and, decreased vascular density. In this section we investigated whether the observed changes in tumor vasculature impacted overall tumor growth. Nude mice were subcutaneously injected with either TC71 or A4573 Ewing's cells. Once the tumors became palpable, the tumor volume was measured and the mice received daily subcutaneous injections of either PBS or AMD 3100. The tumor volumes were recorded twice weekly for the duration of the experiment. Once the longest tumor measurement of a given tumor in the PBS control group reached the maximum size of 2 centimeters, the entire experiment was terminated. We found that AMD 3100 treatment led to a trend towards decreased tumor volume; however, AMD 3100 did not statistically decrease tumor growth rate.

These observations prompted us to investigate whether AMD 3100 treatment and loss of BM-derived pericytes stabilized tumor growth instead and prolonged the overall survival of the tumor-bearing mice. To test this hypothesis, we repeated the experiment as previously described but this time, we sacrificed the mice individually once the longest tumor measurement recorded reached a maximum of 2 centimeters. We found that AMD 3100 did not increase overall survival of the tumor-bearing mice.

Pericytes are present in a low number in tumors and until recently, these cells have been considered abnormal and dysfunctional in tumors and therefore, they have been neglected as potential targets for anti-vascular therapy (42). Pericytes remain a functional constituent of the tumor vasculature and a study in 2007 showed that inhibiting PDGF-B

with the aptamer AX102 led to loss of pericytes and reduced vasculature in a Lewis lung carcinoma model and pancreatic islet cancers. However, the loss in pericytes did not retard tumor growth (58). In contrast, a study in pancreatic islet cancers showed that targeting both endothelial cells as well as pericytes resulted in more efficient reduction of tumor vasculature and tumor growth than targeting one or the other alone (48).

All together, this data suggests a potential therapeutic effect for AMD 3100 as an anti-vascular agent if administered in combination with an anti-VEGF agent rather than a single anti-vascular agent alone in the treatment of Ewing's sarcoma.

Chapter 8.

Appendix

The *pdgf-b*/pGL3 vector is functional

To test whether the *pdgf-b*/pGL3 luciferase construct we generated was functional, we transfected the parental TC71 Ewing's sarcoma cell line, which endogenously expresses PDGF-B, with 50ng/ml of either the *pdgf-b*/PGL3 construct we generated or the PGL3 control vector for 48 hours. The cells were lysed and the luciferase signal was measured and quantified to analyze the *pdgf-b* promoter activity. We found that the *pdgf-b* promoter was activated and our *pdgf-b*/pGL3 construct was indeed functional (Figure A1).

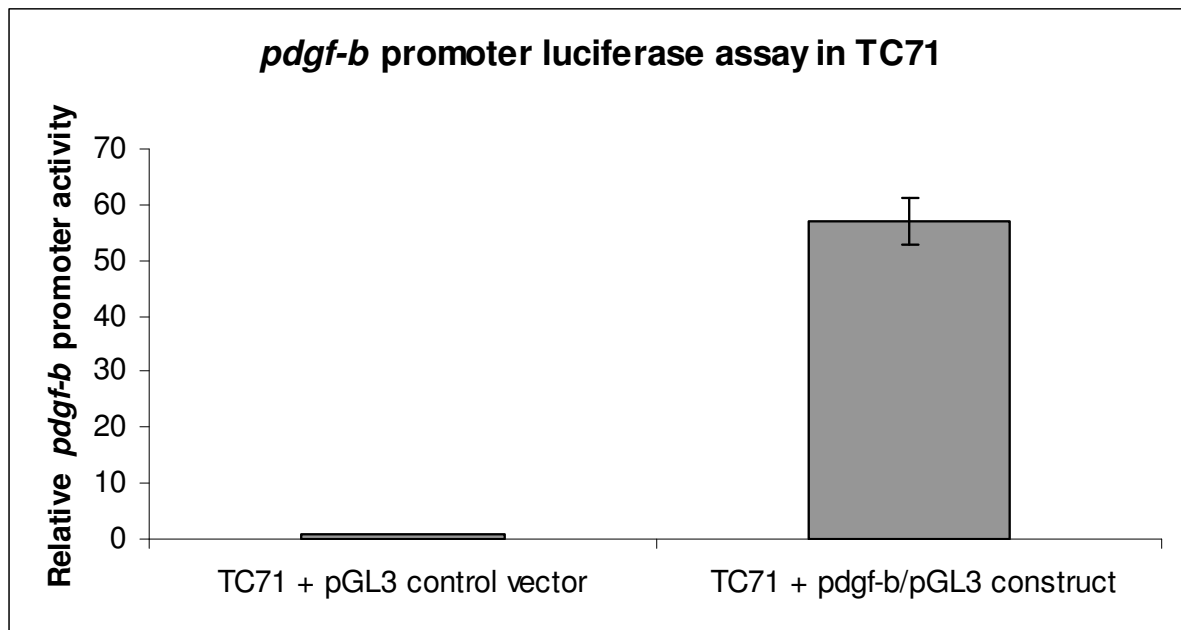


Figure A1. The *pdgf-b*/pGL3 construct is functional. Luciferase assay. The TC71 Ewing's sarcoma parental cell line from which we generated the VEGF₁₆₅-inhibited TC/siVEGF₇₋₁ cell line, endogenously expresses both SDF-1 α and PDGF-B compared to TC/siVEGF₇₋₁. We transfected the TC71 cells with 50 ng/mL of either the *pdgf-b*/ pGL3 construct or the pGL3 control vector for 48 hours. The cells were lysed and the promoter activity analyzed by measuring the total luciferase signal. The *pdgf-b* promoter is activated in TC71 Ewing's sarcoma cells.

SDF-1 α induces the phosphorylation of the ELK-1 transcription factor at serine 383 with a peak at 30 minutes in TC/siVEGF₇₋₁ cells

The ELK-1 transcription factor is activated by phosphorylation at serine 383 (S383) (59, 71). To demonstrate that the recombinant human SDF-1 α protein activated the ELK-1 transcription factor, TC/siVEGF₇₋₁ cells were plated in the absence of growth factors and supplements for 24 hours and treated with either the recombinant human SDF-1 α or 9SDF-1 α inactive protein for 15, 30 or, 60 minutes. The cells were lysed and the nuclear versus cytoplasmic protein extracts were isolated. We performed western blot analysis for total and phosphorylated serine 383 ELK-1 (pELK-1-S383) using lamin B as a nuclear loading control. Both total and p-ELK-1-S383 were normalized to lamin B by densitometry and the ratio of phospho p-ELK-1-S383 to total ELK-1 was measured. We found that SDF-1 α phosphorylated the ELK-1 transcription factor at S383 with a peak at 30 minutes (Figure A2). These findings supported our previous observations that SDF-1 α induced binding of ELK-1 to the *pdgf-b* promoter with a peak at 30 minutes (chapter 3).

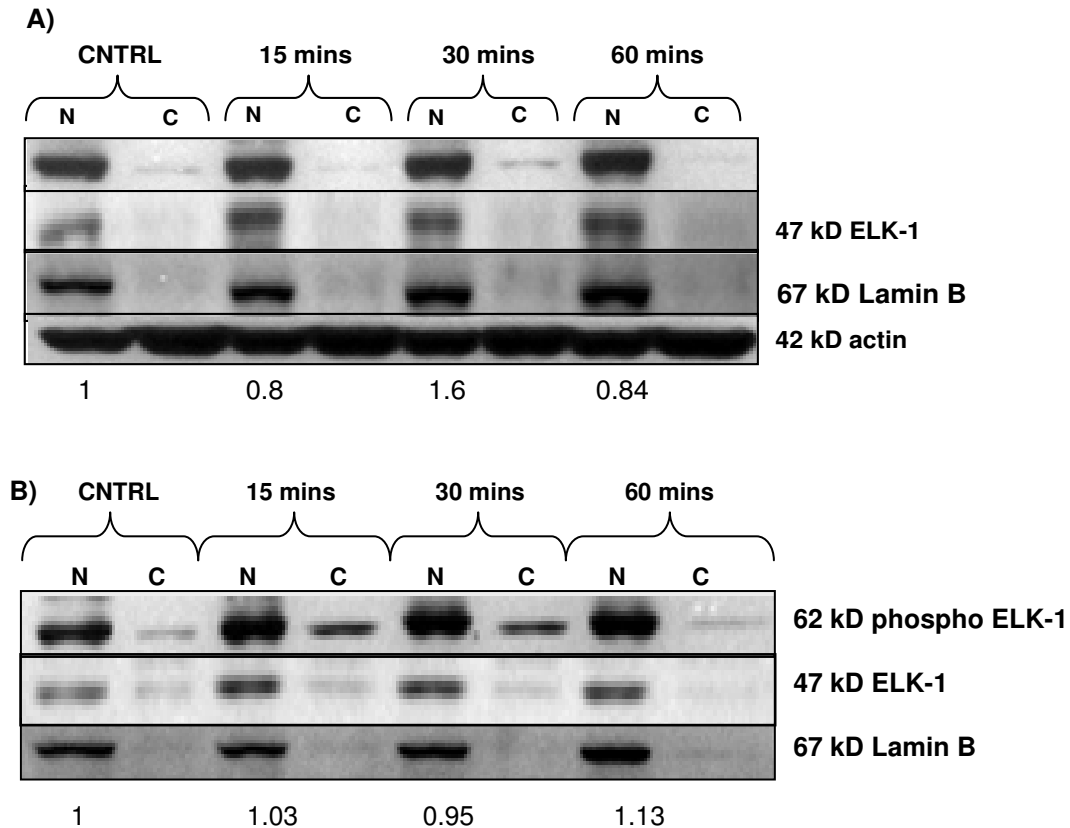


Figure A2. The ELK-1 transcription factor is phosphorylated at S383 in response to SDF-1 α stimulation in TC/siVEGF₇₋₁ cells. Western blot for pELK-1(S383). TC/siVEGF₇₋₁ cells were plated in the absence of growth factors and supplements for 24 hours and then treated with 100 ng/mL of either (A) the recombinant human SDF-1 α protein or (B) the 9SDF-1 α inactive protein for 15, 30 or, 60 minutes. The nuclear versus cytoplasmic extracts were isolated and western blot for total ELK-1, pELK-1-S383 and, lamin B was performed. Actin in panel (A) was used as a loading control to verify the efficiency of the nuclear versus cytoplasmic separation. Densitometry was performed on the bands and both total and p-ELK-1-S383 were normalized to lamin B. The numbers below both panels represent the ratio of normalized pELK-1-S383 relative to normalized total ELK-1 protein. SDF-1 α induces the phosphorylation of ELK-1 at S383 with a peak at 30 minutes post stimulation compared to 9SDF-1 α .

Chapter 9.

Discussion and future directions

Discussion

SDF-1 α regulates PDGF-B by a transcriptional mechanism which involves the ELK-1 transcription factor

We previously demonstrated that inhibiting VEGF₁₆₅ in TC71 tumor cells (TC/siVEGF₇₋₁) resulted in smaller tumors with decreased vasculogenesis and infiltration of bone marrow cells (BMCs) to the tumor site (16, 23, 40). Intratumoral injections with an adenoviral vector containing the SDF-1 α gene (Ad-SDF-1 α) up-regulated the expression of SDF-1 α , increased BM-derived pericytes surrounding the tumor vessels and, rescued tumor growth. Because PDGF-B is involved in pericyte differentiation, we examined sections from the tumors treated with Ad-SDF-1 α for the expression of PDGF-B and found that SDF-1 α gene therapy increased PDGF-B mRNA levels as well as SDF-1 α expression. In contrast, SDF-1 α had no effect on VEGF₁₆₅ (40). These findings suggested a correlation between SDF-1 α , PDGF-B and the formation of pericytes from BMCs.

Platelet derived growth factor B (PDGF-B), a member of the PDGF family of growth factors, is a mitogen for cells of mesenchymal origin such as fibroblasts and smooth muscle cells. When synthesized and secreted in its homodimer form, PDGF-BB binds to its tyrosine kinase receptor, PDGFR- β (49, 53). The expression of PDGF-B and PDGFR- β is usually restricted to a limited number of cell types in areas of vascular development. However, many cancers, including colorectal cancer, pancreatic cancer, glioma, and sarcoma, have been shown to over-express PDGF-B (53, 54, 66). The mechanisms by which PDGF-B is up-regulated in areas of vascular remodeling remain unclear.

PDGF-B expression can be regulated by several mechanisms, including transcriptional regulation (60). Studies by Onimaru and colleagues in 2009 demonstrated that VEGFC can regulate vascular stabilization by controlling PDGF-B expression (67). In the current study, we are the first to demonstrate that SDF-1 α regulates PDGF-B. We stained the tumor sections from the Ad-SDF-1 α treated TC/siVEGF₇₋₁ tumors and confirmed that SDF-1 α up-regulated PDGF-B protein levels as well as mRNA levels (chapter 2). Furthermore, treating two different cell lines (TC/siVEGF₇₋₁ and HEK293) with the recombinant human SDF-1 α increased the expression of PDGF-B mRNA and protein levels *in vitro*. In contrast, an shRNA specific for SDF-1 α down-regulated both SDF-1 α and PDGF-B (chapter 2). We cloned the *pdgf-b* promoter into the pGL3 reporter vector and demonstrated that SDF-1 α activated the *pdgf-b* promoter. These findings demonstrated that SDF-1 α regulates PDGF-B via a transcriptional mechanism (chapter 3).

SDF-1 α or CXCL12 is an alpha chemokine that binds to the 7-transmembrane G-protein coupled receptor CXCR4 (68, 72). Signaling through the SDF-1 α /CXCR4 pathway initiates multiple downstream signaling pathways linked to transcription and expression through MEK1/2 and ERK1/2 for example. ERK can phosphorylate and activate other cellular proteins as well as translocate to the nucleus and phosphorylate and /or activate transcription factors (68). Although the JAK/STAT signaling pathway has also been shown to be activated in response to the SDF-1 α /CXCR4 axis, the involvement of the STAT proteins in signaling in response to CXCR4 activation may depend on the cell type. Several studies have investigated the role of this pathway in hematopoietic cells; however, the effect of SDF-1 α on the JAK/STAT pathway and its role in cell signaling remain an area of investigation (28).

The binding of SDF-1 α to CXCR4 induces phosphorylation of the mitogen-activated protein kinases (MAPKs) p44 ERK-1 and p42 ERK-2, which subsequently initiates the phosphorylation of the nuclear transcription factor ELK-1 (64). The ELK-1 nuclear transcription factor is a member of the 3 ternary complex factors (TCFs), a subfamily of the ETS-domain transcription factors. TCFs are involved in several biological processes and have been shown to be important in regulating angiogenesis and vasculogenesis (59, 62, 63, 73). A study by Kujoth and colleagues in 1998 demonstrated that binding of ETS family members is important for the function of the c-sis/PDGF-B TATA neighboring promoter sequence in K562 human erythroleukemia cells treated with 12-O-tetradecanoylphorbol-13-acetate (60). We therefore investigated whether the ELK-1 transcription factor binds to the *pdgf-b* promoter in response to SDF-1 α stimulation.

We identified potential ELK-1 binding sites both within the *pdgf-b* promoter region at the - 600bp and the transcription start site (TS) and, within the transcribed region at the +1 Kb site. We treated both TC/siVEGF₇₋₁ and HEK293 cells with SDF-1 α for 15, 30 or, 60 minutes and performed chromatin immunoprecipitation (ChIP) on the samples. Real time PCR (q-PCR) showed that the ELK-1 transcription factor bound with high affinity to the *pdgf-b* promoter at the - 600 bp site with a peak at 30 minutes post SDF-1 α stimulation. In contrast, ELK-1 did not bind with high affinity to the TS site in either cell line. We observed a large deviation in binding of ELK-1 at the TS site as indicated by the error bars in the graphs. We hypothesize that this deviation is a result of a cycling between the bound and unbound state of the transcription factor, attributed to the low affinity of ELK-1 for the TS site. The ELK-1 transcription factor recognizes the binding site, but is quickly released. These findings suggest that binding of ELK-1 at the TS site is not critical for the activation

of the *pdgf-b* promoter. As for the + 1 Kb site, we found that while ELK-1 bound to this site in the TC/siVEGF₇₋₁ cells, it did not bind in the HEK293 cells. Further studies are needed to determine the role of this site in the transcription of PDGF-B in the TC/siVEGF₇₋₁ cells.

These observations, combined with our previous findings that SDF-1 α activated the 2 kb *pdgf-b* promoter, suggested that binding of ELK-1 to the – 600 bp site within the *pdgf-b* promoter is sufficient for promoter activation. However, while we demonstrated that ELK-1 is involved in the transcription of PDGF-B, it is difficult to conclude that ELK-1 binding is absolutely essential in this process and whether this transcription factor binds as a single moiety or within a transcriptional protein complex. Members of the ETS family of transcription factors have been shown to bind co-regulator proteins such as the serum response factor (SRF) protein (62). Additional studies would require inhibiting ELK-1 from binding to the – 600 bp site by directly mutating the ELK-1 – 600 bp binding site within the *pdgf-b* promoter for example. An immunoprecipitation assay could also be performed to test whether ELK-1 is binding to the promoter site as a protein complex with the SRF.

The SDF-1 α /PDGF-B pathway plays a critical role in BM-derived pericyte differentiation during vasculogenesis of Ewing's sarcoma

As mentioned above, previous findings from our group demonstrated that treating TC/siVEGF₇₋₁ tumors with Ad-SDF-1 α up-regulated PDGF-B mRNA levels while also restoring vasculogenesis with infiltration of BMCs into the tumor site to a perivascular area where they differentiated into pericytes (40). These observations suggested an association between SDF-1 α , PDGF-B and the formation of pericytes from BMCs. In chapters 2 and 3, we confirmed that SDF-1 α regulated PDGF-B mRNA and protein expression both *in vitro* and *in vivo*. We therefore hypothesized that the increased BM-derived pericyte coverage

observed in the TC/siVEGF₇₋₁ tumors after SDF-1 α gene therapy was a result of the up-regulation of PDGF-B by SDF-1 α .

PDGF-B and its receptor, PDGFR- β , are mainly expressed in the developing vasculature (51). PDGF-B is produced by endothelial cells and PDGFR- β is expressed by pericytes and vascular smooth muscle cells (49). PDGF-B and PDGFR- β have been shown to play a critical role in the process of pericyte maturation. Over expression of PDGF-B in colorectal and pancreatic cancer increased pericyte content (66) whereas lack of PDGFR- β signaling led to pericyte loss, which in turn resulted in endothelial cell changes and capillary dilation and rupture (51, 53). Furthermore, PDGFR- β + pericyte progenitor cells (PPPs) have been shown to migrate to sites of tumor growth, where they differentiated into NG2+, desmin+, and α -SMA+ pericytes (57). In fact, studies by Gabriele Bergers and colleagues showed that HIF1- α , a direct effector of hypoxia, induced recruitment of BM-derived myeloid cells, as well as endothelial and pericyte progenitor cells to promote neo-vascularization in glioblastoma through increases in SDF-1 α (39, 68).

To determine whether the SDF-1 α /PDGF-B pathway played a critical role in the process of pericyte maturation *in vitro*, we established an *in vitro* pericyte differentiation model and investigated the effect of SDF-1 α on PDGFR- β + BMCs collected from the hind femurs of mice. Fresh BMCs expressed the early pericyte marker PDGFR- β but, they did not express the mature pericyte markers, NG2 and desmin. Conditioned medium containing both SDF-1 α and PDGF-B induced PDGFR- β + BMCs to acquire a pericyte-like morphology and to express both NG2 and desmin, indicating pericyte differentiation. This effect was abolished when SDF-1 α was inhibited and PDGF-B expression was decreased. Taken together, our data support the concept of an SDF-1 α /PDGF-B pathway that plays a

critical role in the differentiation of BMCs into mature pericytes *in vitro*. We therefore anticipated that inhibiting SDF-1 α in the Ewing's sarcoma tumor microenvironment would also down-regulate PDGF-B expression and inhibit BMC differentiation into pericytes, with a subsequent negative impact on tumor growth and metastasis.

Pericytes, also known as smooth muscle cells or mural cells, wrap around endothelial cells which together form the basement membrane of the vessel wall (42). Pericytes are recruited by PDGF-B-expressing endothelial cells to the sites of vessel remodeling, where they play a role in vascular stabilization, maturation, and survival (43, 57). Since pericytes appear sparse and detached from the vessel wall in tumors (57), they have been neglected as a potential target for anti-vascular therapy. However, recent studies demonstrated that pericytes are important constituents of the tumor vessel wall (57). Depleting pericytes in a Lewis lung carcinoma tumor model using a DNA oligonucleotide aptamer (AX102) which selectively binds to PDGF-B resulted in regression of the tumor (58).

We investigated the role of SDF-1 α in neo-vascularization of Ewing's sarcoma tumors; specifically, the role of the SDF-1 α /PDGF-B pathway in the differentiation of BMCs into pericytes. We used the SDF-1 α antagonist AMD 3100, a bicyclam molecule which specifically disrupts the SDF-1 α /CXCR4 axis. This drug is currently used in the clinic in patients undergoing allogeneic transplantation due to its effectiveness in mobilizing BMCs from the BM into the peripheral blood while displaying low or no toxic side effects (69, 70). We performed a BMT from GFP⁺ mice into nude mice. one month following engraftment, the mice were subcutaneously injected with either TC71 or A4573 Ewing's sarcoma cells. Once the tumors became palpable, the mice received daily

subcutaneous injections of either PBS or 5 mg/kg AMD 3100 for the duration of the experiment. The experiment was terminated once the maximum tumor side measurement in the PBS control group reached the maximum size of 2 centimeters (~ 3 weeks). The tumors were resected and tumor sections were analyzed by immunohistochemistry (IHC).

We analyzed the effect of AMD 3100 on tumor blood vessel morphology and perfusion in both the TC71 and A4573 Ewing's tumors. Prior to sacrificing the mice, we intravenously (i.v.) injected them with the Hoechst33342 dye in order to label perfused vessels. Tumor sections were stained for the CD31 endothelial cell marker as well to label the blood vessels. We found that inhibiting SDF-1 α signaling in both TC71 and A4573 tumors resulted in smaller vessels with smaller lumens and decreased vessel perfusion compared to PBS. Although our findings cannot determine the effect of SDF-1 α on vessel functionality, they do support the conclusion that the vessels in the AMD 3100 group are less efficient in delivering blood to the tumor mass compared to the PBS control group. To further validate these observations, we performed TUNEL staining on the tumor sections and showed that AMD 3100 treatment increased tumor apoptosis. Taken together, our findings demonstrate that SDF-1 α signaling plays a critical role in tumor vascular development.

To further characterize the role of SDF-1 α signaling in the process of Ewing's sarcoma tumor vascular development, specifically in the differentiation of BMCs into pericytes during vasculogenesis, we stained the tumor sections for GFP to label BMCs, CD31 to label tumor vasculature and, desmin and NG2 to detect mature pericytes. We found that AMD 3100 did not inhibit migration of BMCs to the tumor site. However, the distribution of the BMCs relative to the tumor vasculature *was* affected. The BMCs

preferentially differentiated into endothelial cells and did not form thick perivascular layers surrounding the tumor vessels like the BMCs in the PBS control group. Furthermore, the infiltrating GFP⁺ BMC population did not differentiate into desmin and NG2 positive pericytes.

Taking into consideration our previous studies which demonstrated that VEGF₁₆₅ is over expressed in both TC71 and A4573 Ewing's sarcoma tumors and that this growth factor is the chemotactic stimulus for BMC migration to the tumor site (16, 23); we concluded that the infiltration of BMCs into the AMD 3100- treated mice could be attributed to the expression of VEGF₁₆₅ in the tumor microenvironment. Our previous studies showed that introducing SDF-1 α into VEGF₁₆₅-inhibited tumors did not affect the expression of VEGF₁₆₅ (40). These observations suggest that VEGF₁₆₅ is up-stream of SDF-1 α in the signaling cascade. Therefore, we anticipate that inhibiting SDF-1 α signaling should have no effect on VEGF₁₆₅ expression in both TC71 and A4573 tumors. To summarize, our findings demonstrated a critical role for SDF-1 α signaling in the process of pericyte differentiation during vasculogenesis of Ewing's sarcoma.

We analyzed the overall residual pericyte population in the AMD 3100 treated group by staining for CD31⁺ endothelial cells in combination with desmin and NG2 mature pericyte markers. We found that AMD 3100 decreased the overall number of pericytes compared to PBS within both TC71 and A4573 tumors. We attributed this decrease in pericyte number to the previous findings that inhibiting SDF-1 α signaling inhibited BM-derived pericyte differentiation. We characterized the few remaining pericytes as locally-derived pericytes and not BM-derived as they were negative for GFP. These residual

pericytes remained in close proximity with the CD 31⁺ endothelial cell layer and could potentially function to support the remaining tumor vasculature.

In chapters 2 and 3, we showed that SDF-1 α regulated PDGF-B expression via a transcriptional mechanism and that the SDF-1 α /PDGF-B pathway played a critical role in the differentiation of BMCs into pericytes *in vitro*. To demonstrate that SDF-1 α induces the differentiation of BMCs into pericytes by regulating PDGF-B expression in the tumor microenvironment, we analyzed the effect of AMD 3100 on PDGF-B expression in both TC71 and A4573 tumors. We stained the tumor sections from the AMD 3100 treated tumors for PDGF-B expression and confirmed that inhibiting SDF-1 α signaling *in vivo*, down-regulated PDGF-B. We concluded that the loss in BM-derived pericyte differentiation observed in the AMD 3100-treated mice was an effect of the down-regulation in PDGF-B expression. These findings helped further validate our hypothesis that the SDF-1 α /PDGF-B pathway plays a critical role in BM-derived pericyte differentiation during vasculogenesis of Ewing's sarcoma.

A possible alternative for the decrease in pericyte content observed in the AMD 3100-treated mice could be argued. The loss of pericytes could be attributed to the negative impact of AMD 3100 directly on the blood vessels themselves. Pericytes are defined as the supportive cell layer which surrounds the endothelial cells and maintains the vessel wall (42). Therefore, if the endothelial cell layer is not there to begin with, then that could explain the decrease in BM-derived pericytes. However, several studies including a study by Donald McDonald and colleagues in 2007, demonstrated that inhibiting PDGF-B in Lewis lung carcinomas led to pericyte loss and reduced tumor vascularity. More specifically, they showed that the tumor vascular reduction was in fact secondary to

pericyte loss and suggested that the pericyte layer is necessary for the endothelial cells to form the vessel wall (58). These observations validate our findings that the SDF-1 α /PDGF-B pathway plays a critical role in BM-derived pericyte differentiation.

AMD 3100 as an anti-vascular therapeutic agent

Until recently, pericytes have been considered abnormal and dysfunctional in tumors and therefore, they have been neglected as potential targets for anti-vascular therapy (42). However, recent studies in Lewis lung carcinomas by Donald McDonald and colleagues (58) and in pancreatic islet cancers by Gabriele Bergers and colleagues (42, 48) have demonstrated that although pericytes are present in a smaller number within tumors, targeting pericytes in addition to endothelial cells, resulted in more efficient reduction in tumor vasculature than targeting one or the other alone (48). In the current study, we showed that inhibiting SDF-1 α signaling down-regulated PDGF-B expression and simultaneously inhibited differentiation of BMCs into pericytes which reduced the tumor vasculature (chapters 5 and 6).

We also investigated the effect of inhibiting BM-derived pericyte differentiation on tumor growth in both TC71 and A4573 Ewing's sarcoma tumors. We performed a BMT as previously described (Figure 1). Following engraftment, we subcutaneously injected the mice with either TC71 or A4573 Ewing's cells. Once the tumors became palpable, we measured the tumor volume and started daily subcutaneous injections of either PBS or 5mg/kg AMD 3100. We recorded the tumor volumes twice weekly for the duration of the experiment. The experiment was terminated once the longest tumor side measurement within the PBS control group reached the maximum size of 2 centimeters (3 weeks post tumor cell inoculation). We found that even though AMD 3100 had reduced the tumor

vasculature and resulted with a trend towards smaller tumor volumes, this difference was not statistically significant. We then investigated whether targeting BM-derived pericytes stabilized tumor growth and increased overall mice survival. We performed a survival study where we repeated the experimental design as previously described. This time however, we sacrificed the mice individually once their longest tumor side measurement reached the maximum size of 2 centimeters. We found that AMD 3100 did not statistically prolong survival of the tumor-bearing mice. These findings demonstrated that AMD 3100 had no therapeutic effect when administered as a single anti-vascular agent.

To help interpret our findings, we concluded that inhibiting BM-derived pericyte differentiation specifically was not sufficient to impact overall tumor growth. Even though pericyte content was decreased, we still detected a population of residual locally-derived pericytes. Surprisingly, normal vessels in mice have been shown to tolerate substantial decreases in pericyte density. A study by Abramsson and colleagues in 2003, showed that only a reduction higher than 90% was embryonic lethal (42, 55). These observations suggest that even such a small number of residual pericytes, such as the ones observed in the AMD 3100-treated mice, could be functional and sufficient for vessel stability and endothelial-cell survival.

Targeting pericytes alone is less efficient than targeting both endothelial cells and pericytes individually (42). Similar to our findings, Donald McDonald's study in 2007 where the aptamer AX102 was used to inhibit PDGF-B in Lewis lung carcinomas and pancreatic islet cancers, loss of pericytes resulted in reduced tumor vasculature but did not retard tumor growth (58). In contrast, a study in pancreatic islet cancers by Gabriel Bergers and colleagues in 2003 showed that targeting *both* endothelial cells and pericytes using

anti-VEGF receptors and anti- PDGF receptors in combination was more effective at reducing tumor growth and promised a more effective therapeutic approach (48). To further validate our findings, pericytes in general are less abundant within tumors. In fact, glioblastomas have been shown to contain a substantial number of vessels that are not covered by pericytes. In these tumors, the vessels are more dependent on VEGF signaling for endothelial cell survival. Therefore, targeting VEGF in this tumor type is more efficient at reducing both the tumor vasculature and growth (42, 74). Therefore, we propose to investigate the effect of AMD 3100 on tumor growth when administered in combination with another anti-VEGF agent and anticipate a more efficient vascular reduction and tumor growth inhibition.

Overall, our study demonstrated and suggested a potential mechanism by which SDF-1 α regulates the expression of PDGF-B in the tumor microenvironment during tumor vascular remodeling. Specifically, our findings elucidate the critical role of the SDF-1 α /PDGF-B axis in the differentiation process of BM-derived pericytes which supports vasculogenesis of Ewing's sarcoma. Taking into consideration that most solid tumors rely on an extensive vascular network for their survival and growth and for metastasis to distant organs (6), our study becomes significant and promising not only in targeting Ewing's sarcoma but other solid tumors as well. A tumor vascular system is comparable to a subway system necessary for the delivery of basic resources, such as oxygen and nutrients, to the different "zip codes" in a city. We anticipate that targeting the vascular wall by targeting both endothelial cells and pericytes would induce the vessel wall to collapse and therefore inhibit tumor growth.

Most anti-vascular agents, including those used in the treatment of Ewing's sarcoma, target VEGF as the key regulator of vascular remodeling (75, 76). However, several studies, including our own, have shown that SDF-1 α expression can be induced in the tumor microenvironment and can play a role in tumor neo-vascularization (39, 40). We therefore speculate that SDF-1 α could potentially confer the tumor with an alternate pathway for vascular remodeling in a VEGF-independent manner. We propose that in the absence of VEGF, BMCs can still migrate to the tumor site in response to SDF-1 α where they can participate in tumor neo-vascularization and therefore circumvent the effect of the various anti-VEGF agents currently used in the clinic. Our current study supports these speculations and emphasizes the importance of identifying new growth factors and signaling pathways such as the SDF-1 α /PDGF-B axis as targets for anti-vascular therapy. Our findings also predict a promising effect for AMD 3100 (69, 70) if used in combination with other drugs to target the vasculature in patients with solid tumors.

Understanding the interaction between the tumor and its host environment is essential in establishing new targeted therapies. However, it is important to remember that the tumor mass, as well as the pathways and growth factors its triggers, are heterogeneous. Therefore, uncovering these various signaling pathways and their implications in tumor survival will allow us to engineer new combinational therapies, such as combining anti-VEGF and anti-SDF-1 α (Avastin and AMD 3100) for example, to target both local angiogenesis and vasculogenesis and more efficiently inhibit tumor growth and increase patient survival.

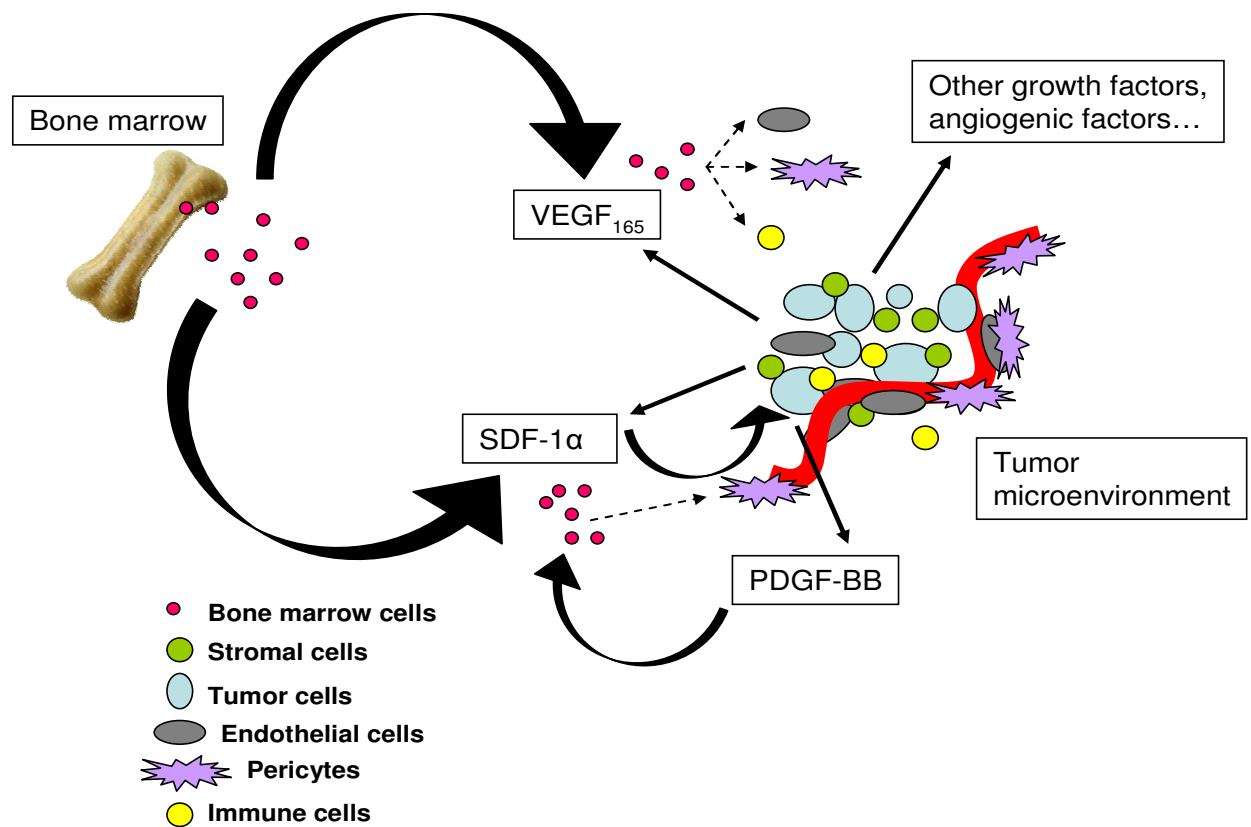


Figure 22. Summary. The tumor and its cell constituents form a heterogeneous microenvironment where different signaling pathways and growth factors such as VEGF₁₆₅, SDF-1α and, PDGF-B are induced. These growth factors play a critical role in promoting both local angiogenesis and vasculogenesis to support tumor neo-vascularization, growth, survival and, invasion. In our current study, we demonstrate that SDF-1α is produced in the tumor microenvironment, acts as a chemotactic factor for BMCs and, induces the expression and secretion of PDGF-BB. PDGF-BB can then bind to its receptor, PDGFR-β, expressed on the surface of infiltrating BMCs and induce their differentiation into mature pericytes. These findings demonstrate the importance of the tumor microenvironment in supporting tumor growth and the need to better understand the signaling pathways that govern tumor survival and progression in order to devise new therapeutic approaches.

Conclusion

SDF-1 α regulates the expression of PDGF-B via a transcriptional mechanism which involves binding of the ELK-1 transcription factor to the *pdgf-b* promoter. This SDF-1 α /PDGF-B pathway plays a critical role in the differentiation of BMCs into pericytes during vasculogenesis of Ewing's sarcoma.

We demonstrated:

1. SDF-1 α regulates the expression of PDGF-B *in vitro* and *in vivo*

We treated TC/siVEGF₇₋₁ tumors in which VEGF₁₆₅ has been down-regulated, with Ad-SDF-1 and showed that it up-regulated PDGF-B mRNA and protein levels. *In vitro*, we treated both the TC/siVEGF₇₋₁ and HEK293 cells with SDF-1 α and showed it up-regulated PDGF-B mRNA and protein levels. In contrast, we down-regulated SDF-1 α in 10T1/2 cells and showed that it down-regulated PDGF-B.

2. SDF-1 α regulates PDGF-B via a transcriptional mechanism

We cloned the *pdgf-b* promoter into a reporter vector and showed that SDF-1 α activated the *pdgf-b* promoter in both TC/siVEGF₇₋₁ and HEK293 cells.

3. SDF-1 α induces binding of the ELK-1 transcription factor to the *pdgf-b* promoter

We treated TC/siVEGF₇₋₁ and HEK293 cells with SDF-1 α and showed that SDF-1 α induced binding of the ELK-1 transcription to the *pdgf-b* promoter with a peak at 30 minutes post-stimulation.

4. The SDF-1 α /PDGF-B pathway plays a critical role in the differentiation of BMCs into pericytes *in vitro*

We showed that BMCs collected from the hind femurs of mice differentiated into mature pericytes which express desmin and NG2 in the presence of SDF-1 α and PDGF-B. In

contrast, we showed that down-regulating SDF-1 α down-regulated PDGF-B and abolished differentiation of BMCs into pericytes.

5. The SDF-1 α /PDGF-B pathway plays a critical role in the differentiation of BMCs into pericytes during vasculogenesis of Ewing's sarcoma

We treated the TC71 and A4573 tumor-bearing mice with the SDF-1 α antagonist AMD 3100 and showed that AMD 3100 led to smaller vessels with smaller lumens, decreased microvessel density and increased tumor apoptosis. We also showed that AMD 3100 down-regulated PDGF-B expression and decreased the differentiation of BMCs into pericytes.

6. AMD 3100 treatment alone did not display a therapeutic advantage in the treatment of TC71 and A4573 Ewing's sarcoma primary tumors

We treated the TC71 and A4573 tumor-bearing mice with the SDF-1 α antagonist AMD 3100 and showed that while AMD 3100 affected the tumor vascular density and morphology, it did not statistically decrease the overall tumor volume or increase the survival of tumor-bearing mice when administered as a single agent in both the TC71 or A4573 Ewing's sarcoma primary tumors.

Future directions

Investigate the therapeutic effect of AMD 3100 on Ewing's sarcoma metastasis

The role of SDF-1 α as a chemotactic gradient for CXCR4⁺ cells and the implication of the SDF-1 α /CXCR4 axis in tumor metastasis has been extensively described (77, 78). For example, recent studies showed that cancer cells which express CXCR4 home to the bone in a manner similar to the homing and retention of hematopoietic stem cells within the bone in response to SDF-1 α gradients (79-81). Ewing's sarcoma, a member of the Ewing's sarcoma family of tumors (ESFT), is the second most common pediatric bone tumor after osteosarcoma (1, 2). Ewing's sarcoma tumors display an aggressive behavior with a tendency towards recurrence following resection and are highly metastatic to the lungs (50%), bone (25%) and bone marrow (20%) (1-3). Despite a survival of about 65 – 75% in non-metastatic Ewing's sarcoma patients, patients with recurrent disease or metastasis at the time of diagnosis, still have only about 20 – 25% overall survival (5). The need for improvement in therapy for patients with Ewing's sarcoma is evident. The SDF-1 α antagonist, AMD 3100 specifically disrupts the SDF-1 α /CXCR4 axis and is currently used in the clinic in patients undergoing allogeneic transplantation due to its effectiveness in mobilizing BMCs from the BM into the peripheral blood while displaying low or no toxic side effects (69, 70). We propose that the SDF-1 α /CXCR4 axis plays a role in Ewing's sarcoma metastasis and therefore, investigating the effect of AMD 3100 as a therapeutic approach for the treatment of the metastatic disease in a mouse model is well merited.

The TC71-PM4 Ewing's cell line is a highly metastatic cell line which was generated from the TC71 parental cell line by repeated cycling through the lungs as

previously described (82). Nude mice will receive daily subcutaneous injections of either PBS or 5mg/kg AMD 3100 starting 3 days prior to them receiving an intravenous injection (i.v.) of the PM4 cells and, daily thereafter for the duration of the experiment. The experiment will be terminated 3-4 weeks following tumor cell inoculation and treatment. The mice will be sacrificed and the lungs resected and analyzed for micrometastasis. We anticipate that inhibiting the SDF-1 α /CXCR4 axis using AMD 3100 should decrease the occurrence of PM4 lung metastasis in mice.

Investigate the possibility of a BM pre-metastatic niche in the lungs which could function to support Ewing's sarcoma metastasis post treatment with AMD 3100

Metastasis is defined as the spread of tumors to distant sites away from the primary tumor and is responsible for the majority of cancer-related deaths (83). In 1889, Stephen Paget observed that circulating tumor cells did not randomly migrate to distant sites and metastasize, but rather, they would only form metastasis when the tumor cell, “seed” found the right microenvironment and factors to support its growth, the “congenial soil” (84). Several studies since have focused on better understanding the changes that take place within the distant metastatic “soil” in order to better understand tumor cell metastasis (80). David Kaplan and colleagues looked at the role of BMCs in the process of tumor metastasis. They demonstrated that VEGFR-1⁺ hematopoietic BM progenitor cells (HPCs) play an essential role in tumor metastasis by initiating the pre-metastatic niche. The BM-derived VEGFR-1⁺ cells were observed in the metastatic sites as early as 14 days after tumor implantation and prior to the arrival of the metastatic tumor cells. Antibodies specific to VEGFR-1 inhibited the formation of the pre-metastatic niches and prevented tumor metastasis. Furthermore, SDF-1 α was highly expressed in the fully formed metastatic

niches which suggested that SDF-1 α mediated the recruitment and adherence of the incoming CXCR4⁺ cells (80, 85).

In our current study, we used the SDF-1 α antagonist AMD 3100 due to its specificity in disrupting the SDF-1 α /CXCR4 axis. This drug is currently used in the clinic in patients undergoing allogeneic transplantation due to its effectiveness in mobilizing BMCs from the BM into the peripheral blood while displaying low or no toxic side effects (69, 70). Although AMD 3100 inhibited BMCs from infiltrating and differentiating into pericytes within the Ewing's sarcoma tumors, we anticipate that AMD 3100 induces a high influx of BMCs from the BM into the circulation. Here, we propose investigating whether this influx of BMCs can promote the formation of a pre-metastatic niche which could subsequently increase the tumor metastasis incidence post AMD 3100 treatment. These studies are important and clinically relevant prior to using AMD 3100 as an anti-vascular therapy. For even if AMD 3100 could be beneficial as an anti-vascular approach for the treatment of primary tumors; it may in fact be detrimental and augment tumor invasiveness and metastasis and, thereby, negatively impact overall patient survival.

A bone marrow transplant (BMT) from GFP⁺ transgenic mice into nude mice will be performed (Figure 1). Following a period of 1 month for engraftment, the mice will receive a subcutaneous injection of either TC71 or A4573 Ewing's sarcoma tumors. Once the tumors become palpable, the mice will receive daily subcutaneous injections of either PBS or 5mg/kg AMD 3100 for a period of 3 weeks. Mice from each group will be sacrificed the day treatment is started and twice a week while treatment is being administered and the lungs collected and analyzed for the presence of GFP⁺ BMCs and micrometastasis. At the end of 3 weeks, all primary tumors will be surgically resected and

the mice allowed to recover. Mice from each group will continue to be sacrificed twice weekly post surgery and their lungs collected and analyzed for GFP⁺ BMCs and micrometastasis.

We anticipate that as long as AMD 3100 is being administered, BMCs and CXCR4⁺ tumor cells should not be able to stick and adhere within the lungs in response to SDF-1 α signaling specifically. However, it is possible that other angiogenic growth factors are being expressed in the lungs such as VEGF which could compensate for the loss in SDF-1 α signaling and consequently allow the BMCs to form a pre-metastatic niche and promote metastasis via an SDF-1 α -independent mechanism. On the other hand, SDF-1 α inhibition by AMD 3100 is reversible; therefore, we anticipate that once we stop delivering the AMD 3100 drug, the mobilized BMCs should be able to stick, adhere and, form a pre-metastatic niche which might increase the incidence of tumor metastasis to the lungs.

Investigate the therapeutic effect of AMD 3100 in combination with DC101 anti-VEGFR-2 in Ewing's sarcoma

In the current study, we demonstrated that SDF-1 α played a critical role in vasculogenesis of Ewing's sarcoma; specifically, in the differentiation of BMCs into pericytes during tumor neo-vascularization. Treating tumor-bearing mice with the SDF-1 α antagonist, AMD 3100, led to smaller vessels with smaller lumens, decreased vessel perfusion, and, increased tumor apoptosis (chapter 5); however, when we analyzed the therapeutic effect of AMD 3100 on the primary Ewing's sarcoma tumors, we found that inhibiting SDF-1 α did not statistically decrease overall tumor volume or increase the survival of the tumor-bearing mice (chapter 8). Our findings correlated with the observations made by Donald McDonald and colleagues in Lewis lung carcinomas and

pancreatic islet cancers where they used the aptamer AX102 to inhibit PDGF-B and showed that although the tumor vasculature was reduced, it did not retard the tumor growth (58). On the other hand, Gabriel Bergers and colleagues in 2003 showed that targeting both endothelial cells and pericytes by targeting both VEGF and PDGF receptors in combination, was more effective at reducing tumor growth and promised a more effective therapeutic approach (48). Furthermore, our lab demonstrated that vasculogenesis is essential for Ewing's sarcoma and that VEGF₁₆₅ is the chemotactic stimulus for BMC migration to the tumor site (10, 16, 23). We used DC101, a VEGF receptor 2 inhibiting antibody and showed that DC101 significantly inhibited the growth of Ewing's sarcoma (25). All together, the essential roles of both SDF-1 α and VEGF in tumor vascular development of Ewing's sarcoma imply that administering AMD 3100 not as a single agent but rather, in combination with a compound such as DC101 in order to target VEGF may result in increased tumor growth inhibition. Findings from these studies could be used as preliminary insights into the potential of clinical trials involving combination studies using AMD 3100 with bevacizumab or avastin (anti-VEGF) for targeting both angiogenesis and vasculogenesis simultaneously and consequently result with a more effective anti-vascular approach for the treatment of this disease.

Chapter 10.
Materials and Methods

Cell lines and culture

We used the human Ewing's sarcoma cell lines A4573, TC71 and, VEGF₁₆₅ - inhibited TC/siVEGF₇₋₁ generated by stable transfection of VEGF₁₆₅ siRNA into TC71. TC/siVEGF₇₋₁ cells express all the VEGF isoforms except VEGF₁₆₅ (24). Human embryonic kidney 293 (HEK293) cells and C3H/10T1/2 murine embryonic mesenchymal cells were purchased from ATCC (Manassas, VA; CRL-1573, CCL-226). TC/siVEGF₇₋₁ and HEK293 cells express low levels of endogenous SDF-1 α and PDGF-B compared with C3H/10T1/2 cells. All cells were cultured in complete Dulbecco's modified Eagle's medium (DMEM) supplemented with 10% fetal bovine serum (FBS), 2 mM L-glutamine, 1 mM nonessential amino acids, 1 mM penicillin-streptomycin, and 2x vitamin solution (Gibco BRL, Grand Island, NY).

Proteins and antibodies

Recombinant human SDF-1 α was purchased from R&D Systems (Minneapolis, MN; 350-NS-010/CF). The inactive 9SDF-1 α recombinant protein used as a negative control was a generous gift from Dr. Qing Ma at The University of Texas MD Anderson Cancer Center. Rabbit polyclonal immunoglobulin (IgG) to human ELK-1, rabbit polyclonal IgG to mouse desmin and, chicken polyclonal IgG to GFP were purchased from Abcam (Cambridge, MA; ab28831, ab15-200, ab13970). ChromPure rabbit control IgG was purchased from Jackson ImmunoResearch Laboratories (West Grove, PA; 011-000-003). Rabbit polyclonal IgG to mouse PDGF-BB (N-30) and rabbit polyclonal IgG to mouse PDGFR- β (P-20) were purchased from Santa Cruz Biotechnology (CA; sc-127, sc-339). Rabbit polyclonal IgG to mouse NG2 chondroitin sulfate proteoglycan was purchased from Millipore (Bedford, MA; AB5320). Rabbit polyclonal IgG to phospho-ELK-1 (serine

383) and ELK-1 were purchased from Cell Signaling Technology (Danvers, MA; 9181, 9182).

q-PCR

TC/siVEGF₇₋₁ and HEK293 cells were cultured in vitro in the absence of growth factors and supplements for 8 hours and then treated with 100ng/mL of either the recombinant human SDF-1 α protein or the inactive 9SDF- α inactive protein for 24 hours. RNA was collected by the TRIzol method (Invitrogen, Grand Island, NY). Briefly, the medium was removed and the cells were treated with 1mL of TRIzol for 5 minutes at room temperature (RT). The cells were collected, and 200 μ L of chloroform (Fisher Scientific, Pittsburgh, PA) was added for 3 minutes at RT. The mixture was then centrifuged in the Centrifuge 5415-R (Eppendorf, Westbury, NY) for 15 minutes at 4°C. The upper clear phase was collected, and 500 μ L of isopropanol (Fisher Scientific) was added for 10 minutes at RT. The solution was centrifuged for 10 minutes at 4°C, and the pellet was re-suspended and washed 2 times with 75% ethanol for 5 minutes at 4°C. The pellet was air-dried, re-suspended in 30 μ L of nuclease-free water (Promega, Sunnyvale, CA), and incubated at 65°C for 5 minutes. cDNA was synthesized using a reverse-transcription system (Promega). Real-time quantitative reverse-transcription polymerase chain reaction (q-PCR) was performed using iQ-SYBR Green Supermix with the iCycler iQ (Bio-Rad Laboratories, Hercules, CA).

ELISA

TC/siVEGF₇₋₁ and HEK293 cells were cultured in vitro in the absence of growth factors and supplements for 8 hours and then treated with 100ng/mL of either SDF-1 α or the inactive 9SDF-1 α protein for 36 hours. The supernatant was collected and concentrated using Amicon Ultra-15, PLGC Ultracel-PL Membrane, 10 kDa (Millipore) by centrifuging

at 2500rpm for 30 minutes at 4°C in the Centrifuge 5804R (Eppendorf). PDGF-B protein levels were measured by enzyme-linked immunosorbent assay (ELISA) (R&D Systems, Minneapolis, MN; MBB00) according to the manufacturer's protocol.

ShRNA knockdown of SDF-1 α in C3H/10T1/2 cells

SDF-1 shRNA Plasmid (m) (sh-SDF-1) and Control shRNA Plasmid-A (sh-control) were purchased from Santa Cruz Biotechnology (sc-39368-SH, sc-108060). C3H/10T1/2 (10T1/2) cells were cultured in vitro and transfected with 1 μ g of either sh-SDF-1 or sh-control using FuGENE 6 (Roche Applied Science, Indianapolis, IN) according to the manufacturer's directions. At 48 hours after transfection, the medium was replaced with fresh DMEM and the cells were cultured under puromycin selection (2 μ g/mL) (InvivoGen, San Diego, CA). RNA was isolated using the TRIzol method, and cDNA was synthesized using a reverse-transcription system (Promega). Down-regulation of SDF-1 α was confirmed by q-PCR.

***pdgf-b* promoter cloning**

DNA was isolated from TC71 Ewing's sarcoma cells. The 2-kb *pdgf-b* promoter DNA fragment was isolated by PCR. Briefly, primers were designed and synthesized using Integrated DNA Technologies (IDT). All sequences are available upon request. The PCR product was run on a 1% agarose gel, and the 2-kb *pdgf-b* promoter DNA fragment was isolated and purified using the QIAquick Gel Extraction Kit (QIAGEN, Valencia, CA; 28704). The purified sequence was ligated into the pCR2.1-TOPO expression vector using the TOPO TA Cloning Kit (Invitrogen, Carlsbad, CA; K4560-01). The vector was isolated and purified with the QIAprep Spin Miniprep Kit (QIAGEN; 27104) according to the manufacturer's directions, and the DNA sequence was verified by SeqWright DNA

Technology Services (Houston, TX). The 2 kb *pdgf-b* promoter DNA fragment was then isolated and cloned into the pGL3-Basic luciferase reporter vector (Promega BioSciences, San Luis Obispo, CA; E1751). The *pdgf-b*/pGL3 reporter vector sequence was verified by SeqWright DNA Technology Services. To test the functionality of the *pdgf-b*/pGL3 construct, we used 50ng of the construct to transfect TC71 cells and the *pdgf-b* promoter activity was tested by measuring the luciferase signal.

Dual-luciferase reporter assay

We used 50 ng of either the *pdgf-b*/pGL3 reporter construct or the pGL3-Control vector (Promega BioSciences; E1761) to transfect TC/siVEGF₇₋₁ and HEK293 cells using FuGENE 6 (Roche Applied Science) according to the manufacturer's directions. Beginning 48 hours after transfection, the cells were cultured in the absence of growth factors and supplements for 24 hours and then treated with 100 ng/mL of either the recombinant SDF-1 α or the inactive 9SDF-1 α protein for 8 hours. The cells were lysed and the luciferase signal measured using the Dual-Luciferase Reporter Assay System (Promega BioSciences; E1910) according to the manufacturer's instructions.

Western blot analysis

TC/siVEGF₇₋₁ cells were cultured in the absence of growth factors and supplements for 24 hours and then treated with 100 ng/mL of either the recombinant human SDF-1 α or 9SDF-1 α inactive proteins for 15, 30 or, 60 minutes. The cells were lysed and the nuclear versus cytoplasmic extracts were isolated according to the manufacturers instructions (Active Motif, Carlsbad, CA; 40010). Protein concentration was measured by the Bradford protein assay. 50 μ g of protein was mixed with (2x) SDS loading dye, boiled at 100°C for 5 minutes and, loaded on a 10% acrylamide gel for 3 hours at 95 volts. The proteins were then

transferred onto a nitrocellulose membrane at 95 volts for 1 hour at RT. The gel was discarded and the membrane collected, blocked with 5% bovine serum albumin (BSA) for 1 hour at RT and probed for either phospho-ELK-1 S383 or total ELK-diluted 1:500 in BSA blocking solution O/N at 4°C. The membrane was washed 3 times for 10 minutes in 1x TBST and probed with the ECL anti-rabbit IgG horseradish peroxidase-linked whole antibody (GE Healthcare, Little Chalfont Buckinghamshire, UK; NA934V) at 1:1500 in blocking solution for 1 hour. The membrane was washed 3 times for 10 minutes with 1x TBST and exposed with the ECL Western Blotting Analysis System (RPN2109) for 2 minutes at RT.

ChIP assay

Potential ELK-1 binding sites within the 2-kb *pdgf-b* promoter region were identified using the GeneRegulation.com MATCH software. 2 sites at -600bp and at the transcription start site (TS) which scored > 85% were analyzed by chromatin immunoprecipitation (ChIP) (Millipore) according to the manufacturer's instructions. Briefly, TC/siVEGF₇₋₁ and HEK293 cells were cultured in the absence of growth factors and supplements for 24 hours and then treated with 100 ng/mL recombinant human SDF-1 α for 15, 30, or 60 minutes. The cells were collected and the proteins cross-linked to the DNA by incubating in 36% formaldehyde for 10 minutes at RT. The cells were sonicated and the DNA sheered using the Sonicator 3000 (Misonix, Farmingdale, NY) to produce fragments of 400- 800 bp. The lysates were pre-cleared with protein A/G agarose for 2 hours at 4°C and incubated with the anti-ELK-1 rabbit polyclonal antibody (Abcam) O/N at 4°C. The ELK-1/DNA/Ab complex was immunoprecipitated, isolated, and washed. Cros- linking was reversed with 5% NaCl at

65°C O/N. The DNA was isolated using the QIAquick PCR Purification Kit (Qiagen). We confirmed binding of ELK-1 by q-PCR.

Primer sequences

Primers for the human *pdgf-b* promoter and for human PDGF-B were designed and synthesized using Integrated DNA Technologies (IDT, Coralville, IA). Primers for human ELK-1 binding sites, for mouse SDF-1 α and PDGF-B, and, for real time (q-PCR) were synthesized using Sigma-Genosys.com. Please refer to table 1 for primer sequences.

<u>Target</u>	<u>Forward primer</u>	<u>Reverse primer</u>
Human PDGF-B	TGCTGTTGAGGTGGTGTAGATGGT	AGTCGTGGCTGGGTTGGAATATGA
Human <i>pdgf-b</i> promoter	TGTCCGGTGGAAGAGGGTTTTT	CTCCCGGCTGCAGGAGGAGA
Human ELK-1 (-600bp) binding site	GGAGATAGTAAACAGCAGGGTGACTGACGG	CTCCTAGCTGGTTGCCTGGCACAAC
Human ELK-1 (TS) binding site	CCAGAAGAGGAAAGGCTGTCTCCACCCAC	CTGCAGGAGGAGAAGTTGCCACCCTTTC
Human ELK-1 (+1Kb) binding site	GGAGTCGGCATGAATCGCTGCTGG	CAACTCACCTCGGCGCTGACCAGA C
Mouse SDF-1 α	CTTCATCCCCATTCTCTCTCA	GACTCTGCTCTGGTGGAAGG
Mouse PDGF-B	AAAGACACCTTCTTGAGGGA	ATTAAGGTGGCGCGATAGGTCCTT
RT human PDGF-B	CTTGACACTTCCCCATCTT	CTTGGGGATCTTTCCCTTC
RT mouse SDF-1 α	CCAAACTGTGCCCTTCAGAT	TGGGCTGTTGTGCTTACTTG
RT mouse PDGF-B	GGCCACACACCTTCTCTGAT	AAATGAACCGGAAGTGAACG

Table 1. Forward and reverse primers.

In vitro pericyte differentiation model

Whole BMCs were isolated from nude mice by flushing their hind femurs with sterile PBS. Fresh BMCs were analyzed for PDGFR- β , desmin, and NG2 expression. Briefly, the cells were collected and then cytospun onto glass slides by centrifuging at 30 rpm for 2mins at RT in the Shandon Cytospin 2 centrifuge (Shandon Southern Products, Astmore, United

Kingdom). To establish an in vitro pericyte differentiation model, we collected BMCs and cultured the cells in a 2-well Culture-Slide (BD Biosciences, Woburn, MA; 354102) either in complete DMEM alone or in conditioned medium obtained from 10T1/2, sh-SDF-1-10T1/2 or sh-control- 10T1/2 cells (previously generated). Supernatant from the corresponding cells was collected, spun down at 1200 rpm for 5 minutes at 4°C in the Centrifuge 5804R (Eppendorf) to remove any debris or floating cells, and added to the freshly collected BMCs. BMCs were kept in culture for 2 weeks and stained for the expression of PDGFR- β , desmin, and NG2 pericyte markers.

2-well chamber immunocytochemistry staining

BMCs were collected and cultured as previously described. The cells were fixed with cold acetone for 10 minutes, washed with PBS 3 times for 3 minutes, and incubated with blocking solution (4% normal fish serum in PBS) for 20 minutes at RT. Anti-PDGFR- β , anti-desmin, or anti-NG2 (1:600) in 4% blocking solution was added to the slides O/N at 4°C. The slides were washed with PBS 3 times for 3 minutes and incubated in blocking solution for 10 minutes at RT. Alexa Fluor-594 secondary (Molecular Probes, Eugene, OR; 1:1000 in blocking solution) was added for 1 hour at RT, and the slides were washed with PBS 3 times for 3 minutes. Nuclei were stained with Hoechst 33342 dye (Molecular Probes; 1:10,000 in PBS) for 1 minute and the slides were washed with PBS 3 times for 3 minutes. Images were captured using a Zeiss Axioplan fluorescence microscope (Carl Zeiss MicroImaging, Thornwood, NY) equipped with a 100-W Hg lamp and narrow bandpass excitation filters. Images were obtained using a cooled charge-coupled device Hamamatsu C5810 camera (Hamamatsu Photonics, Bridgewater, NJ).

Statistical analysis

We used STATISTICA 6.0, Anova on-way software to analyze all the q-PCR, ELISA and ChIP results. For ChIP, the sample values minus the control values were used in one-way analysis of variance, with post hoc analysis using the Fisher least significant difference to determine significant differences. For the animal studies and quantification data, we used the SimplePCI and the Mann-Whitney 2-tailed U-test software. $P < 0.05$ was considered statistically significant.

Animals

All animal experiments were approved by the Institutional Animal Care and Use Committee at The University of Texas M.D. Anderson Cancer Center. GFP⁺ transgenic mice used as donor mice in our BMT experiments, were purchased from Jackson laboratories (Strain c57bl/6-tg (actb-egfp)1osb/j). BALB/cAnN nude mice were purchased at four to six weeks old from either the National Cancer Institute (strain 01B70) or Charles River (strain nu/nu 088).

TC71 and A4573 Ewing's sarcoma tumor models

Nude mice were implanted subcutaneously with either TC71 (2×10^6 cells/0.2mL sterile PBS) or A4573 (6×10^6 total cells given as 2 separate injections of 3×10^6 /0.2 mL sterile PBS at day 1 and day 3 following the one month period of engraftment) Ewing's sarcoma cells. The cells were checked for mycoplasma prior to injection and used at passages three to seven. All injections were performed using a 30 gage needle and using a 1 cc disposable syringe. Tumors were resected once the longest tumor side measurement in the PBS control group reached 2 centimeters. Resected tumors were snap frozen in Optimal Cutting

Temperature (OCT) solution (Sakura Finetek USA, Torrance, CA) and stored at -80°C for further analysis.

SDF-1 α gene therapy on TC/siVEGF₇₋₁ Ewing's sarcoma tumors

TC/siVEGF₇₋₁ cells were implanted subcutaneously on the ventral side of nude mice (4×10^6 /mouse). 3 days post tumor cell inoculation, the mice received intratumoral injections of Ad-SDF-1 α or Ad-control (2.53×10^8 pfu/50 μL /administration/mouse). A total of 5 injections were administered over a period of 3 weeks. On day 23 after tumor cell inoculation, all tumors were carefully excised, weighed, placed in OCT, snap-frozen in liquid nitrogen, and stored at -80°C for further analysis (40).

Bone marrow transplant model (BMT; Figure 1)

Bone marrow cells (BMCs) were collected from GFP transgenic by removing the hind femurs of mice, cutting the bone ends with sterile scissors and, flushing the bone marrow with sterile PBS using a 10 mL sterile syringe and 30 gauge needle. BMCs were then pelleted and re-suspended in sterile PBS. Meanwhile, nude mice were subjected to whole body lethal irradiation (900 rad) using a Cesium irradiator (137Cs Mark 1 Irradiator; J. L. Shepherd & Associates, Glendale, CA) to eradicate the endogenous BMCs. We then rescued the irradiated mice by injecting them intravenously (i.v.) with the previously collected GFP⁺ BMCs. At least 1×10^6 GFP⁺ BMCs/ mouse are needed to ensure successful reconstitution. The mice were allowed to recover for a period of one month prior to tumor cell injection to ensure BMC engraftment. Transplant success was confirmed by collecting BMCs as previously described from at least three representative mice and tested for GFP expression by flow cytometry (BD FACS Aria, BD Biosciences). A transplant was considered successful if at least 90% of BMCs were GFP⁺.

PDGF-B immunohistochemistry and microscopy

Frozen Tumor sections were cut, fixed with cold acetone for 5 minutes, acetone/chloroform for 5 minutes and, cold acetone for another 5 minutes. The slides were washed with PBS 3 times for 3 minutes and incubated with blocking solution (5% normal horse serum + 1% normal goat serum in PBS) for 20 minutes at RT. PDGF-B rabbit polyclonal IgG diluted at 1:100 in blocking solution was added to the slides O/N at 4°C. The slides were washed with PBS 3 times for 3 minutes and incubated with blocking solution for 10 minutes at RT. Biotinylated goat anti-rabbit IgG (Biocare Medical, Concord, CA; GR608H) was added for 30 minutes at RT, and the slides were washed with PBS 3 times for 3 minutes. The slides were incubated with 4plus streptavidin horseradish peroxidase (HRP) (Biocare Medical; HP604H) for 30 minutes at RT and washed with PBS 3 times for 3 minutes with PBS. 3,3'-Diaminobenzidine (DAB) (Research Genetics, Huntsville, AL) was added for 5-10 minutes, and the slides were washed with distilled water 3 times for 3 minutes. The slides were counterstained with Gill's hematoxylin #3 (Sigma-Aldrich, St. Louis, MO; GHS316). Images were captured using a Nikon Microphot-FXA microscope (Nikon Instruments, Melville, NY).

Hoechst perfusion assay

Nude mice were injected with either TC71 or A4573 Ewing's sarcoma cells as previously described. However, in order to label vessel perfusion, we performed intravenous (i.v.) injections of the Hoechst nuclear dye (Molecular Probes, Invitrogen, CA; 33342). 1.2mg/0.1mL of the Hoechst33342 was intravenously (i.v.) injected 2 minutes prior to sacrificing the mice by cervical dislocation.

Fluorescent immunohistochemistry analysis (IHC)

Tumor sections were fixed with cold acetone for 10 minutes, washed with PBS 3 times for 3 minutes and incubated with blocking solution (4% fish serum in PBS) for 20 minutes at RT. Primary IgGs were diluted in blocking solution and added to the slides O/N at 4°C (refer to table 2). The slides were washed with PBS 3 times for 3 minutes and incubated with blocking solution for 10 minutes at RT. All secondary IgGs were diluted 1:1000 in blocking solution and added to the slides for 1 hour at RT (refer to table 2). The slides were washed with PBS 3 times for 3 minutes, incubated with Hoechst33342 (nuclear stain) diluted 1:10,000 in PBS for 30 seconds and, washed with PBS 3 times for 3 minutes.

<u>Primary antibody</u>	<u>Dilution factor</u>	<u>Company</u>
Chicken anti- GFP	1: 800	Abcam, Cambridge, MA
Rabbit anti- mouse desmin	1: 400	Abcam, Cambridge, MA
Rabbit anti- mouse NG2	1: 600	Millipore, Billerica, MA
Rat anti- mouse CD31	1:500	BD Biosciences, Franklin Lakes, NJ
<u>Secondary antibody</u>		
Alexa Flour 488 (anti-rat/anti-rabbit)	1: 1000	Molecular Probes, Eugene, OR
Alexa Flour 594 (anti-rabbit/anti-chicken)	1: 1000	Molecular Probes, Eugene, OR

Table 2. Immunohistochemistry primary and secondary antibodies.

TUNEL staining and microscopy

Frozen Tumor sections were cut and fixed with 4% paraformaldehyde in PBS 20 minutes at RT. The slides were washed with PBS 3 times for 3 minutes and distilled water 1 time for 3 minutes then treated with proteinase K (20mg/mL) diluted 1:1000 in distilled water for 10 minutes at RT. The slides were washed with distilled water 4 times for 1 minute, incubated

with 3% H₂O₂ in methanol for 12 minutes and, washed with distilled water 4 times for 1 minute and with 1x TdT buffer in water for 2 minutes. The slides were then incubated with Terminal Transferase diluted 1:400 + Biotin 16dUTP diluted 1:200 in 1x TdT buffer O/N at 4°C. Next, the slides were washed with PBS 2 times for 5 minutes and distilled water 3 times for 1 minute then incubated with 5% normal horse serum diluted in 2% bovine serum albumin in distilled water for 10 minutes at RT. The slides were washed with distilled water 3 times for 1 minute and PBS 1 time for 1 minute then incubated with 4plus streptavidin horseradish peroxidase (HRP; Biocare Medical; HP604H) for 30 minutes at RT. The slides were washed with PBS 3 times for 3 minutes. 3,3'-Diaminobenzidine (DAB; Research Genetics, Huntsville, AL) was added for 3 minutes and the slides were washed with distilled water 3 times for 3 minutes. The slides were counterstained with Gill's hematoxylin #3 (Sigma-Aldrich, St. Louis, MO; GHS316). Images were captured using a Nikon Microphot-FXA microscope (Nikon Instruments, Melville, NY).

Microscopy

Images were captured with a Zeiss Axioplan fluorescence microscope (Carl Zeiss, Inc., Thornwood, NY) equipped with a 100-W Hg lamp and narrow bandpass excitation filters and the representative pictures were obtained using a cooled charge-coupled device Hamamatsu C5810 camera (Hamamatsu Photonics, Bridgewater, NJ) with the Optimas imaging software (Media Cybernetics, Bethesda, MD).

Immunohistochemistry quantification

Five random fields at either 10x or 20 x-magnification were captured from each slide from both the PBS and the AMD 3100-treated groups. The total positive pixels for each marker were measured using the SimplePCI software (Hamamatsu, Sewickley, PA). We then

measured the mean pixel area of positive fluorescence for each of the protein of interests from each tumor section. For the pericyte differentiation studies, the ratio of desmin or NG2 positive to GFP positive pixels was measured.

Bibliography

1. Balamuth, N. J., and R. B. Womer. Ewing's sarcoma. *Lancet Oncol* 11:184-192.
2. Riggi, N., and I. Stamenkovic. 2007. The Biology of Ewing sarcoma. *Cancer Lett* 254:1-10.
3. Weber, K. L., and F. H. Sim. 2001. Ewing's sarcoma: presentation and management. *J Orthop Sci* 6:366-371.
4. Leavey, P. J., and A. B. Collier. 2008. Ewing sarcoma: prognostic criteria, outcomes and future treatment. *Expert Rev Anticancer Ther* 8:617-624.
5. Anderson, P., L. Kopp, N. Anderson, K. Cornelius, C. Herzog, D. Hughes, and W. Huh. 2008. Novel bone cancer drugs: investigational agents and control paradigms for primary bone sarcomas (Ewing's sarcoma and osteosarcoma). *Expert Opin Investig Drugs* 17:1703-1715.
6. Folkman, J. 1971. Tumor angiogenesis: therapeutic implications. *N Engl J Med* 285:1182-1186.
7. Doi, Y., H. Kudo, T. Nishino, and S. Fujimoto. 2003. [Vasculogenesis and angiogenesis]. *J UOEH* 25:409-417.
8. Kopp, H. G., C. A. Ramos, and S. Rafii. 2006. Contribution of endothelial progenitors and proangiogenic hematopoietic cells to vascularization of tumor and ischemic tissue. *Curr Opin Hematol* 13:175-181.
9. Asahara, T., and A. Kawamoto. 2004. Endothelial progenitor cells for postnatal vasculogenesis. *Am J Physiol Cell Physiol* 287:C572-579.

10. Bolontrade, M. F., R. R. Zhou, and E. S. Kleinerman. 2002. Vasculogenesis Plays a Role in the Growth of Ewing's Sarcoma in Vivo. *Clin Cancer Res* 8:3622-3627.
11. Schmidt, A., K. Brixius, and W. Bloch. 2007. Endothelial precursor cell migration during vasculogenesis. *Circ Res* 101:125-136.
12. Asahara, T., H. Masuda, T. Takahashi, C. Kalka, C. Pastore, M. Silver, M. Kearne, M. Magner, and J. M. Isner. 1999. Bone marrow origin of endothelial progenitor cells responsible for postnatal vasculogenesis in physiological and pathological neovascularization. *Circ Res* 85:221-228.
13. Yamaguchi, J., K. F. Kusano, O. Masuo, A. Kawamoto, M. Silver, S. Murasawa, M. Bosch-Marce, H. Masuda, D. W. Losordo, J. M. Isner, and T. Asahara. 2003. Stromal cell-derived factor-1 effects on ex vivo expanded endothelial progenitor cell recruitment for ischemic neovascularization. *Circulation* 107:1322-1328.
14. Lyden, D., K. Hattori, S. Dias, C. Costa, P. Blaikie, L. Butros, A. Chadburn, B. Heissig, W. Marks, L. Witte, Y. Wu, D. Hicklin, Z. Zhu, N. R. Hackett, R. G. Crystal, M. A. Moore, K. A. Hajjar, K. Manova, R. Benezra, and S. Rafii. 2001. Impaired recruitment of bone-marrow-derived endothelial and hematopoietic precursor cells blocks tumor angiogenesis and growth. *Nat Med* 7:1194-1201.
15. Ribatti, D., A. Vacca, B. Nico, L. Roncali, and F. Dammacco. 2001. Postnatal vasculogenesis. *Mech Dev* 100:157-163.
16. Lee, T. H., M. F. Bolontrade, L. L. Worth, H. Guan, L. M. Ellis, and E. S. Kleinerman. 2006. Production of VEGF165 by Ewing's sarcoma cells induces vasculogenesis and the incorporation of CD34+ stem cells into the expanding tumor vasculature. *Int J Cancer* 119:839-846.

17. Yu, L., B. Su, M. Hollomon, Y. Deng, V. Facchinetti, and E. S. Kleinerman. Vasculogenesis driven by bone marrow-derived cells is essential for growth of Ewing's sarcomas. *Cancer Res* 70:1334-1343.
18. Reddy, K., Z. Zhou, K. Schadler, S. F. Jia, and E. S. Kleinerman. 2008. Bone marrow subsets differentiate into endothelial cells and pericytes contributing to Ewing's tumor vessels. *Mol Cancer Res* 6:929-936.
19. Costa, C., R. Soares, and F. Schmitt. 2004. Angiogenesis: now and then. *APMIS* 112:402-412.
20. Hicklin, D. J., and L. M. Ellis. 2005. Role of the vascular endothelial growth factor pathway in tumor growth and angiogenesis. *J Clin Oncol* 23:1011-1027.
21. Brown, L. F., M. Detmar, K. Claffey, J. A. Nagy, D. Feng, A. M. Dvorak, and H. F. Dvorak. 1997. Vascular permeability factor/vascular endothelial growth factor: a multifunctional angiogenic cytokine. *EXS* 79:233-269.
22. Zhou, Z., M. F. Bolontrade, K. Reddy, X. Duan, H. Guan, L. Yu, D. J. Hicklin, and E. S. Kleinerman. 2007. Suppression of Ewing's sarcoma tumor growth, tumor vessel formation, and vasculogenesis following anti vascular endothelial growth factor receptor-2 therapy. *Clin Cancer Res* 13:4867-4873.
23. Reddy, K., Y. Cao, Z. Zhou, L. Yu, S. F. Jia, and E. S. Kleinerman. 2008. VEGF(165) expression in the tumor microenvironment influences the differentiation of bone marrow-derived pericytes that contribute to the Ewing's sarcoma vasculature. *Angiogenesis*.

24. Guan, H., Z. Zhou, H. Wang, S. F. Jia, W. Liu, and E. S. Kleinerman. 2005. A small interfering RNA targeting vascular endothelial growth factor inhibits Ewing's sarcoma growth in a xenograft mouse model. *Clin Cancer Res* 11:2662-2669.
25. Zhou, Z., K. Reddy, H. Guan, and E. S. Kleinerman. 2007. VEGF(165), but not VEGF(189), stimulates vasculogenesis and bone marrow cell migration into Ewing's sarcoma tumors in vivo. *Mol Cancer Res* 5:1125-1132.
26. Juarez, J., L. Bendall, and K. Bradstock. 2004. Chemokines and their receptors as therapeutic targets: the role of the SDF-1/CXCR4 axis. *Curr Pharm Des* 10:1245-1259.
27. Mackay, C. R. 2001. Chemokines: immunology's high impact factors. *Nat Immunol* 2:95-101.
28. Kucia, M., K. Jankowski, R. Reca, M. Wysoczynski, L. Bandura, D. J. Allendorf, J. Zhang, J. Ratajczak, and M. Z. Ratajczak. 2004. CXCR4-SDF-1 signalling, locomotion, chemotaxis and adhesion. *J Mol Histol* 35:233-245.
29. Ganju, R. K., S. A. Brubaker, J. Meyer, P. Dutt, Y. Yang, S. Qin, W. Newman, and J. E. Groopman. 1998. The alpha-chemokine, stromal cell-derived factor-1alpha, binds to the transmembrane G-protein-coupled CXCR-4 receptor and activates multiple signal transduction pathways. *J Biol Chem* 273:23169-23175.
30. Maksym, R. B., M. Tarnowski, K. Grymula, J. Tarnowska, M. Wysoczynski, R. Liu, B. Czerny, J. Ratajczak, M. Kucia, and M. Z. Ratajczak. 2009. The role of stromal-derived factor-1--CXCR7 axis in development and cancer. *Eur J Pharmacol* 625:31-40.

31. Lapidot, T., and O. Kollet. 2002. The essential roles of the chemokine SDF-1 and its receptor CXCR4 in human stem cell homing and repopulation of transplanted immune-deficient NOD/SCID and NOD/SCID/B2m(null) mice. *Leukemia* 16:1992-2003.
32. Hernandez, P. A., R. J. Gorlin, J. N. Lukens, S. Taniuchi, J. Bohinjec, F. Francois, M. E. Klotman, and G. A. Diaz. 2003. Mutations in the chemokine receptor gene CXCR4 are associated with WHIM syndrome, a combined immunodeficiency disease. *Nat Genet* 34:70-74.
33. Teicher, B. A., and S. P. Fricker. CXCL12 (SDF-1)/CXCR4 pathway in cancer. *Clin Cancer Res* 16:2927-2931.
34. Ma, Q., D. Jones, and T. A. Springer. 1999. The chemokine receptor CXCR4 is required for the retention of B lineage and granulocytic precursors within the bone marrow microenvironment. *Immunity* 10:463-471.
35. Li, M., and R. M. Ransohoff. 2009. The roles of chemokine CXCL12 in embryonic and brain tumor angiogenesis. *Semin Cancer Biol* 19:111-115.
36. De Falco, E., D. Porcelli, A. R. Torella, S. Straino, M. G. Iachininoto, A. Orlandi, S. Truffa, P. Biglioli, M. Napolitano, M. C. Capogrossi, and M. Pesce. 2004. SDF-1 involvement in endothelial phenotype and ischemia-induced recruitment of bone marrow progenitor cells. *Blood* 104:3472-3482.
37. Moore, M. A., K. Hattori, B. Heissig, J. H. Shieh, S. Dias, R. G. Crystal, and S. Rafii. 2001. Mobilization of endothelial and hematopoietic stem and progenitor cells by adenovector-mediated elevation of serum levels of SDF-1, VEGF, and angiopoietin-1. *Ann N Y Acad Sci* 938:36-45; discussion 45-37.

38. Hattori, K., B. Heissig, K. Tashiro, T. Honjo, M. Tateno, J. H. Shieh, N. R. Hackett, M. S. Quitarano, R. G. Crystal, S. Rafii, and M. A. Moore. 2001. Plasma elevation of stromal cell-derived factor-1 induces mobilization of mature and immature hematopoietic progenitor and stem cells. *Blood* 97:3354-3360.
39. Du, R., K. V. Lu, C. Petritsch, P. Liu, R. Ganss, E. Passegue, H. Song, S. Vandenberg, R. S. Johnson, Z. Werb, and G. Bergers. 2008. HIF1alpha induces the recruitment of bone marrow-derived vascular modulatory cells to regulate tumor angiogenesis and invasion. *Cancer Cell* 13:206-220.
40. Reddy, K., Z. Zhou, S. F. Jia, T. H. Lee, J. Morales-Arias, Y. Cao, and E. S. Kleinerman. 2008. Stromal cell-derived factor-1 stimulates vasculogenesis and enhances Ewing's sarcoma tumor growth in the absence of vascular endothelial growth factor. *Int J Cancer* 123:831-837.
41. Aghi, M., K. S. Cohen, R. J. Klein, D. T. Scadden, and E. A. Chiocca. 2006. Tumor stromal-derived factor-1 recruits vascular progenitors to mitotic neovasculature, where microenvironment influences their differentiated phenotypes. *Cancer Res* 66:9054-9064.
42. Bergers, G., and S. Song. 2005. The role of pericytes in blood-vessel formation and maintenance. *Neuro Oncol* 7:452-464.
43. Hirschi, K. K., and P. A. D'Amore. 1996. Pericytes in the microvasculature. *Cardiovasc Res* 32:687-698.
44. Majno, G., G. E. Palade, and G. I. Schoefl. 1961. Studies on inflammation. II. The site of action of histamine and serotonin along the vascular tree: a topographic study. *J Biophys Biochem Cytol* 11:607-626.

45. Rucker, H. K., H. J. Wynder, and W. E. Thomas. 2000. Cellular mechanisms of CNS pericytes. *Brain Res Bull* 51:363-369.
46. Crocker, D. J., T. M. Murad, and J. C. Geer. 1970. Role of the pericyte in wound healing. An ultrastructural study. *Exp Mol Pathol* 13:51-65.
47. Raza, A., M. J. Franklin, and A. Z. Dudek. Pericytes and vessel maturation during tumor angiogenesis and metastasis. *Am J Hematol* 85:593-598.
48. Bergers, G., S. Song, N. Meyer-Morse, E. Bergsland, and D. Hanahan. 2003. Benefits of targeting both pericytes and endothelial cells in the tumor vasculature with kinase inhibitors. *J Clin Invest* 111:1287-1295.
49. Fredriksson, L., H. Li, and U. Eriksson. 2004. The PDGF family: four gene products form five dimeric isoforms. *Cytokine Growth Factor Rev* 15:197-204.
50. Bondjers, C., M. Kalen, M. Hellstrom, S. J. Scheidl, A. Abramsson, O. Renner, P. Lindahl, H. Cho, J. Kehrl, and C. Betsholtz. 2003. Transcription profiling of platelet-derived growth factor-B-deficient mouse embryos identifies RGS5 as a novel marker for pericytes and vascular smooth muscle cells. *Am J Pathol* 162:721-729.
51. Hellstrom, M., M. Kalen, P. Lindahl, A. Abramsson, and C. Betsholtz. 1999. Role of PDGF-B and PDGFR-beta in recruitment of vascular smooth muscle cells and pericytes during embryonic blood vessel formation in the mouse. *Development* 126:3047-3055.
52. Lindahl, P., B. R. Johansson, P. Leveen, and C. Betsholtz. 1997. Pericyte loss and microaneurysm formation in PDGF-B-deficient mice. *Science* 277:242-245.

53. Westermarck, B., and C. H. Heldin. 1993. Platelet-derived growth factor. Structure, function and implications in normal and malignant cell growth. *Acta Oncol* 32:101-105.
54. Fomchenko, E. I., and E. C. Holland. 2007. Platelet-derived growth factor-mediated gliomagenesis and brain tumor recruitment. *Neurosurg Clin N Am* 18:39-58, viii.
55. Abramsson, A., P. Lindblom, and C. Betsholtz. 2003. Endothelial and nonendothelial sources of PDGF-B regulate pericyte recruitment and influence vascular pattern formation in tumors. *J Clin Invest* 112:1142-1151.
56. Rajantie, I., M. Ilmonen, A. Alminae, U. Ozerdem, K. Alitalo, and P. Salven. 2004. Adult bone marrow-derived cells recruited during angiogenesis comprise precursors for periendothelial vascular mural cells. *Blood* 104:2084-2086.
57. Song, S., A. J. Ewald, W. Stallcup, Z. Werb, and G. Bergers. 2005. PDGFRbeta+ perivascular progenitor cells in tumours regulate pericyte differentiation and vascular survival. *Nat Cell Biol* 7:870-879.
58. Sennino, B., B. L. Falcon, D. McCauley, T. Le, T. McCauley, J. C. Kurz, A. Haskell, D. M. Epstein, and D. M. McDonald. 2007. Sequential loss of tumor vessel pericytes and endothelial cells after inhibition of platelet-derived growth factor B by selective aptamer AX102. *Cancer Res* 67:7358-7367.
59. Buchwalter, G., C. Gross, and B. Wasylyk. 2004. Ets ternary complex transcription factors. *Gene* 324:1-14.
60. Kujoth, G. C., D. F. Robinson, and W. E. Fahl. 1998. Binding of ETS family members is important for the function of the c-sis/platelet-derived growth factor-B

TATA neighboring sequence in 12-O-tetradecanoylphorbol-13-acetate-treated K562 cells. *Cell Growth Differ* 9:523-534.

61. Khurana, A., and C. S. Dey. 2002. Involvement of Elk-1 in L6E9 skeletal muscle differentiation. *FEBS Lett* 527:119-124.
62. Sharrocks, A. D. 2001. The ETS-domain transcription factor family. *Nat Rev Mol Cell Biol* 2:827-837.
63. Lelievre, E., F. Lionneton, F. Soncin, and B. Vandenbunder. 2001. The Ets family contains transcriptional activators and repressors involved in angiogenesis. *Int J Biochem Cell Biol* 33:391-407.
64. Majka, M., J. Ratajczak, M. A. Kowalska, and M. Z. Ratajczak. 2000. Binding of stromal derived factor-1alpha (SDF-1alpha) to CXCR4 chemokine receptor in normal human megakaryoblasts but not in platelets induces phosphorylation of mitogen-activated protein kinase p42/44 (MAPK), ELK-1 transcription factor and serine/threonine kinase AKT. *Eur J Haematol* 64:164-172.
65. Reddy, K., Y. Cao, Z. Zhou, L. Yu, S. F. Jia, and E. S. Kleinerman. 2008. VEGF165 expression in the tumor microenvironment influences the differentiation of bone marrow-derived pericytes that contribute to the Ewing's sarcoma vasculature. *Angiogenesis* 11:257-267.
66. McCarty, M. F., R. J. Somcio, O. Stoeltzing, J. Wey, F. Fan, W. Liu, C. Bucana, and L. M. Ellis. 2007. Overexpression of PDGF-BB decreases colorectal and pancreatic cancer growth by increasing tumor pericyte content. *J Clin Invest* 117:2114-2122.

67. Onimaru, M., Y. Yonemitsu, T. Fujii, M. Tanii, T. Nakano, K. Nakagawa, R. Kohno, M. Hasegawa, S. Nishikawa, and K. Sueishi. 2009. VEGF-C regulates lymphangiogenesis and capillary stability by regulation of PDGF-B. *Am J Physiol Heart Circ Physiol* 297:H1685-1696.
68. Teicher, B. A., and S. P. Fricker. CXCL12 (SDF-1)/CXCR4 Pathway in Cancer. *Clin Cancer Res*.
69. De Clercq, E. 2009. The AMD3100 story: the path to the discovery of a stem cell mobilizer (Mozobil). *Biochem Pharmacol* 77:1655-1664.
70. Cashen, A. F., B. Nervi, and J. DiPersio. 2007. AMD3100: CXCR4 antagonist and rapid stem cell-mobilizing agent. *Future Oncol* 3:19-27.
71. Tian, J., and M. Karin. 1999. Stimulation of Elk1 transcriptional activity by mitogen-activated protein kinases is negatively regulated by protein phosphatase 2B (calcineurin). *J Biol Chem* 274:15173-15180.
72. Horuk, R. 2001. Chemokine receptors. *Cytokine Growth Factor Rev* 12:313-335.
73. Kasza, A., P. Wyrzykowska, I. Horwacik, P. Tymoszek, D. Mizgalska, K. Palmer, H. Rokita, A. D. Sharrocks, and J. Jura. Transcription factors Elk-1 and SRF are engaged in IL1-dependent regulation of ZC3H12A expression. *BMC Mol Biol* 11:14.
74. Benjamin, L. E., D. Golijanin, A. Itin, D. Pode, and E. Keshet. 1999. Selective ablation of immature blood vessels in established human tumors follows vascular endothelial growth factor withdrawal. *J Clin Invest* 103:159-165.
75. Veeravagu, A., A. R. Hsu, W. Cai, L. C. Hou, V. C. Tse, and X. Chen. 2007. Vascular endothelial growth factor and vascular endothelial growth factor receptor

- inhibitors as anti-angiogenic agents in cancer therapy. *Recent Pat Anticancer Drug Discov* 2:59-71.
76. DuBois, S. G., N. Marina, and J. Glade-Bender. Angiogenesis and vascular targeting in Ewing sarcoma: a review of preclinical and clinical data. *Cancer* 116:749-757.
 77. Chen, G., Z. Wang, X. Y. Liu, and F. Y. Liu. High-Level CXCR4 Expression Correlates with Brain-Specific Metastasis of Non-Small Cell Lung Cancer. *World J Surg.*
 78. Ma, L., H. Qiao, C. He, Q. Yang, C. H. Cheung, J. R. Kanwar, and X. Sun. Modulating the interaction of CXCR4 and CXCL12 by low-molecular-weight heparin inhibits hepatic metastasis of colon cancer. *Invest New Drugs.*
 79. Muller, A., B. Homey, H. Soto, N. Ge, D. Catron, M. E. Buchanan, T. McClanahan, E. Murphy, W. Yuan, S. N. Wagner, J. L. Barrera, A. Mohar, E. Verastegui, and A. Zlotnik. 2001. Involvement of chemokine receptors in breast cancer metastasis. *Nature* 410:50-56.
 80. Kaplan, R. N., B. Psaila, and D. Lyden. 2006. Bone marrow cells in the 'pre-metastatic niche': within bone and beyond. *Cancer Metastasis Rev* 25:521-529.
 81. Kaifi, J. T., E. F. Yekebas, P. Schurr, D. Obonyo, R. Wachowiak, P. Busch, A. Heinecke, K. Pantel, and J. R. Izbicki. 2005. Tumor-cell homing to lymph nodes and bone marrow and CXCR4 expression in esophageal cancer. *J Natl Cancer Inst* 97:1840-1847.

82. Jia, S. F., R. R. Zhou, and E. S. Kleinerman. 2003. Nude mouse lung metastases models of osteosarcoma and Ewing's sarcoma for evaluating new therapeutic strategies. *Methods Mol Med* 74:495-505.
83. Weigelt, B., J. L. Peterse, and L. J. van 't Veer. 2005. Breast cancer metastasis: markers and models. *Nat Rev Cancer* 5:591-602.
84. Ribatti, D., G. Mangialardi, and A. Vacca. 2006. Stephen Paget and the 'seed and soil' theory of metastatic dissemination. *Clin Exp Med* 6:145-149.
85. Kaplan, R. N., R. D. Riba, S. Zacharoulis, A. H. Bramley, L. Vincent, C. Costa, D. MacDonald, D. K. Jin, K. Shido, S. A. Kerns, Z. Zhu, D. Hicklin, Y. Wu, J. L. Port, N. Altorki, E. R. Port, D. Ruggero, S. V. Shmelkov, K. K. Jensen, S. Rafii, and D. Lyden. 2005. VEGFR1-positive haematopoietic bone marrow progenitors initiate the pre-metastatic niche. *Nature* 438:820-827.

Vita

Randala Hamdan, the daughter of Hisham and Afaf Hamdan, was born in the Czech Republic on February 17, 1982. Randala is of Lebanese nationality; however, due to her Father's career as a diplomat, Randala traveled most of her childhood and lived in Prague, Nigeria, Geneva, London and, Beirut. She is fluent in Arabic, English and, French. Randala completed her high school education at Notre Dame de La Delivrande in Araya, Lebanon in 2000 when she moved to Denton, Texas, to start her Bachelor of Science degree in Biochemistry at The University of North Texas. She graduated cum laude in 2004 and moved to Houston, Texas, to work as a research assistant in the laboratory of Dr. Jean-Pierre Issa, MD, where her work contributed to 2 publications in the journals *Cancer Epidemiology, Biomarkers and Prevention* and, *Cancer Prevention Research*. Randala enrolled as a graduate student at The University of Texas, MD Anderson Cancer Center, in 2005 and completed 3 rotations with Dr. Jean-Pierre Issa, MD, Dr. Alan Schroit, PhD, and, Dr. Eugenie Kleinerman, MD. Her 3 months rotation in Dr. Alan Schroit's laboratory resulted in a first author manuscript in the journal, *Biochemistry*. Randala joined Dr. Kleinerman's laboratory to work on her thesis dissertation looking at the role of SDF-1 α and PDGF-B in BM-derived pericyte differentiation in Ewing's sarcoma in the summer of 2006. Since then, she was awarded the City Federation of Women's Clubs Endowed Scholarship in the Biomedical Sciences (2009) and the Marilyn and Frederick R. Lummis, Jr., M.D., Fellowship in the Biomedical Sciences (2009-2010).